Appendix A: Preliminary Analysis for the Six-week Nine-site Data (January 11, 2003 to February 26, 2003).

Appendix A.

Spatial and Temporal Assessment of a Mobile Source Aerosol Indicator During Winter in Boston, MA: A Pilot Study

George A. Allen and Philip R.S. Johnson

Northeast States for Coordinated Air Use Management, Boston MA.

.

Poster # 05-27, presented at "Particulate Matter: Atmospheric Sciences, Exposure and the Fourth Colloquium on PM and Human Health" in Pittsburgh, PA, March 31-April 4, 2003

An International Conference Managed by the American Association for Aerosol Research

Introduction. Many urban locations are expected to be near or over the annual U.S. EPA standard for PM2.5 of 15.0 $\mu g/m^3$. Data from PM2.5 monitors in the same metropolitan area only a few miles apart can be substantially different, with some over and some under the standard. Variation on this spatial scale is often presumed to be driven by local mobile source particle emissions. It is important to define the spatial extent of elevated PM2.5 for compliance, air toxics assessment, and control purposes, as well as for health effects studies. One indicator of local mobile source aerosol in urban areas is black carbon soot (BC, associated with primary Diesel and automotive emissions), which has been shown to be well correlated with integrated elemental carbon (EC) filter samples. BC can be measured in real-time with a commercial instrument (Aethalometer) that is relatively simple to install and operate; the principle is light absorption through a quartz filter (optical density).

Study Design. A pilot study was performed during the winter of 2003 to assess the spatial and temporal variation in the local mobile-source aerosol over the greater Boston area, using BC as an indicator for that PM component. Given that other major mass components of PM2.5 (sulfate, organic carbon) in the northeast U.S. are secondary transported aerosols and tend to be uniform over this scale, the locally generated "tailpipe" component of PM should drive the shape of PM2.5 spatial gradients over the metro area. A series of nine monitoring sites were selected heading WNW from downtown Boston out 35 km (Figure 1), generally away from immediate large sources of local mobile-source emissions. This design avoids coastal influence and allows the pilot study to be more readily generalized to other large metro areas in the Northeast.

Site Locations	**Km**	**Site Description.**
Beacon Hill (Boston)	0.0	Urban Residential (adjacent to the State House)
Roxbury (Boston)*	3.5	Urban Residential/Commercial (Dudley Sq.)
Brigham Cir. (Boston)*	4.1	Urban Residential/Commercial (Harvard Medical Area)
Brighton (Boston)	7.0	Semi-Urban Residential
Newton (Nonantum)†	11.7	Suburban Residential/Light Commercial
Waltham	14.9	Suburban Residential/Light Commercial
Weston †	17.4	Suburban Residential, near I-90/I-95
Wayland †	25.1	Suburban Residential
Stow	35.3	Semi-rural open land; Regional Background site

* existing sites run by other organizations

† Non-core network sites, only run 11 Jan. to 26 Feb. or 6 Mar. 2003

Measurement Methods. BC was measured with Magee Scientific Inc. Aethalometers, models AE-16 and AE-42, with fine-mode size cut inlets. The default "sigma" value of 16.6 was used. All BC data are reported in $\mu g/m^3$ at STP. Leak tests and external flow calibrations were performed on all instruments. Data were collected at 5-minute intervals using the Aethalometer's internal storage; 1-hour mean concentrations of BC were calculated with the Washington University-St. Louis Aethalometer data processor. Hourly data were screened for unusual local source influence, such as woodsmoke; a total of 31, 15, and 9 hours were removed from the Waltham, Beacon Hill, and Wayland sites respectively between 4 Jan. and 6 March 2003. An additional 11 hours were removed for all sites overnight on Saturday evening 18 January.

Figure 1. Site Locations

"+" indicates a core network site; "–" is a temporary site (11 Jan - 26 Feb 2003).

Population Density. Population densities at the nine monitoring sites were generated to assess whether population is a surrogate for local mobile-source aerosol concentrations. Population estimates were generated using LandView5 software, a spatial and demographic database application created by the U.S. EPA, Census Bureau, Geological Survey, and NOAA (http://landview.census.gov). The software tallies Census 2000 block data for those block centroids whose coordinates fall within a circle defined by a prescribed radius. Geographic coordinates for the monitoring sites were used as center points to estimate population density within a 0.5 mile radii or 0.8 square miles.

Data Analysis. The core data set used for most analysis was from the six longer-term "core" sites, from January 4 to March 6, 2003 (data from the three non-core sites were used only in the spatial frequency distribution analysis), since these core sites had more days of data and will continue for a full year. Average spatial and diurnal spatial patterns were segregated by workday vs. non-workday. Population densities at each monitoring site were compared to mean black carbon levels.

Results and Discussion. Data capture for all sites exceeds 97% for each site after editing for local woodsmoke influence. **Figure 2** shows the core six-site network data as 24-hour running averages for the Jan. 4 to Mar. 6, 2003 period; a wide range of spatial and temporal BC concentration is evident, with urban sites consistently higher than non-urban sites. **Figure 3** shows the frequency distributions and means of hourly BC concentrations by site for all nine sites; the order is downtown to background from left to right. As one would expect, the data are lognormally distributed, and there is a general trend of lower BC as sites become less urban. Some sites show clear woodsmoke influence during certain periods. Obvious cases were removed, but it is still likely that some woodsmoke influence remains for the suburban sites, especially Newton and Waltham, during this pilot study period. It is notable that Brighton, only 7.0 km from Beacon Hill and 5.8 km from Roxbury, has a mean BC of less than half that of either Roxbury or Beacon Hill. There is a factor of 3.5 between mean BC in

downtown Boston and the regional background site at Stow, which is important from an air toxics exposure point of view. Based on available annual mean PM2.5 data, the gradient over this range is much smaller (approximately a factor of 1.4), with sites in downtown Boston at or near the annual PM2.5 standard of 15.0 $\mu g/m^3$. The BC data from this pilot study imply that the size of the metro area near the annual PM2.5 standard may be limited to core urban areas.

Preliminary results do not confirm the original hypothesis of mobile source-related "hot-spots", but point to a more homogeneous elevated concentration in the core urban area. The original study design had targeted the Roxbury (near a large city bus station and bus "barns") and Weston (500 meters NW of a major interstate highway exchange and toll booths) sites as likely to have elevated BC from local traffic influence. Neither of these sites was elevated compared to surrounding sites; the mean BC at Roxbury was similar to Beacon Hill, and Weston was similar to the two sites further west. Earlier limited work showed a residential site in South Boston (2.9 km SE from Beacon Hill) to have similar levels of mean BC as Roxbury. This supports the possibility of a fairly uniform spatial pattern of elevated BC in the core urban area for residentially oriented monitoring locations. We plan to investigate this further with a micro-scale study in downtown Boston later this year.

Weather was colder than normal during the study period by approximately 3°C. Two of the sites in this network have been running for 4 years; this provides some context for the effect of weather on data from this study. The following table compares mean BC for Roxbury and Brigham Circle over this period with three previous years:

Jan-Feb mean BC	Roxbury (range)	Brigham Circle (range)	Ratio of means (range)
2000-2002	1.42 (1.25-1.56)	0.83 (0.76 - 0.89)	1.71 (1.39 - 1.92)
2003	0.89	0.62	1.42

Compared to 2000-2002, 2003 Jan-Feb BC was 37% lower at Roxbury, and 25% at Brigham Circle, and was the cleanest of the 4 years by a distinct margin. The ratio of Roxbury to Brigham Circle BC (1.42) was also lower this year than the 3-year mean ratio; this is consistent with overall BC levels being lower, and suggests that the spatial gradients reported for this pilot study may be a lower-end estimate.

Figure 4 shows the diurnal pattern of BC for the six core sites, broken down by work and non-workdays. For workdays, the morning rush hour BC at Beacon Hill and Roxbury is five times higher than the Stow site; diurnal patterns become weaker as sites become less urban. The lack of any distinct workday diurnal pattern at the Stow site confirms that it represents the regional background BC concentration. Non-workday diurnal patterns show no clear time of day effects for most sites, in part because only 19 days of data were available.

Figure 5 shows mean BC across the six core sites, broken down by work and non-workdays. There is a distinct difference only for the three most urban sites, and no difference at Waltham or Stow; this is consistent with the less urbanized sites having more regional and fewer local sources of BC.

Figure 6 shows the relationship between population density (0.5 mile radius) and mean BC at the nine monitoring sites. With the exception of Brighton (whose BC levels were lower than adjacent sites), population estimates decrease linearly as mean BC decreases. The coefficient of determination (R^2) between population density and mean BC is 0.43 for all nine sites but increases to 0.81 without the Brighton site. This indicates that it may be possible to predict spatial gradients in mean BC concentrations across this scale by using local population density, a readily available metric.

Figure 7 is a single 24-hour period showing the effect of poor dispersion on BC levels at all nine sites. Cloud ceiling (from Logan Airport in Boston) is used as a surrogate for the minimum mixing height.

When the ceiling is less than 2000 feet, urban levels of BC increase dramatically, even though this happens after the morning rush hour. During hour 17, the cloud ceiling increases to 6000 feet, and BC levels drop rapidly. **Figure 8** is a five-day time series from the eight sites running during that period, and shows a more typical regional stagnation event. PM2.5 data from the Roxbury site is also shown (on the right-axis). A distinct morning rush hour peak for both BC and PM2.5 occurs on Thursday, but not on Friday. Late Friday evening shows another distinct multi-hour peak; the cause is unclear, but the Celtics were playing Toronto in Boston that evening (they won!). Both peaks show an EC to PM2.5 ratio of 10 at the Roxbury site.

Conclusions. Substantial gradients in BC exist over relatively small distances in the metropolitan Boston area, however there may be a core urban area where levels are elevated but gradients are not distinct. Mean BC varies by a factor of 3.5 from downtown to a regional background site; this factor is larger for sub-daily event periods. Based on spatial, hour-of-day, and day-of-week patterns, BC appears to be a reasonable indicator of local "tailpipe" aerosol despite potential for woodsmoke interference, but it is not highly specific to Diesel or on-road vs. off-road sources. These pilot data suggest that urban PM2.5 attainment areas may not always extend over the entire metropolitan region, but be limited to a somewhat smaller urban zone. Although PM2.5 gradients in greater Boston are no more than a factor of 1.5, the BC gradient of 3.5 and the relatively rapid drop-off within the urban area are important from an air toxics exposure and control strategy point of view.

Study Limitations. The single (and somewhat atypical) cold weather season and limited pilot study spatial scope and duration limit the precision of estimates of both spatial gradients and absolute BC concentrations. Woodsmoke may be an interference especially in suburban locations. The relative contributions of Diesel [on- and/or off- road] vs. automotive engines to observed BC concentrations is

uncertain. Population density data may be imprecise at the 0.5 mile radius level due to the spatial resolution of those data. Traffic density data were not available in a useful form to compare to observed BC patterns.

Future work. Six core BC sites will continue for a full year's operation to allow assessment of seasonal factors and the significance of woodsmoke interference. The question of "hot-spots" will be addressed with micro-scale studies in downtown Boston later this year, and possibly a different site near I-90/I-95 in Weston/Newton. A high elevation site near Boston (Blue Hill, 200 m elevation, 12.5 km south of Roxbury) will be added to the network to further assess regional transport of BC. Further analysis is required to determine whether local population density can be considered a surrogate for local traffic density, which might be a more appropriate metric for predicting BC concentrations.

Acknowledgments. The following organizations and companies have supported this work in kind:
Massachusetts Department of Environmental Protection
U.S. EPA, Region 1
Magee Scientific Company, Berkeley CA
Harvard School of Public Health/Boston EPA-PM Center
Washington University-St. Louis/ STL EPA Supersite
Appalachian Mountain Club, Boston MA
BGI Inc., Waltham MA.
ETA Associates, Newton MA

Figure 2. 24-hour running means of hourly BC, Six Core Sites, Jan 4 - Mar 6, 2003

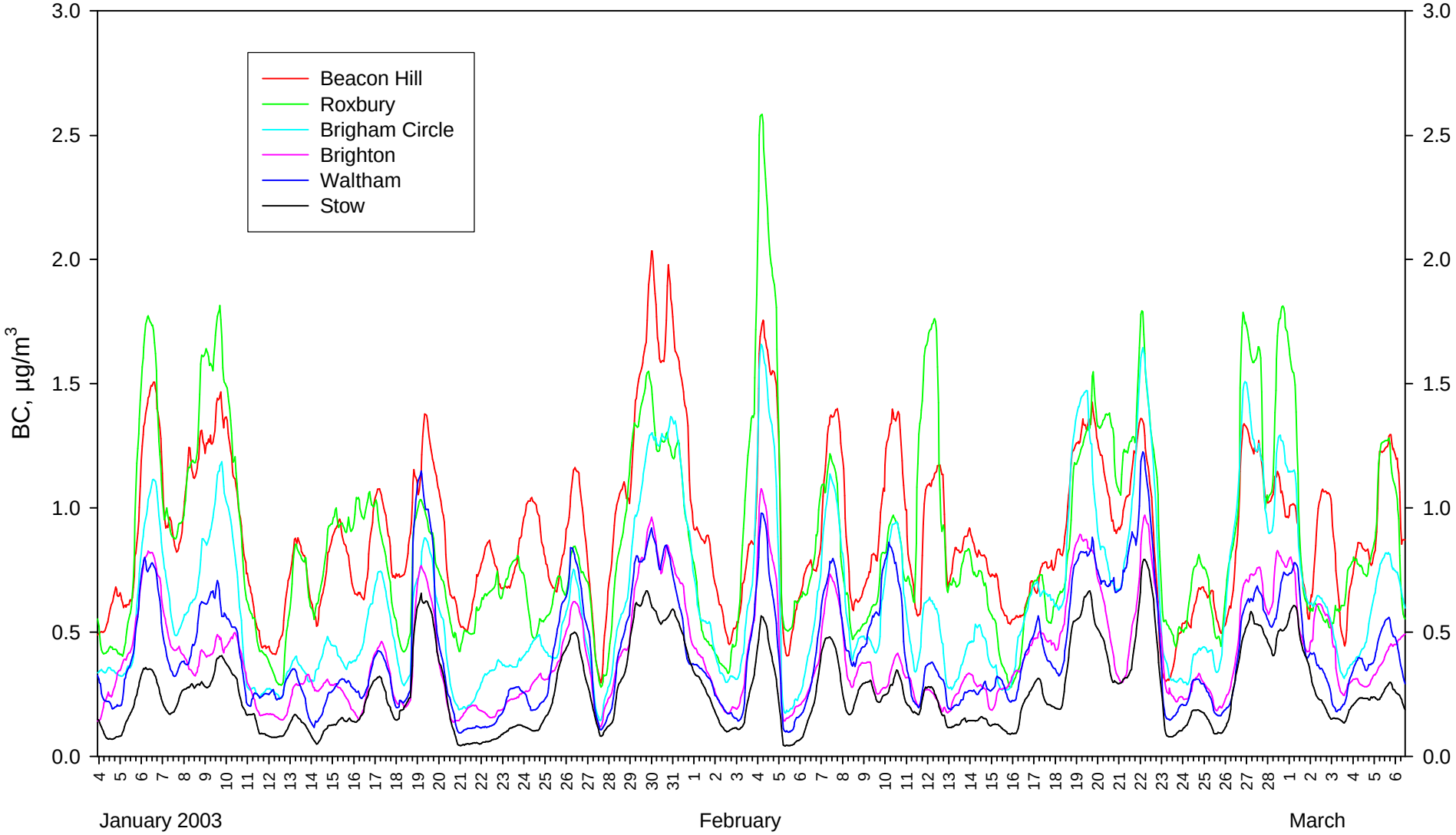

Figure 3. 11 Jan thru 26 Feb 2003 1-Hour Spatial BC Distributions

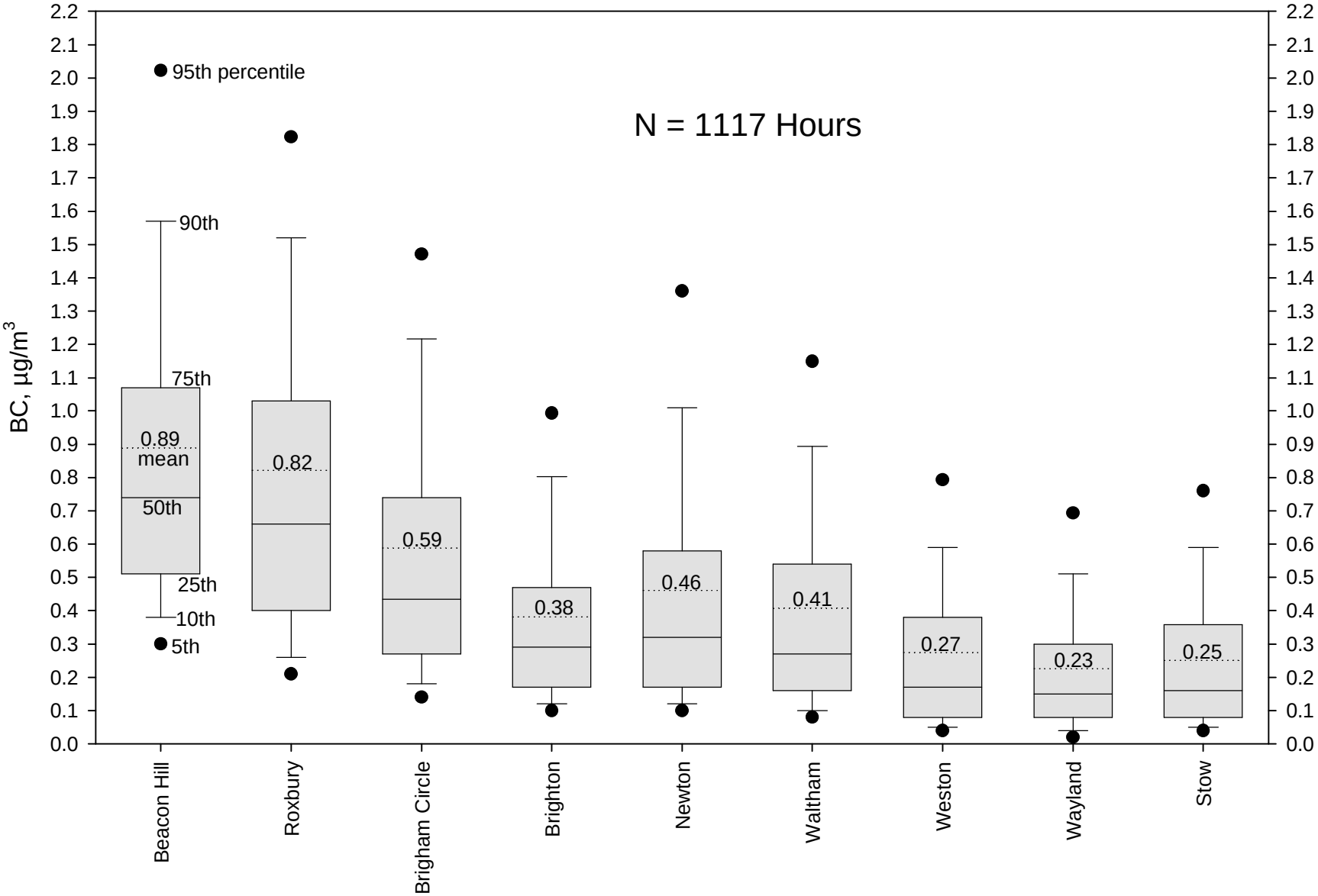

Figure 4. Diurnal BC Jan 04 - Mar 06, 2003

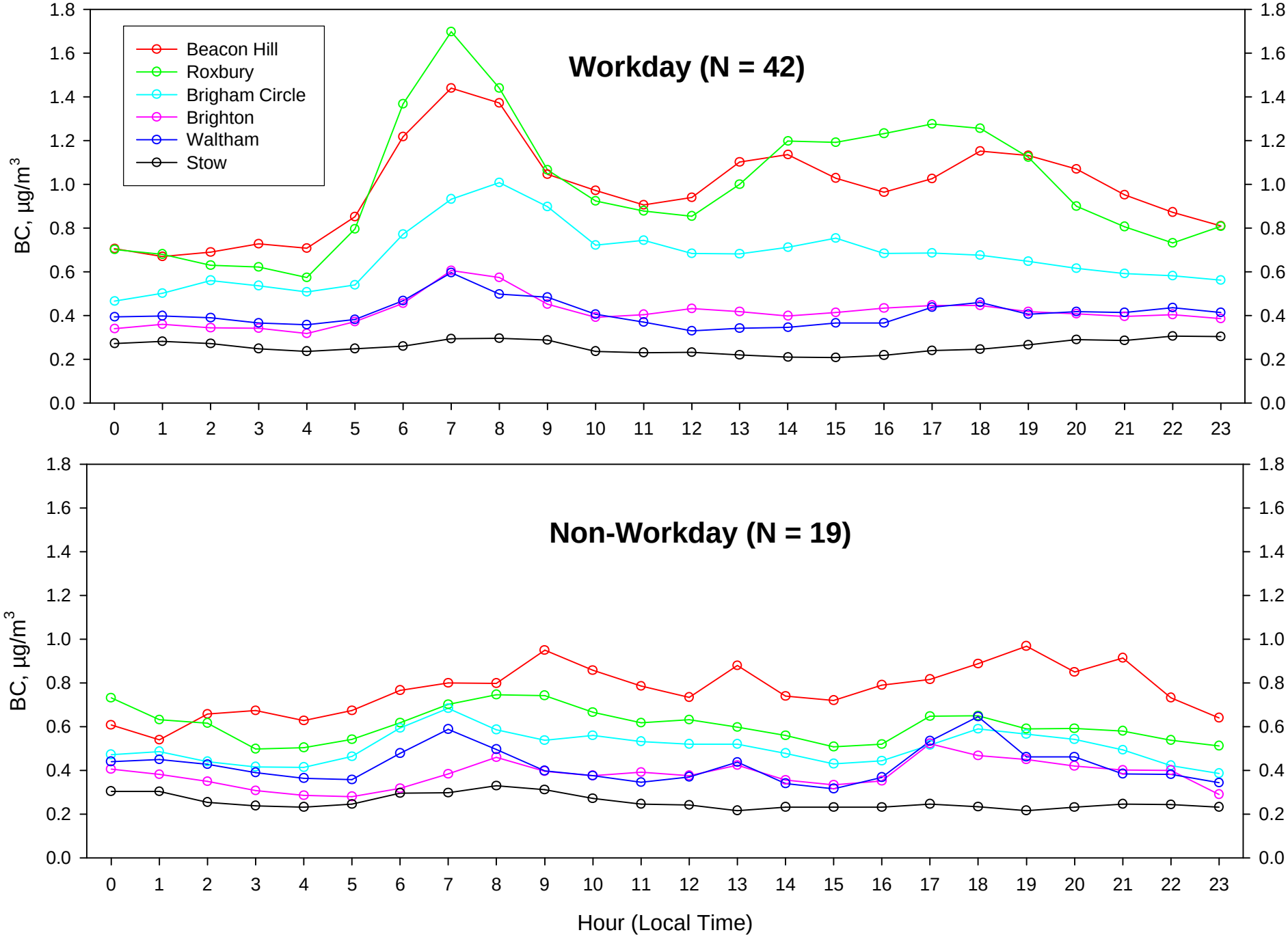

Figure 5.
Workday vs. Non-workday Mean BC
6 Core Sites, Jan 4 through Mar 6, 2003

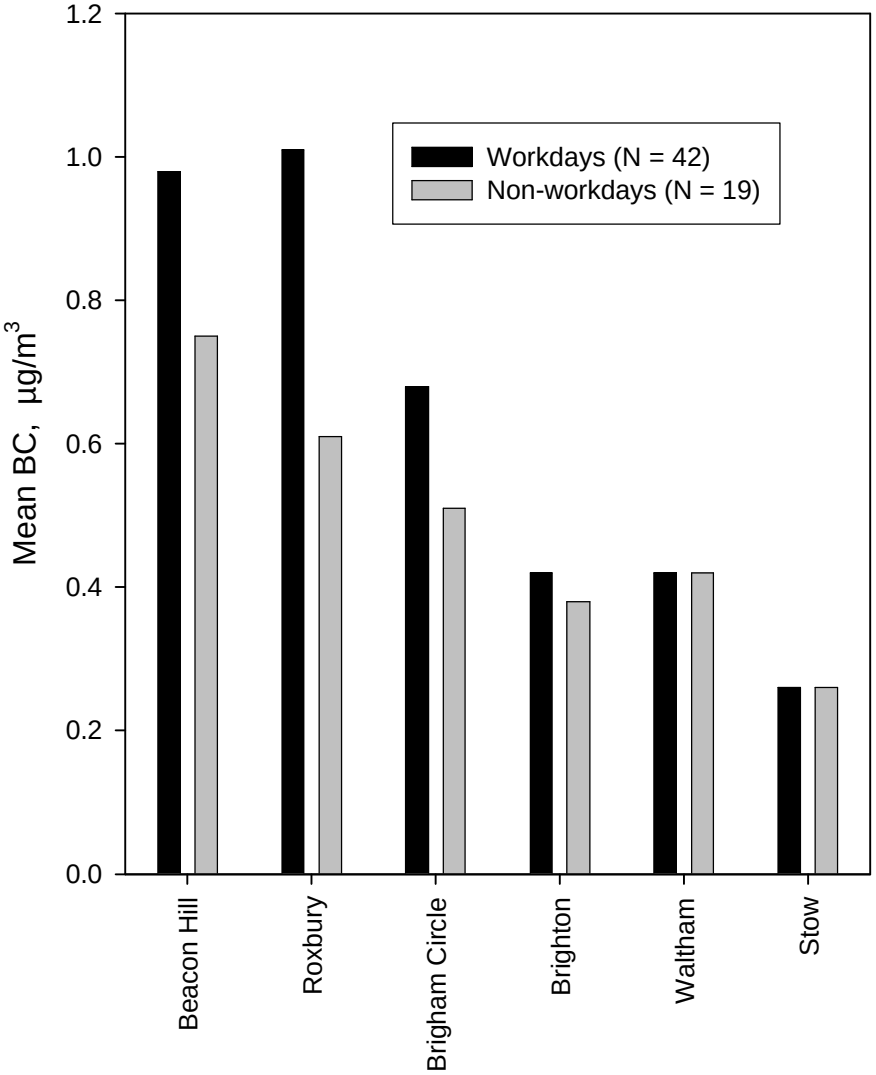

Figure 6.
Population Density (0.5 mile radius)
vs. Mean BC

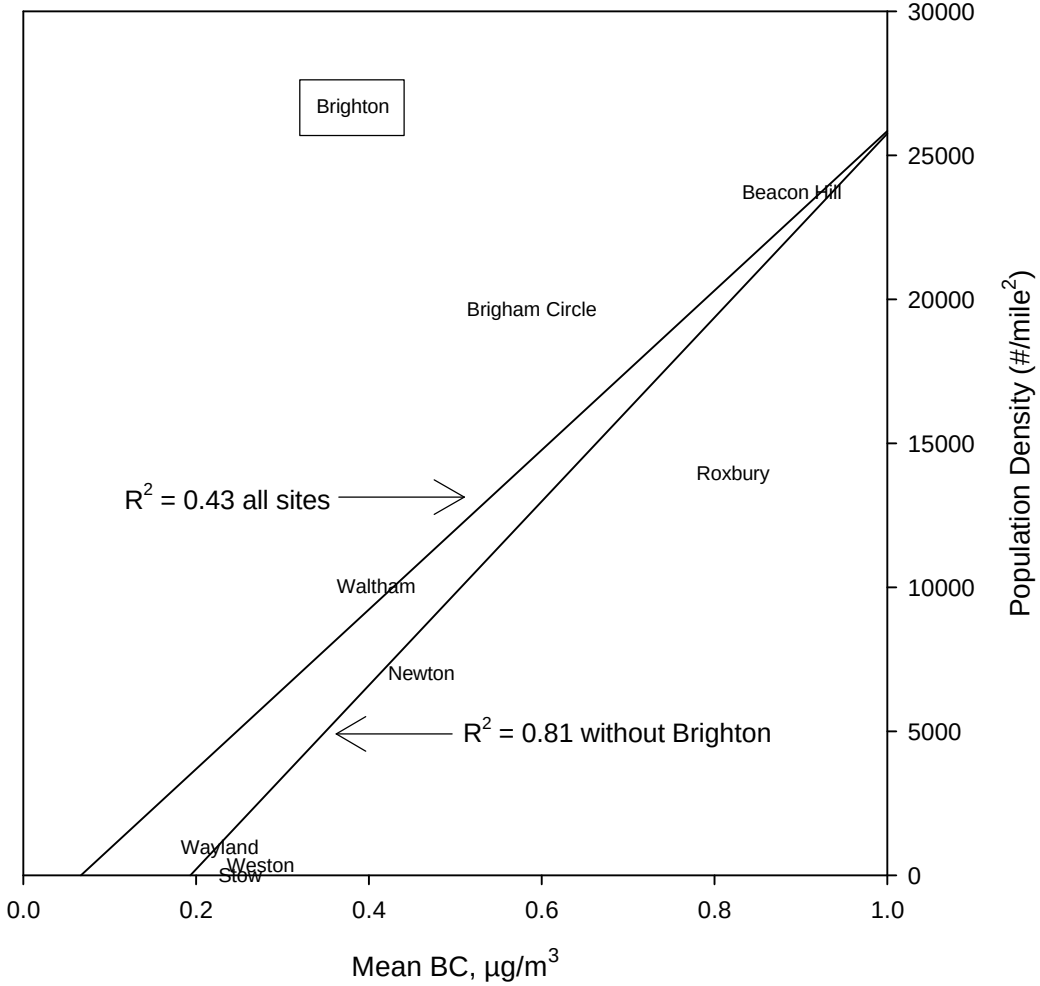

Figure 7. Feb 4 2003 BC Event

15-minute running means of 5-minute data

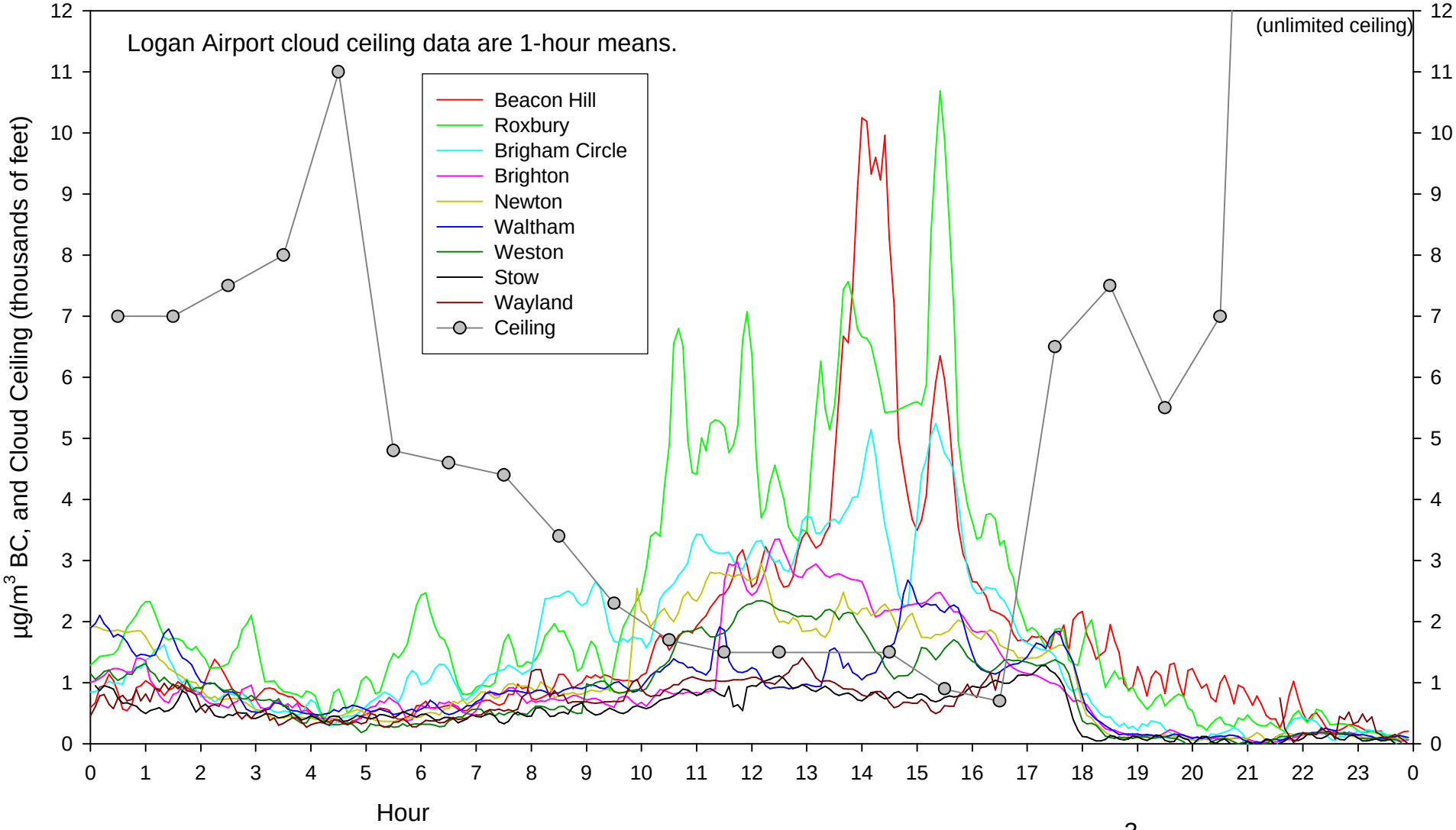

Roxbury PM2.5 dropped from 41 to 5 µg/m^3 between 15:00 and 20:00

Figure 8. Metro-Boston Regional Stagnation Event
BC (left axis) and PM2.5 (right axis) running 3-Hour Means of 1-hour data

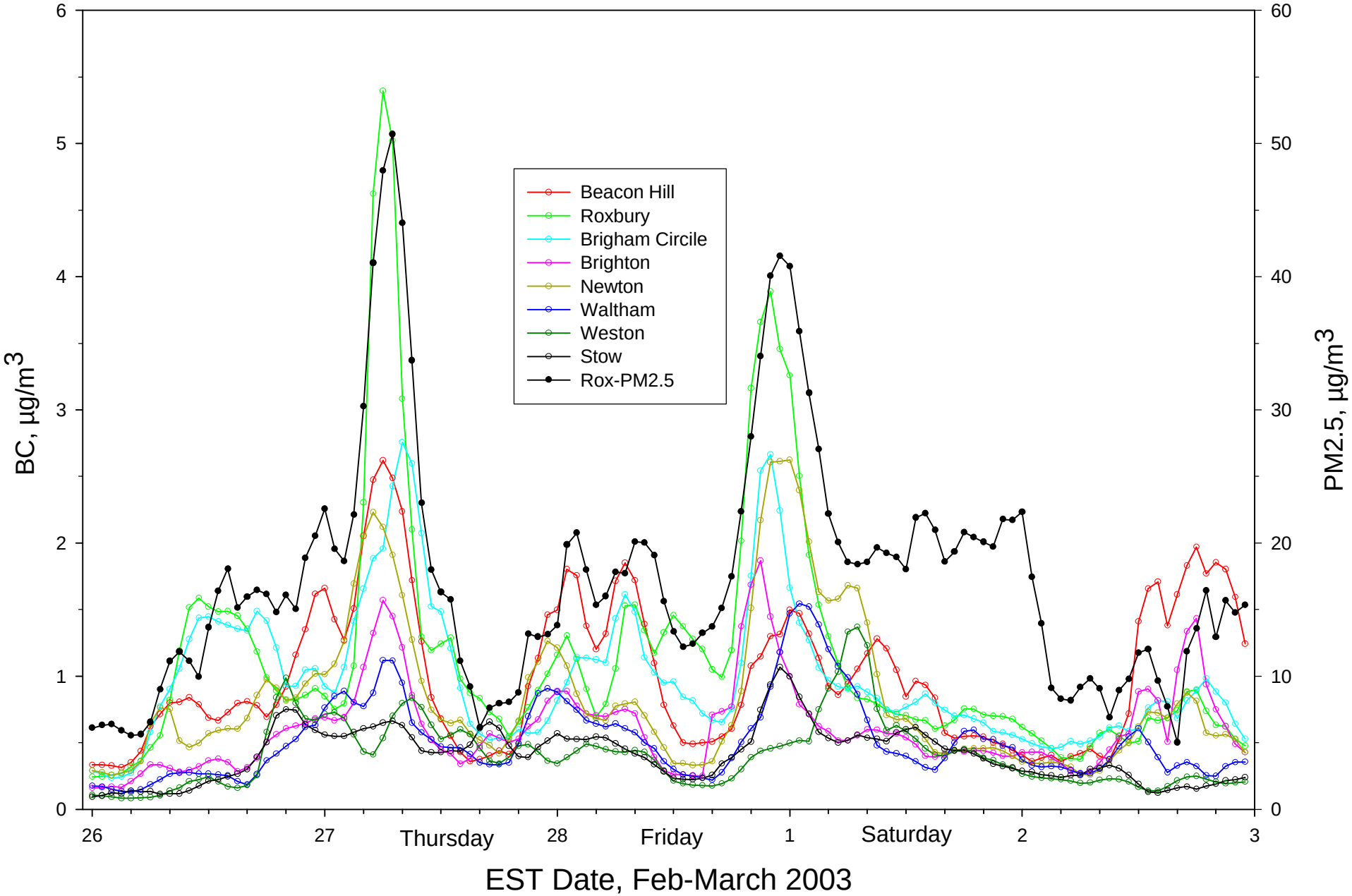

Appendix B: Preliminary Analysis for the One-year Six-site Data (December 20, 2002 to September 9, 2003), including the Summer Core Boston 10-site Data.

Appendix B.

Spatial and Temporal Aspects of Black Carbon Concentrations over the Boston Metro Area: An Update of Work in Progress

George Allen and Philip R.S. Johnson
Northeast States for Coordinated Air Use Management

Based on material presented at the 22nd Annual Conference of the American Association of Aerosol Research
Anaheim, CA October 22, 2003

Rev. 16 Dec 2003

Background

· This study was designed to assess the spatial and temporal variation in "mobile source aerosol" as measured by black carbon in an urban area. Data collection is not yet complete, and all analysis presented here is preliminary and under development.
· By design, this is not a "hotspot" assessment, given that the monitoring sites were located >100 meters from the most intense "source" strength (adjacent major roadways) areas. Higher exposures than those reported here may exist at mobile-source “hotspots” both in the urban area and in non-urban areas as well.
· This study does assess "neighborhood-scale" (0.5 to 4 km) exposure gradients to black carbon across the metropolitan Boston area.
· Limitations of this study include semi-randomized monitor siting and monitor-to-monitor bias that are not accounted for at this time. Wind conditions that may result in dilution of source pollution at any given site have also not been taken into account in this preliminary analysis. The significance of observed gradients will be characterized using ANOVA analyses once the final year-long data set is available.
· This study has begun to characterize the urban mobile source aerosol gradient in greater Boston, has identified future areas for more refined microscale assessment, and has underscored the utility of black carbon as an indicator of fossil fuel combustion, showing that it can be reasonably specific for mobile source-related fine particulate in an urban area.

Introduction.

Need to define the spatial extent of elevated PM2.5 across urban areas:
- Compliance issues (PM2.5 attainment)
- Air toxics exposure assessment, Control assessment
- Health effects studies

Black Carbon (BC):
- Generally associated with fossil fuel combustion; in this study BC is shown to be a useful indicator of local [primary] mobile source aerosol in urban areas
- Not highly specific to diesel for the neighborhood scale siting (non-hotspot) used in this study

Method: Magee Scientific Aethalometer™
- Optical Density measurement, scaled to BC in $\mu g/m^3$
- Well correlated with DRI TOR-EC (less so with NIOSH/STN EC)
- Simple method, easy to deploy and operate
- Method bias across sites is typically 10% or less

Approach:

Previous work: Pilot study, winter of 2003 (AAAR PM conference poster, Spring 2003)

Assess spatial/temporal variation in "local mobile-source aerosol"
9 sites WNW from downtown
Scale: over the greater Boston area – out to 35 km (background)

Pilot results indicated that it was important to expand the work into a larger study:

Strong spatial gradients (>3 on average; more for events)
Look in detail at specific neighborhoods (Beacon Hill, S.Boston similar to Roxbury)
Run 6 sites for full year (address seasonal questions, woodsmoke and space heating interferences): all of 2003
"Neighborhood-Scale" study – Summer 2003: 10 sites in Boston

Detailed Study Description:

Many urban locations are expected to be near or over the annual U.S. EPA standard for PM2.5 of 15.0 μg/m^3. Data from PM2.5 monitors in the same metropolitan area only a few miles apart can be substantially different, with some over and some under the standard. Variation on this urban spatial scale is often presumed to be driven by local mobile source particle emissions. It is important to define the spatial extent of elevated PM2.5 for compliance, air toxics exposure assessment, and control assessment purposes, as well as for health effects studies exposure estimates. One indicator of local mobile source aerosol in urban areas is black carbon soot (BC, associated with primary diesel and automotive emissions), which has been shown to be well correlated with integrated elemental carbon (EC) filter samples. BC can be measured in real-time with a commercial instrument (Aethalometer) that is relatively simple to install and operate; the principle is light absorption through a quartz filter (optical density).

This study assesses the spatial and temporal variation in the local mobile-source aerosol over the greater Boston area, using BC as an indicator for that PM component. Given that other major mass components of PM2.5 (sulfate, organic carbon) in the northeast U.S. are secondary transported aerosols and tend to be uniform over this scale, the locally generated "tailpipe" component of PM should drive the broad shape of PM2.5 spatial gradients over the metro area. A series of monitoring sites was selected heading WNW from downtown Boston out 35 km, using neighborhood-scale siting criteria (generally away from immediate large sources of local mobile-source emissions). The siting design avoids coastal influence; this and the neighborhood-scale siting allows the study to be more readily generalized to other large metro areas in the Northeast. More detail on the spatial scale of representation for monitor siting is in 40CFR58, appendix D: http://www.epa.gov/ttn/amtic/files/cfr/pt58/40cfr58a.pdf

6 Core Site Locations	Km	Site Description
Beacon Hill (Boston)	0.0	Urban Residential (near State House)
Roxbury (Boston)	3.5	Urban Residential/Commercial; EJ
Brigham Cir. (Boston)	4.1	Urban Residential/Commercial
Brighton (Boston)	7.0	Semi-Urban Residential
Waltham	14.9	Suburban Residential/Light Commercial
Stow	35.3	Semi-rural, open land; Regional Background site for Metro Boston

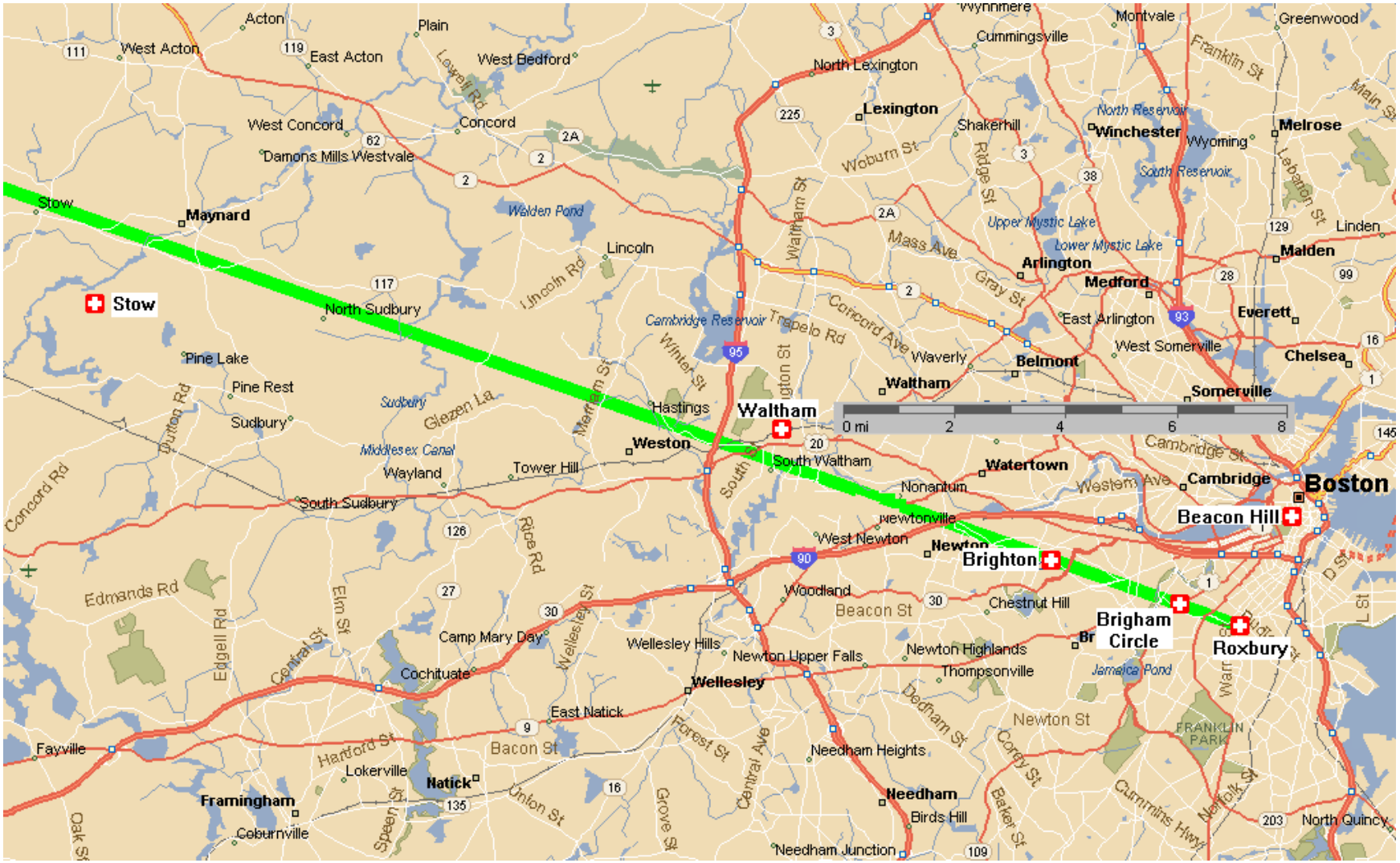

Figure: 6-Site Hourly BC Distributions, Dec. 20, 2002 to Sep. 09, 2003.

This set of boxplots updates the initial "pilot" analysis that was based on 2 months of winter 2003 data and shows the frequency distribution of hourly BC data.

Joy St. [Beacon Hill near State House] BC is essentially identical for all but perhaps the extreme hour values (95th percentile). The measurement methods used can not resolve concentration differences less than 10% between sites (site to site measurement bias).

The ratio between the mean or median BC from the highest urban sites and the Stow background site is between 3 and 3.5.

Brighton and Waltham BC remain essentially identical for these boxplot metrics, both about half of the highest urban sites. Future statistical analysis will quantify the significance of this concentration gradient.

Figure: Diurnal BC, Six Greater Boston Sites Dec. 20, 2002 - Sep. 9, 2003.

This diurnal plot updates the initial "pilot" analysis that was based on 2 months of winter 2003 data and shows the temporal patterns of BC broken down by site and workday vs. non-workday. The much larger sample size and inclusion of both warm and cold weather seasons substantially decrease the uncertainty of in the initial pilot data interpretation.

The three "core" urban Boston sites show a distinct and strong rush-hour peak during workdays, and only a weak and indistinct peak during the same hours for non-workdays. This is consistent with expected traffic patterns and conclusions drawn by others previously. Note that Roxbury rush-hour peak BC is distinctly higher than Joy St. for both morning and afternoon, even though mean BC for these two sites is very similar.

Concentrations observed at Brighton and Waltham BC track remarkably well. The Stow background site shows no significant workday or non-workday diurnal pattern (errorbars are typically about 10% of the parameter value), confirming the lack of significant local traffic influence at that site.

This multi-season weekday/non-weekday diurnal analysis also provides increased confidence that BC is reasonably specific to local tailpipe aerosol, minimizing concerns related to potential interferences at these sites from other sources of BC such as oil-fired space heating and woodsmoke.

Figure: Workday/Non-Workday BC means across sites.

This plot shows the mean BC across sites by work/non-work day. As would be expected, the differences are highest (about 70%) at the sites with the most local traffic influence and highest BC levels, and decrease to about 10% at the Stow background site.

Figure: Cold vs. Warm season mean BC by site.

Although winter might be expected to have more of a local mobile source influence than summer (more and stronger inversions), these data show that all sites had substantially lower mean BC in the winter. This is most likely an artifact due to the unusually stormy weather in winter 2003; compared to Jan-Feb 2000-2002, Roxbury 2003 Jan-Feb mean BC was 37% lower.

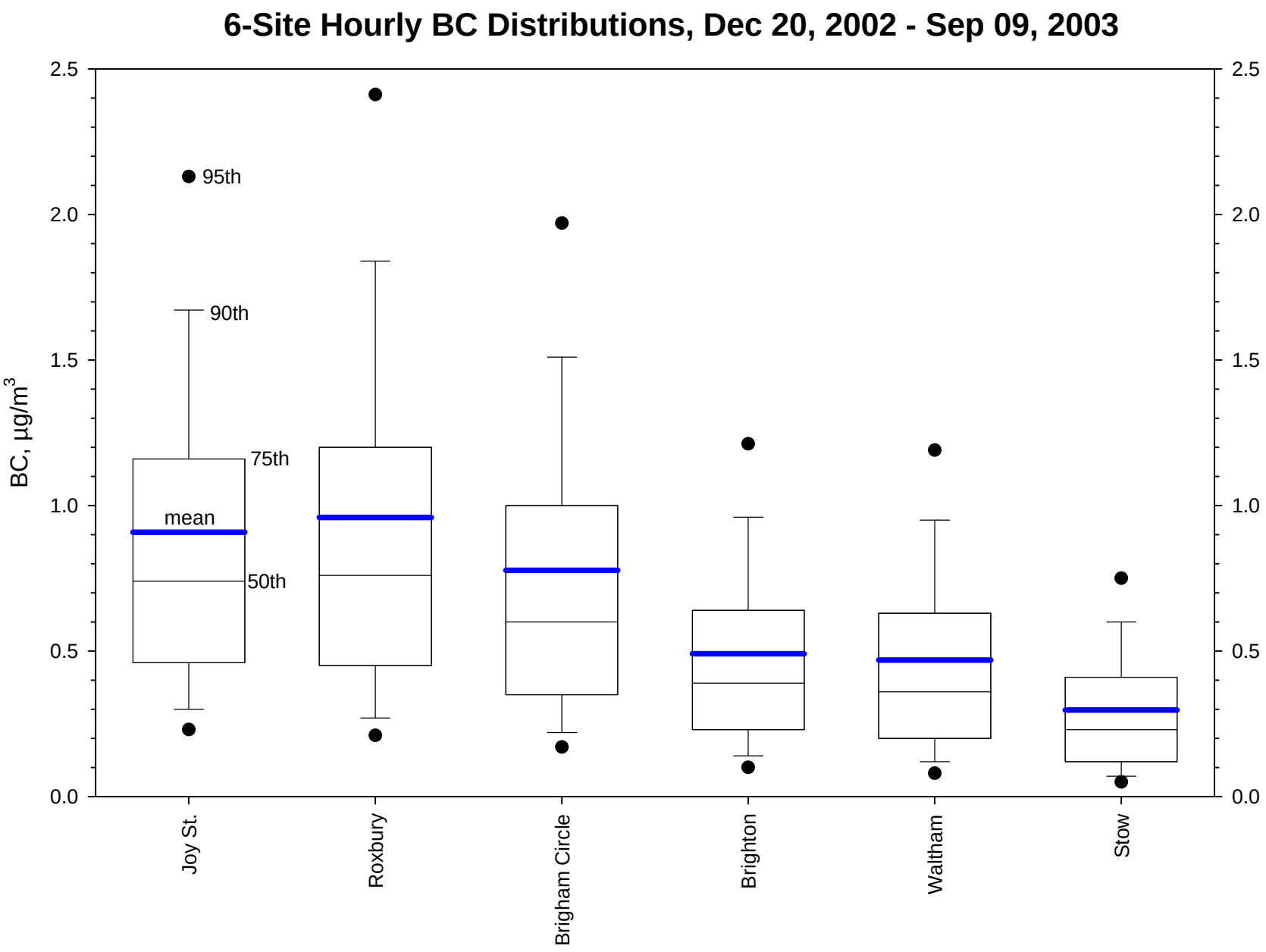
6-Site Hourly BC Distributions, Dec 20, 2002 - Sep 09, 2003
BC, µg/m3
2.5
2.0
1.5
1.0
0.5
0.0
95th
90th
75th
mean
50th
Joy St.
Roxbury
Brigham Circle
Brighton
Waltham
Stow

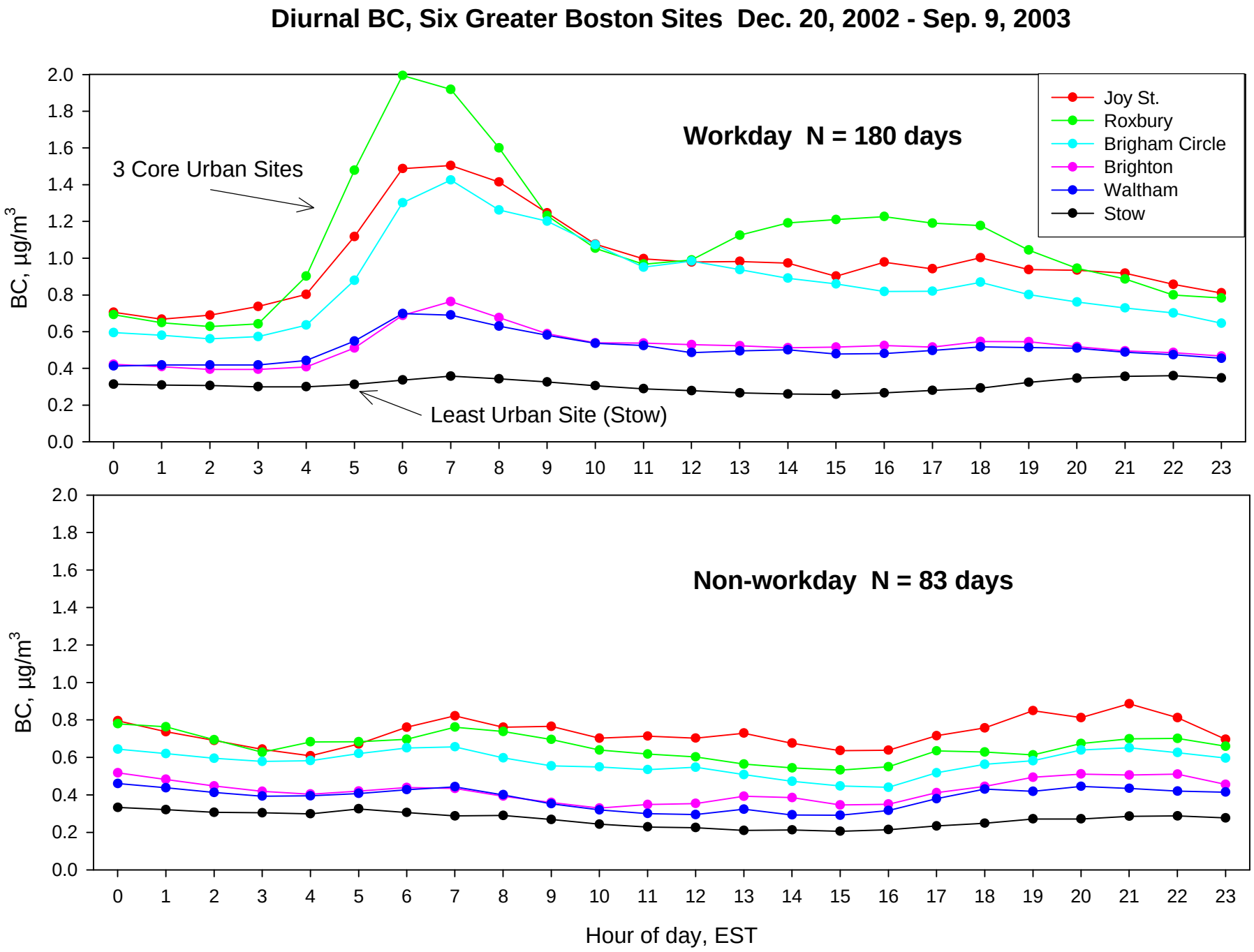
Diurnal BC, Six Greater Boston Sites Dec. 20, 2002 - Sep. 9, 2003
Workday N = 180 days
3 Core Urban Sites
Least Urban Site (Stow)
Joy St.
Roxbury
Brigham Circle
Brighton
Waltham
Stow
Non-workday N = 83 days
BC, µg/m3
Hour of day, EST

Note: This seasonal comparison is not valid due to a recently recognized strong seasonal bias in Aethalometer BC response

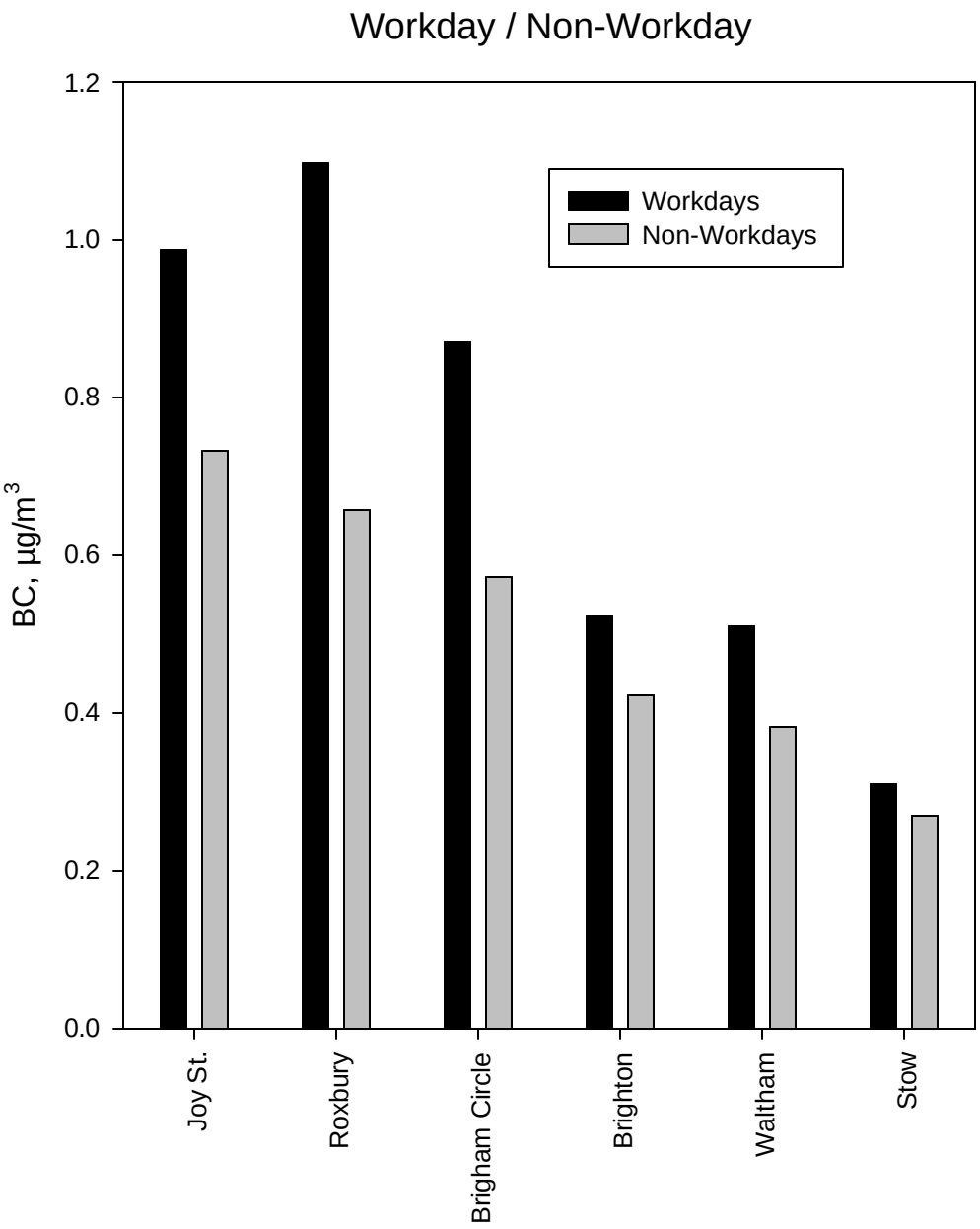

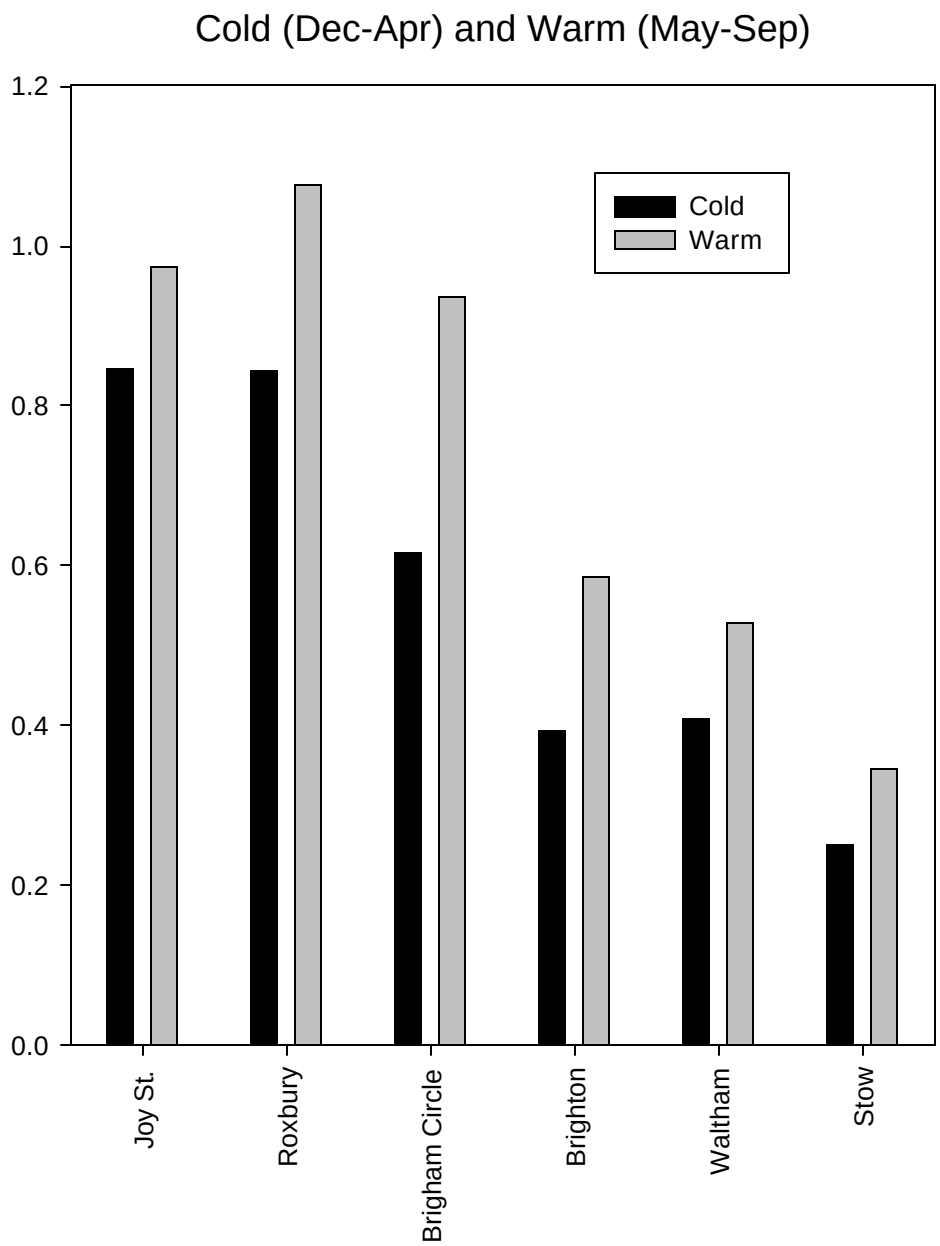

"Neighborhood Scale" study: Summer 2003, for 2 months. 10 of 12 sites are in Boston; 9 are within a radius of 2.5 km; siting is representative of neighborhood scale (not hotspot/microscale) exposure. This table shows distance from the State House (Beacon Hill).

Site Locations	Km	Site Description
Joy St.	0.0	Urban Residential/Commercial. (Beacon Hill, near State House)
Pinckney St.	0.3	Urban Residential (Beacon Hill)
North End	1.1	Urban Residential/Commercial (near the I-93 Expressway)
South St.	1.0	Urban Commercial (near South Station bus and train terminals)
Hereford St.	1.9	Urban Residential (Back Bay)
Albany St.	2.4	Urban Commercial (BU School of Public Health)
South Boston	2.9	Urban Residential
Roxbury	3.5	Urban Residential/Commercial
Brigham Circle	4.0	Urban Residential/Commercial
Brighton	7.0	Semi-Urban Residential

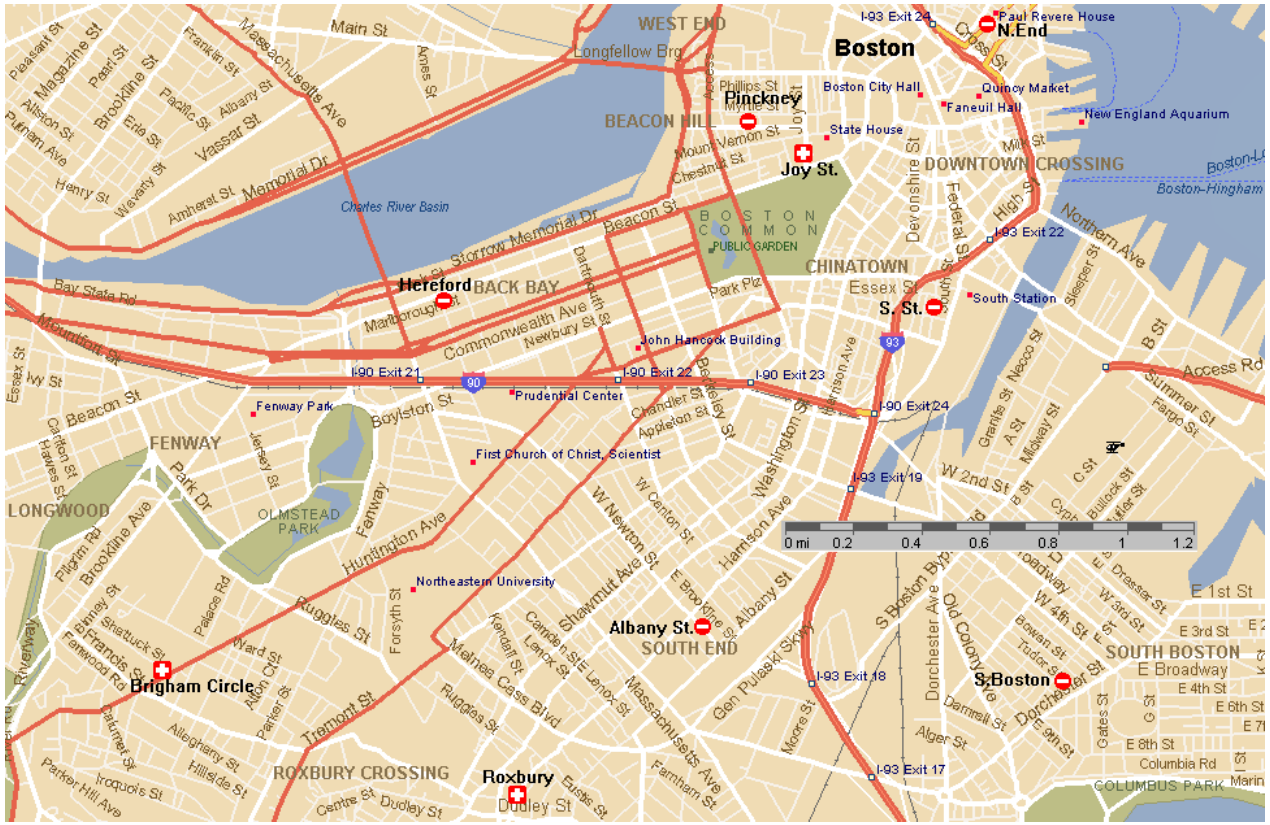

Figure: Summer 2003 1-hour Boston BC frequency distributions

This figure shows the distributions for all 12 BC monitoring sites, limited to days where all sites had data. Approximately 20 days are excluded due to two different sites that each had a 10-day period of missing data.

Mean BC for 8 of the 9 Downtown Boston sites during this study period was within 20% of 1.0 $\mu g/m^3$, suggesting that with few exceptions, gradients for mean BC at neighborhood scale oriented sites in Boston are not substantial. The observed variation across sites could be influenced by variability in monitor siting, mobile source strength gradients, and microscale meteorology. Further data analyses will quantify the significance of these spatial BC concentration gradients.

The exception was the North End, with mean BC of 1.55 $\mu g/m^3$, which might be due to proximity to the Expressway (southbound still above ground) and Callahan tunnel entrance, as well as Big Dig construction activity. This site is on the top of a 4-story building, 100 meters from the tunnel entrance and 200 meters from the southbound lane of the Expressway.

This question will eventually be answered, since this site is a permanent MA-DEP BC monitor; if post-Big Dig BC levels decline relative to the other two long-term BC sites in Boston (Roxbury and Brigham Circle) then it is likely that the local sources noted above were driving the observed elevated levels.

Note that the highest and lowest BC means for these 9 sites (North End and Pinckney St. on Beacon Hill) are only 1.3 km (0.8 miles) apart, with a ratio of 2.0.

Figure: Joy St., Pinckney St. and Roxbury, April - August 2003

This box plot of frequency distributions examines in more detail (more sample days and thus a more stable relationship) the differences between the two sites on Beacon Hill (0.3 km apart) and Roxbury. One question raised by the pilot work last winter (and the rationale for the Pinckney St. site) was "If Joy St. is similar to Roxbury BC on average, what's the cause and scale of the elevated BC on Beacon Hill?". Pinckney St. is about as far removed as possible from through-traffic streets on Beacon Hill.

For this longer period, mean BC for Joy, Pinckney, and Roxbury are 0.94, 0.74, and 1.04 $\mu g/m^3$ respectively. The ratio of Pinckney to Joy St. is 0.79 for both the mean and the 95th percentile values. This suggests that part of Joy St.'s BC is traffic that is very local (micro-scale), but gradients on this scale are not substantial.

Figures: BC vs. Population Density, Winter 9-site and Summer Boston 10-site Regressions

The first plot shows data from the winter 2003 pilot study that suggested that population density might be a useful surrogate for average BC concentrations over a large spatial scale and with a large range of BC concentrations (R^2 of 0.81 if Brighton removed). The same analysis was performed on the 10 Boston sites for the summer neighborhood scale study. The second plot shows that for a smaller spatial scale with smaller dynamic range, population density can not be used to predict BC - the slope is actually reversed with higher BC associated with lower population density ($R^2 = 0.52$). This might be explained by core commercial and transit corridor areas such as the South St. site near South Station having lower population density but high traffic activity.

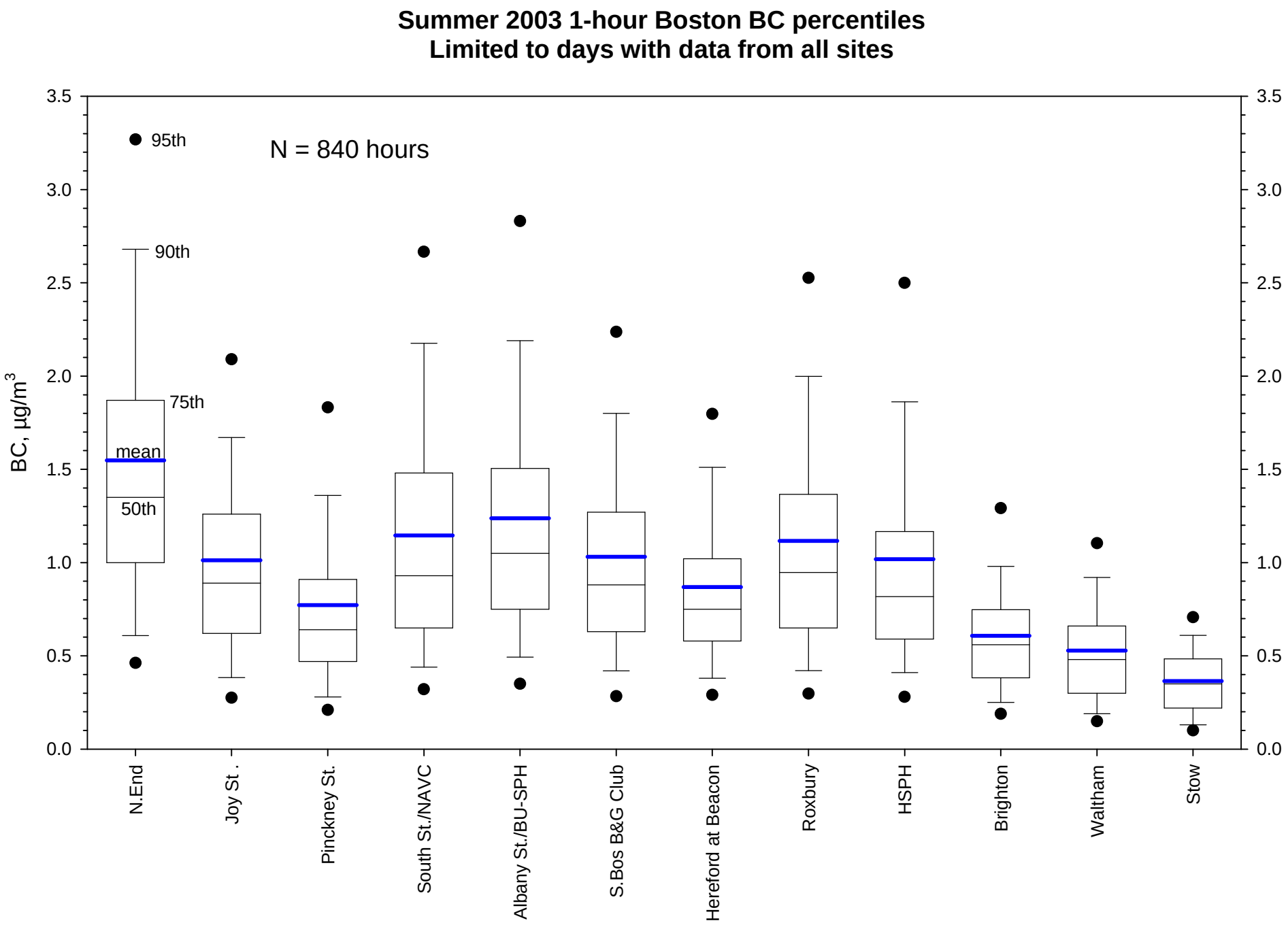
Summer 2003 1-hour Boston BC percentiles
Limited to days with data from all sites
N = 840 hours
95th
90th
75th
mean
50th
BC, µg/m3
3.5
3.0
2.5
2.0
1.5
1.0
0.5
0.0
N.End
Joy St .
Pinckney St.
South St./NAVC
Albany St./BU-SPH
S.Bos B&G Club
Hereford at Beacon
Roxbury
HSPH
Brighton
Waltham
Stow

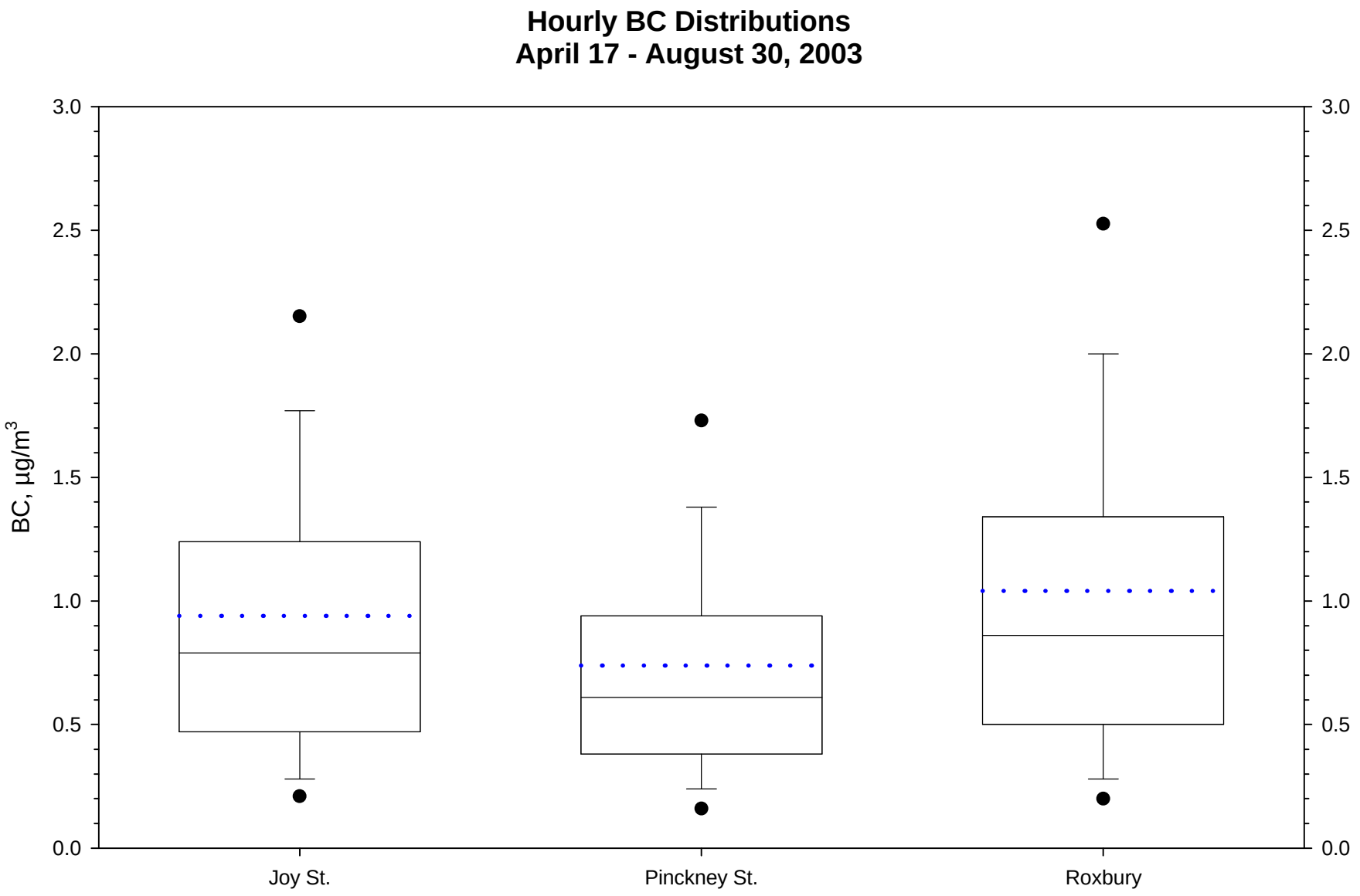
Hourly BC Distributions
April 17 - August 30, 2003
BC, µg/m3
3.0
2.5
2.0
1.5
1.0
0.5
0.0
Joy St.
Pinckney St.
Roxbury

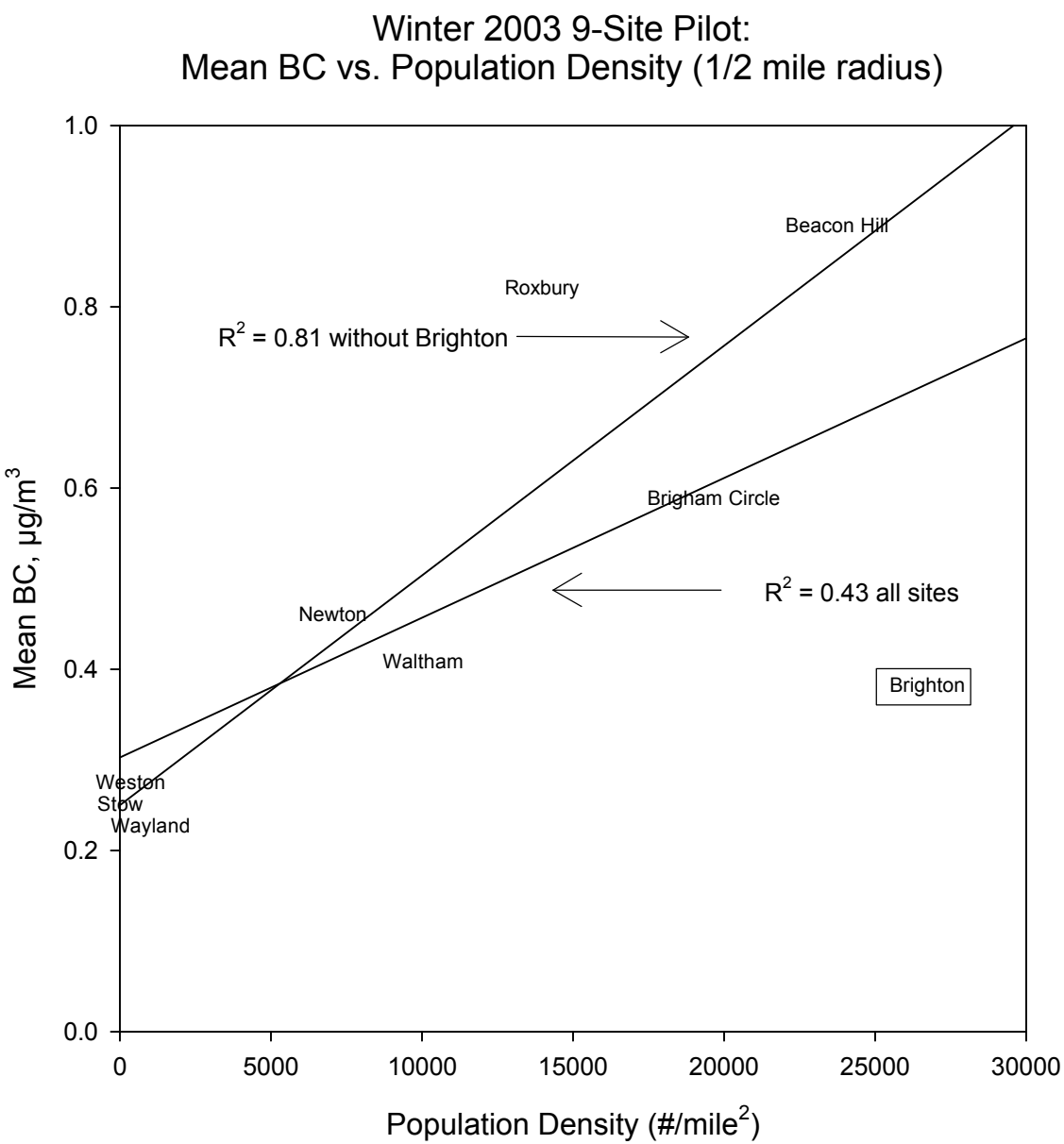
Winter 2003 9-Site Pilot:
Mean BC vs. Population Density (1/2 mile radius)
Mean BC, µg/m3
Population Density (#/mile2)
1.0
0.8
0.6
0.4
0.2
0.0
0
5000
10000
15000
20000
25000
30000
Beacon Hill
Roxbury
R2 = 0.81 without Brighton
Brigham Circle
R2 = 0.43 all sites
Newton
Waltham
Brighton
Weston
Stow
Wayland

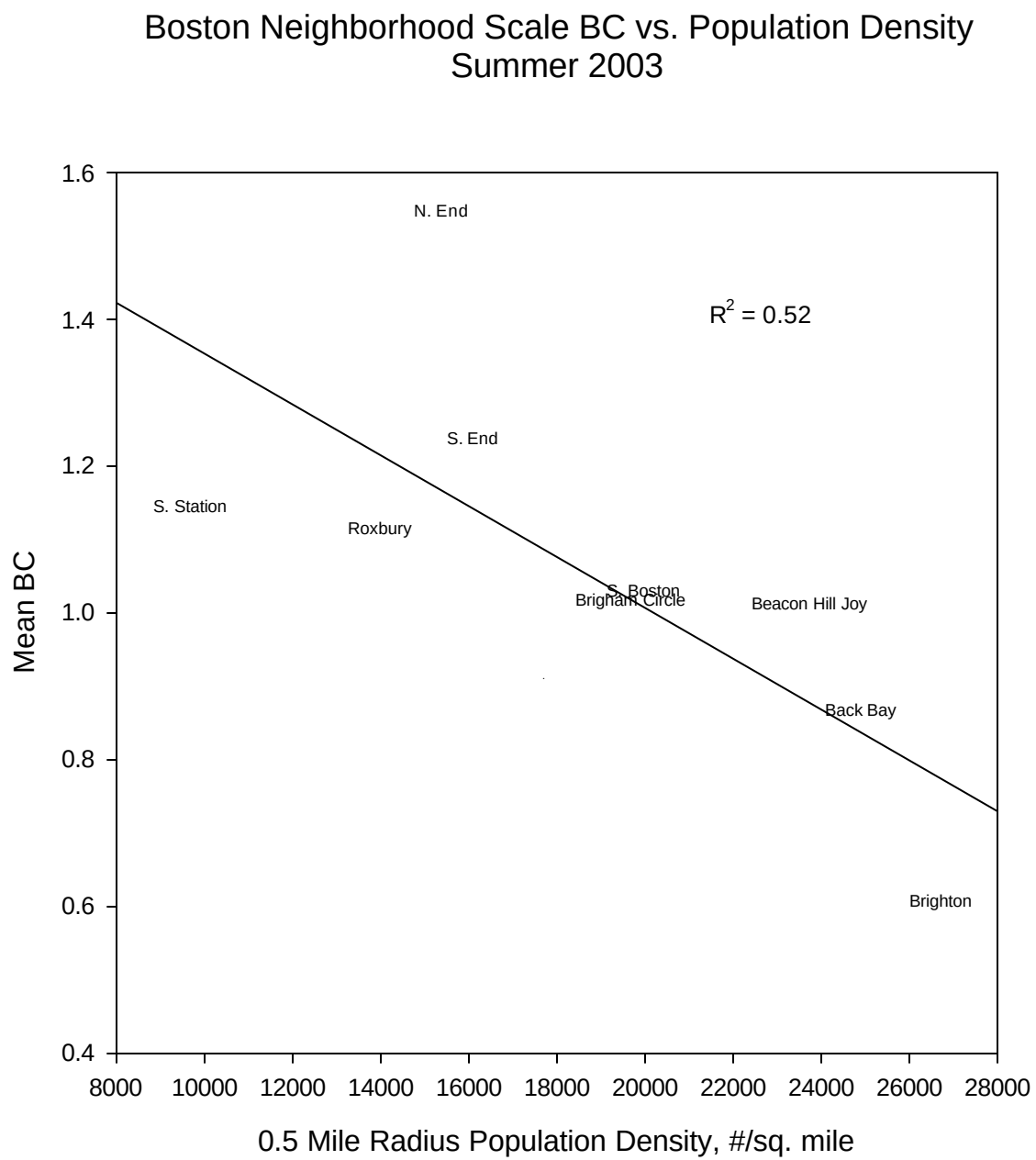
Boston Neighborhood Scale BC vs. Population Density
Summer 2003
Mean BC
0.5 Mile Radius Population Density, #/sq. mile
R^2 = 0.52
N. End
S. End
S. Station
Roxbury
S. Boston
Brigham Circle
Beacon Hill Joy
Back Bay
Brighton
1.6
1.4
1.2
1.0
0.8
0.6
0.4
8000
10000
12000
14000
16000
18000
20000
22000
24000
26000
28000

Figures: Two time series "case study" examples

These two time series plots show examples of short term patterns and gradients of hourly BC across the Boston area. The first, July 13-15, is the 9 core Boston sites and the Stow background site. Tuesday July 15 was one of the dirtier days of the summer with several sites exceeding 4 $\mu g/m^3$ BC for several morning hours. The ratio of these sites to the Stow background site for this peak period is approximately 10, similar to that observed during the winter pilot project.

The second time series is a 5-day period covering August 6 to 11. All 12 sites are included in this plot. Thursday the 7th shows a distinct evening rush-hour peak, not a common feature. The very high peak in South Boston on Friday the 8th at hour 07 EST is substantially higher than other sites, although the other urban sites peak at the same hour. This site could have been influenced by local marine diesel sources, since major Boston Harbor piers are about 1 mile away to the NNE. Winds at Logan Airport were NNE to NE at a few miles/hour during this time. That peak hour was influenced by two contiguous very high 5-minute BC values (22 and 13 $\mu g/m^3$); without those values the mean for this hour is 6 $\mu g/m^3$, more similar to the other sites.

Both of these time-series plots show a very distinct "clean Sunday and dirty work-day" effect.

Figure and Table: August 6-11 case study: hourly scatter plots and correlation matrix

Scatter plots for hourly BC for six site-pairs and a table for all site pairs during this August 5-day period are shown as examples of the short-term relationships across different spatial scales. There is a wide range of correlation, from reasonably high (R^2 = 0.85 for the two Beacon Hill sites) to very low (0.08 for Stow and South St.).

Distance between sites is not always a predictor of good predictor of how well they are correlated. Joy St. and Roxbury (3.5 km apart) have an R^2 of 0.72, while Hereford St. and South St. (2.4 km apart) R^2 is 0.28 for the same time period. Some sites, such as South St. and especially Hereford St. are not well correlated with other urban sites. Others (Roxbury, Joy St., Albany St.) seem to be reasonably well correlated with most urban sites; these three sites also have means that are very similar (within a few percent).

The scatter plots show some interesting patterns for some site-pairs. The two downtown Boston sites with the lowest mean BC (Hereford St. and Pinckney St.) are well correlated when levels are below about 1 $\mu g/m^3$ BC. But when levels are high at either site, they tend to be decoupled temporally. South Boston and South St. are clearly influenced by different sources. North End and Stow, the highest and lowest sites in the study, are pretty well decoupled at this time scale; note that here the axes are not scaled the same; the bottom line is the 1:1 line. Essentially all hours at North End are at or above the Stow BC levels.

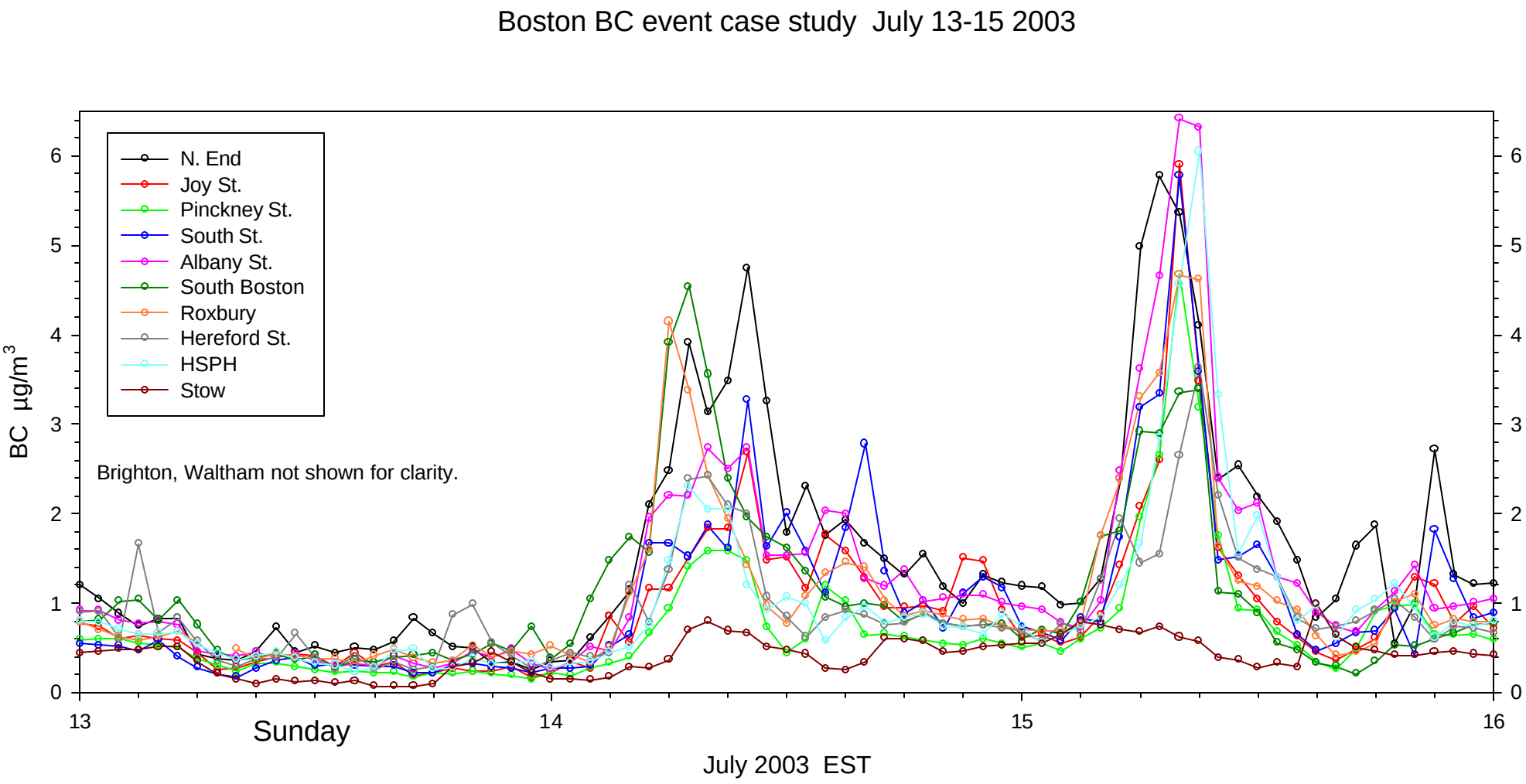
Boston BC event case study July 13-15 2003
N. End
Joy St.
Pinckney St.
South St.
Albany St.
South Boston
Roxbury
Hereford St.
HSPH
Stow
Brighton, Waltham not shown for clarity.
BC µg/m3
0
1
2
3
4
5
6
13
14
15
16
Sunday
July 2003 EST

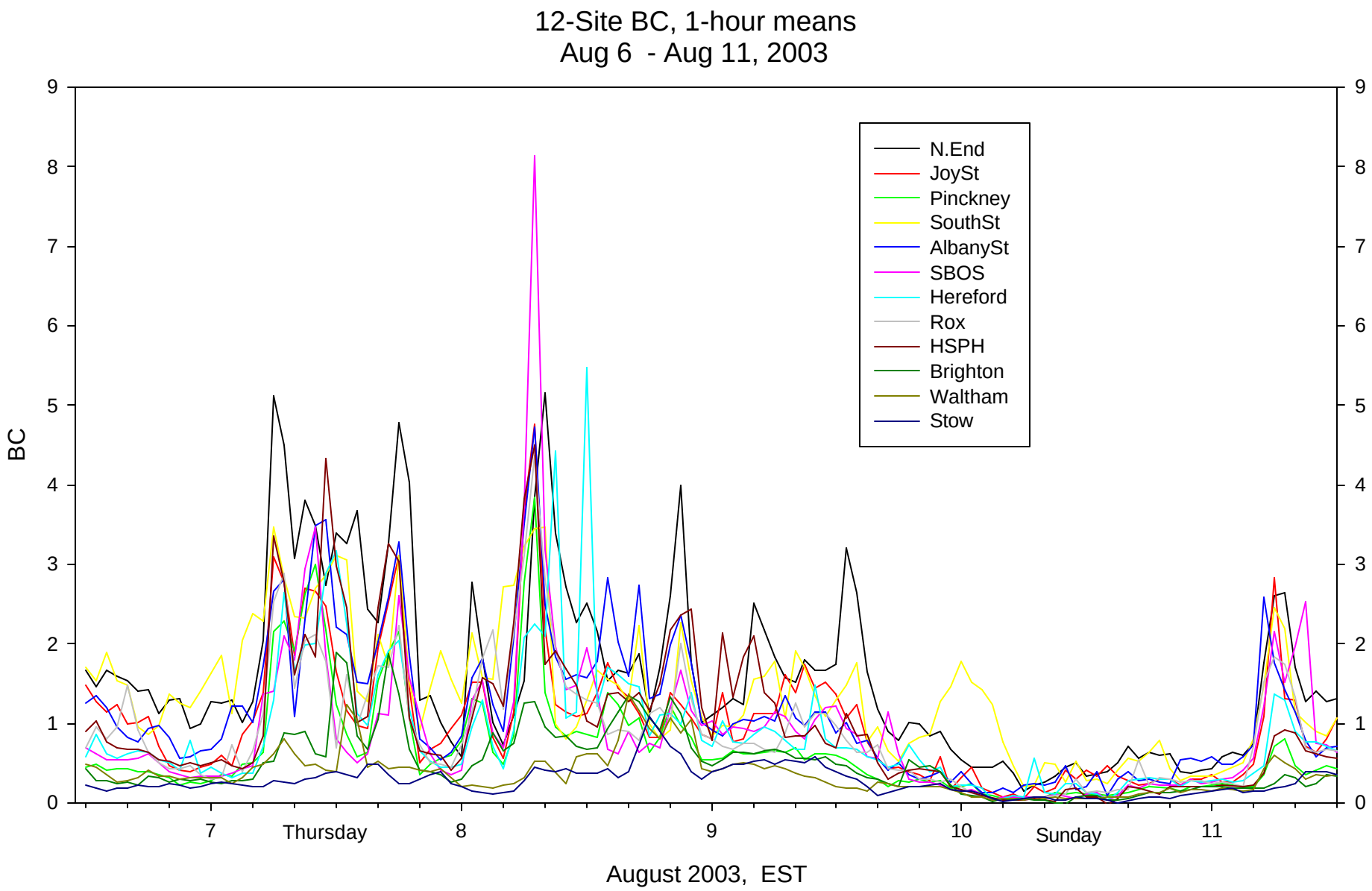
12-Site BC, 1-hour means
Aug 6 - Aug 11, 2003
BC
0
1
2
3
4
5
6
7
8
9
7
Thursday
8
9
10
Sunday
11
August 2003, EST
N.End
JoySt
Pinckney
SouthSt
AlbanySt
SBOS
Hereford
Rox
HSPH
Brighton
Waltham
Stow

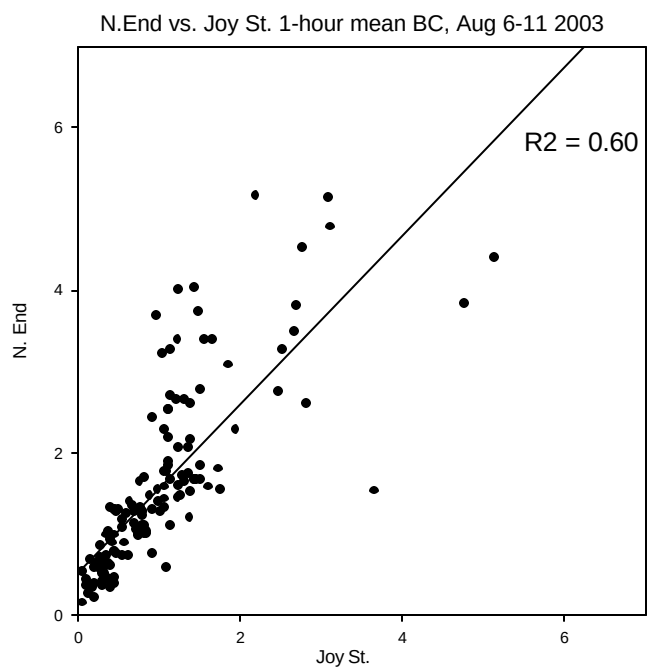
N.End vs. Joy St. 1-hour mean BC, Aug 6-11 2003
R2 = 0.60
N. End
Joy St.

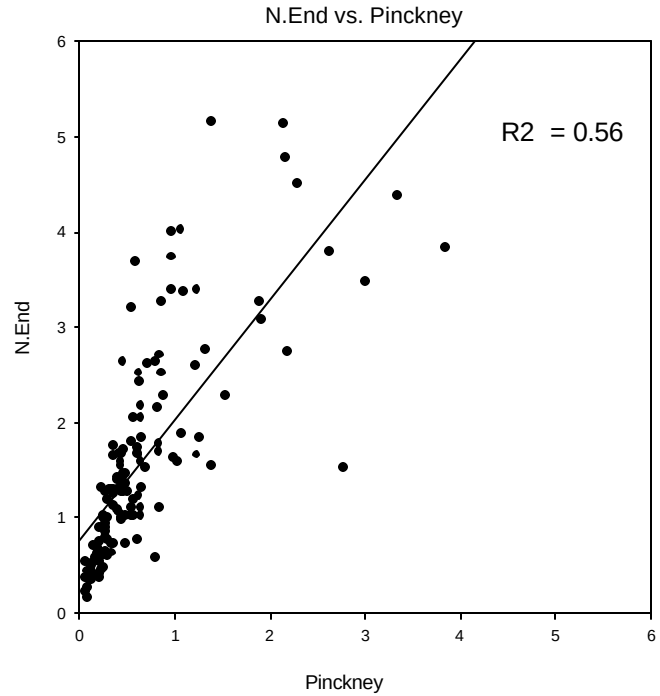
N.End vs. Pinckney
R2 = 0.56
N.End
Pinckney

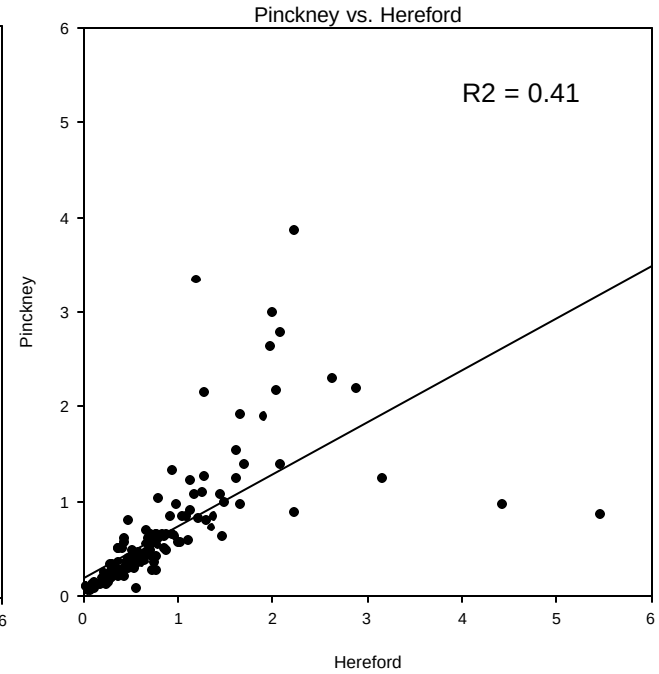
Pinckney vs. Hereford
R2 = 0.41
Pinckney
Hereford

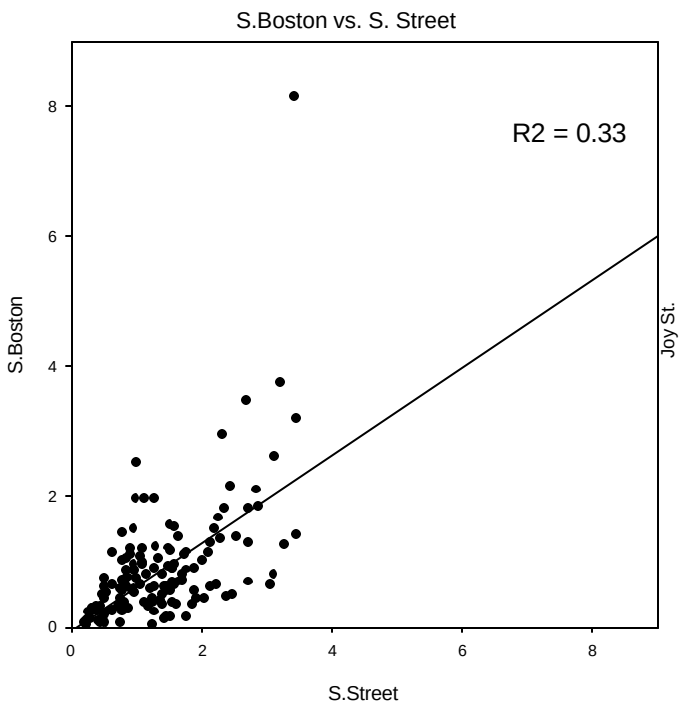
S.Boston vs. S. Street
R2 = 0.33
S.Boston
S.Street

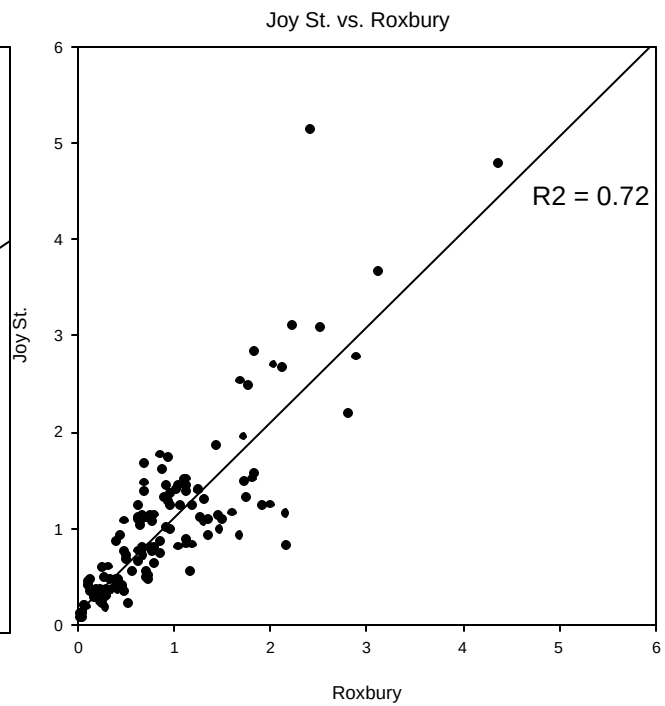
Joy St. vs. Roxbury
R2 = 0.72
Joy St.
Roxbury

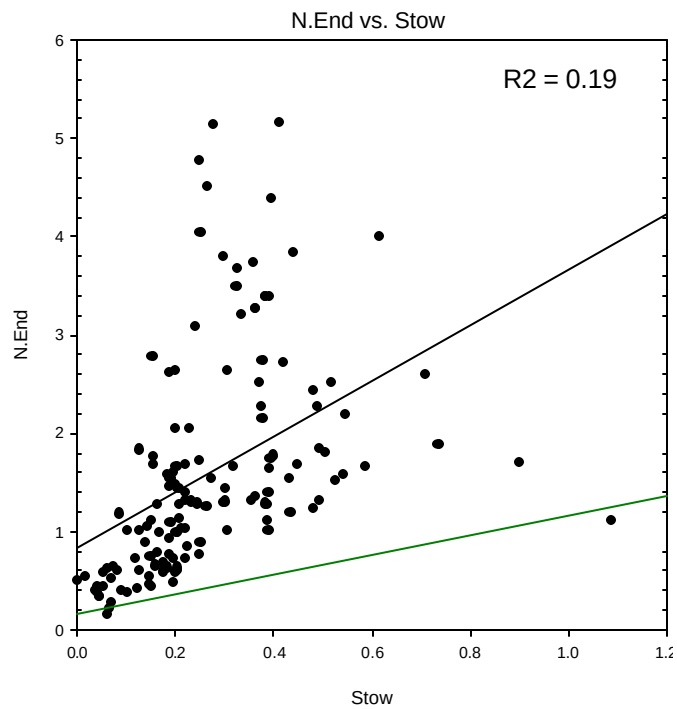
N.End vs. Stow
R2 = 0.19
N.End
Stow

1-hour R^2 Matrix, August 6-11 2003

R2 .70 or higher R2 .50 to .69

	N.End	Joy St.	Pinck-ney St.	S.St	Albany St.	S.Bos.	Hereford St.	Rox	BrigCir	Brighton	Waltham	Stow
N.End	x	.60	.56	.54	.63	.40	.46	.59	.51	.46	.30	.19
Joy	.60	x	.85	.54	.79	.62	.36	.72	.59	.38	.18	.14
Pinckney	.56	.85	x	.51	.79	.64	.41	.69	.67	.44	.19	.13
S. St.	.54	.54	.51	x	.57	.33	.28	.53	.48	.35	.21	.08
Albany	.63	.79	.79	.57	x	.55	.46	.73	.66	.51	.31	.19
S.Bos	.40	.62	.64	.33	.55	x	.34	.70	.48	.24	.09	.10
Hereford	.46	.36	.41	.28	.46	.34	x	.41	.48	.45	.27	.17
Rox	.59	.72	.69	.53	.73	.70	.41	x	.63	.40	.20	.14
Brig.Cir	.51	.59	.67	.48	.66	.48	.48	.63	x	.59	.22	.22
Brighton	.46	.38	.44	.35	.51	.24	.45	.40	.59	x	.44	.39
Waltham	.30	.18	.19	.21	.31	.09	.27	.20	.22	.44	x	.38
Stow	.19	.14	.13	.08	.19	.10	.17	.14	.22	.39	.38	x

Conclusions and Preliminary Findings

Substantial gradients in BC exist over a 35km scale

Mean BC varies by a factor of 3.5 from downtown Boston to the regional background site

==> Much larger factor for sub-daily event periods: 10x or more

These data indicate that the neighborhood spatial scale of "urban excess" PM2.5 for Boston is limited to approximately 10 miles from downtown. This is important from both an air toxics exposure and control strategy perspective.

Core urban area: BC levels at all neighborhood-scale sites are elevated relative to the background site, but urban gradients are not distinct for most of these sites.

Short-term (1-hour) correlations across these sites range from very good to poor; some urban sites are much better indicators of the general downtown area than others.

BC appears to be a reasonable indicator of local "tailpipe" aerosol, not highly specific to diesel or on-road vs. off-road sources. Winter space heating and woodsmoke do not appear to be significant interferences in the urban area.

Limitations of this preliminary report

This study does not assess worst-case "hotspot" exposure scenarios in either urban or non-urban settings, since it is based on neighborhood scale, not mid-scale or micro-scale ("roadway") monitor siting. As such, these findings should not be construed tp suggest that meaningful exposures do not occur outside of urban areas. Potential instrument bias has not yet been removed that could effect gradient assessments. ANOVA analysis to assess the significance of gradients has not yet been performed, and may result in modification of these preliminary conclusions.

Limitations of this study include semi-randomized monitor siting and monitor-to-monitor bias that are not accounted for at this time. Meteorological conditions that may influence observed BC concentrations at any given site have also not been taken into account in this preliminary analysis. The statistical significance of observed gradients will be characterized using ANOVA analyses once the final year-long data set is available.

Appendix C: Change in Reported BC Without and With Spot Loading Correction for Two Sites in 2003-2004 (Scatter and time-series plots for HSPH and North End).

Appendix C.

Change in reported BC without and with spot loading correction for two sites in 2003-2004.

The Aethalometer BC has an artifact that results in under-reporting of BC concentrations that varies over time on the scale of hours to seasons. This artifact was examined for the HSPH and N.End sites during 2003 and 2004 using both scatter and time-series plots. Figures 1 and 2 are regressions of correct vs. original (raw) 1-hour BC data for these two sites. There is a bias of approximately 20 percent at both sites, with errors approaching a factor of two for some hours.

Figure 1. HSPH Corrected vs. Raw 1-hour BC, 2003

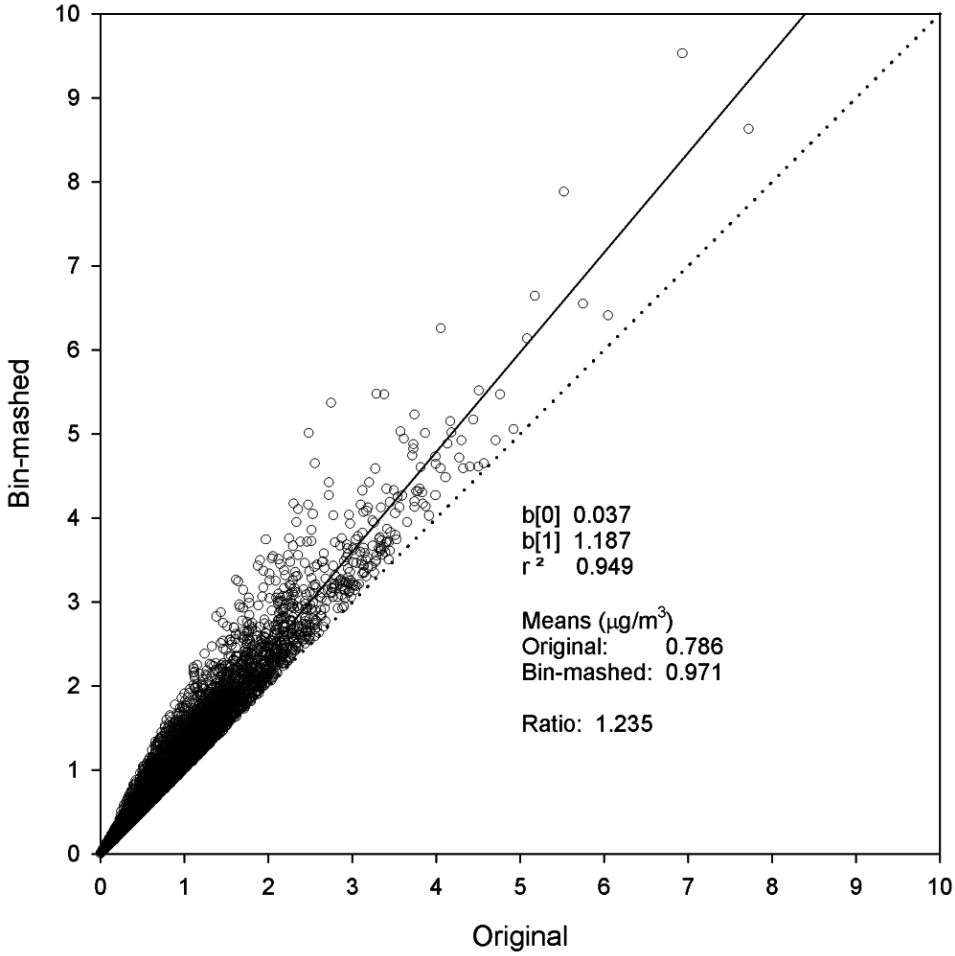

Figure 2. North End Corrected vs. Raw 1-hour BC, 2003-2004

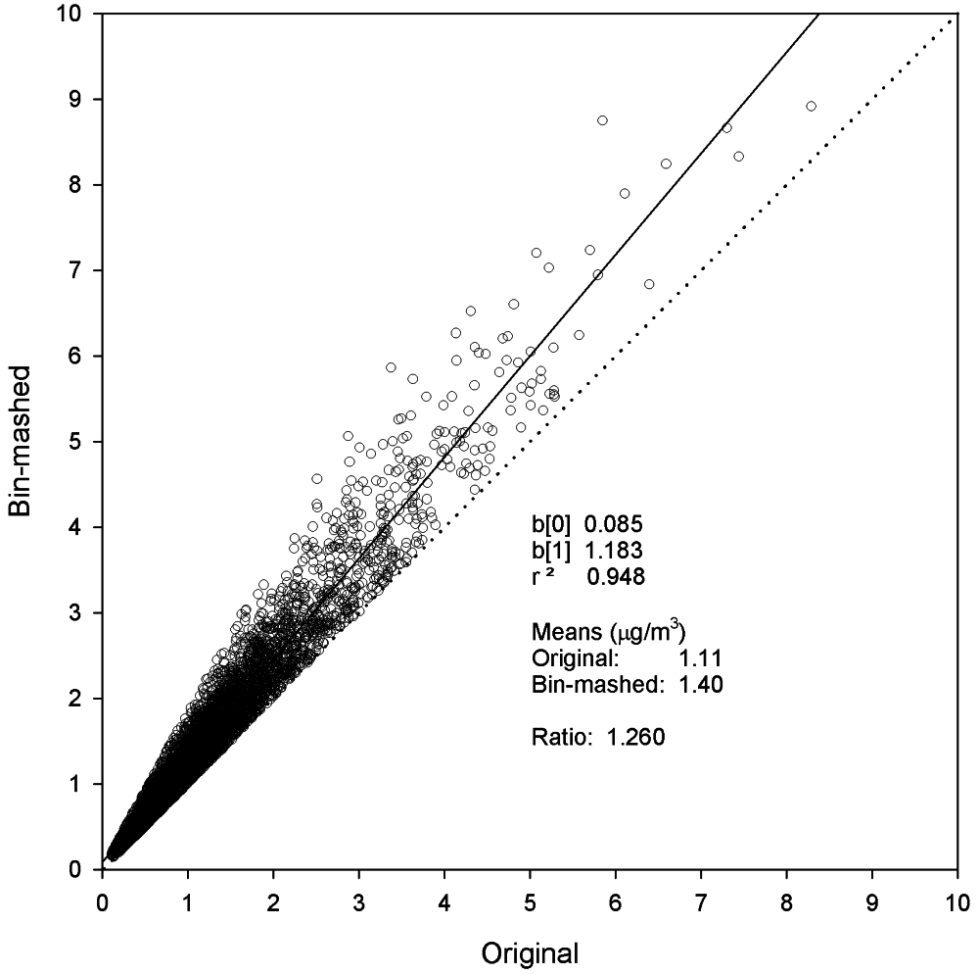

Figures 3 and 4 show this artifact error as a function of time over the same periods. The red line is the ratio of hourly corrected to original BC concentrations, and changes both at hourly time-scales (from aerosol loading during measurements on a single spot on the sample tape) and seasonal scales (from changes in the aerosol composition).

Figure 4. HSPH 1-hour BC and Ratio of Corrected to Original BC Concentration

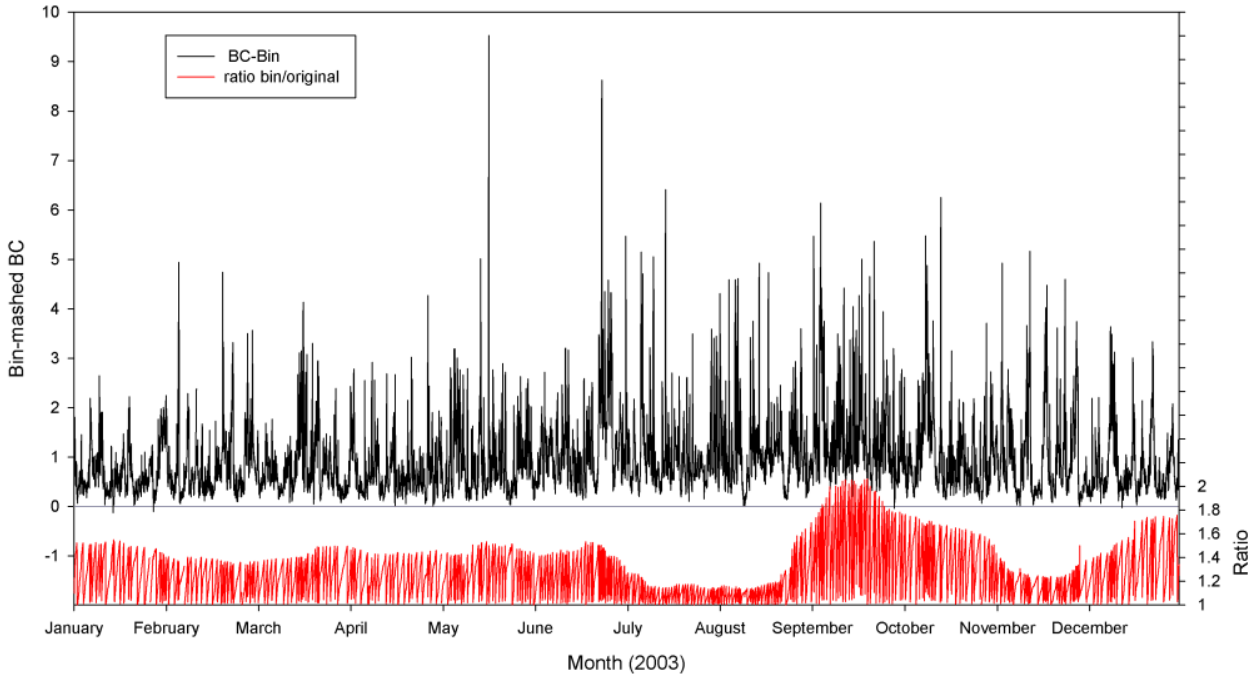

Figure 3. N.End 1-hour BC and Ratio of Corrected to Original BC Concentration

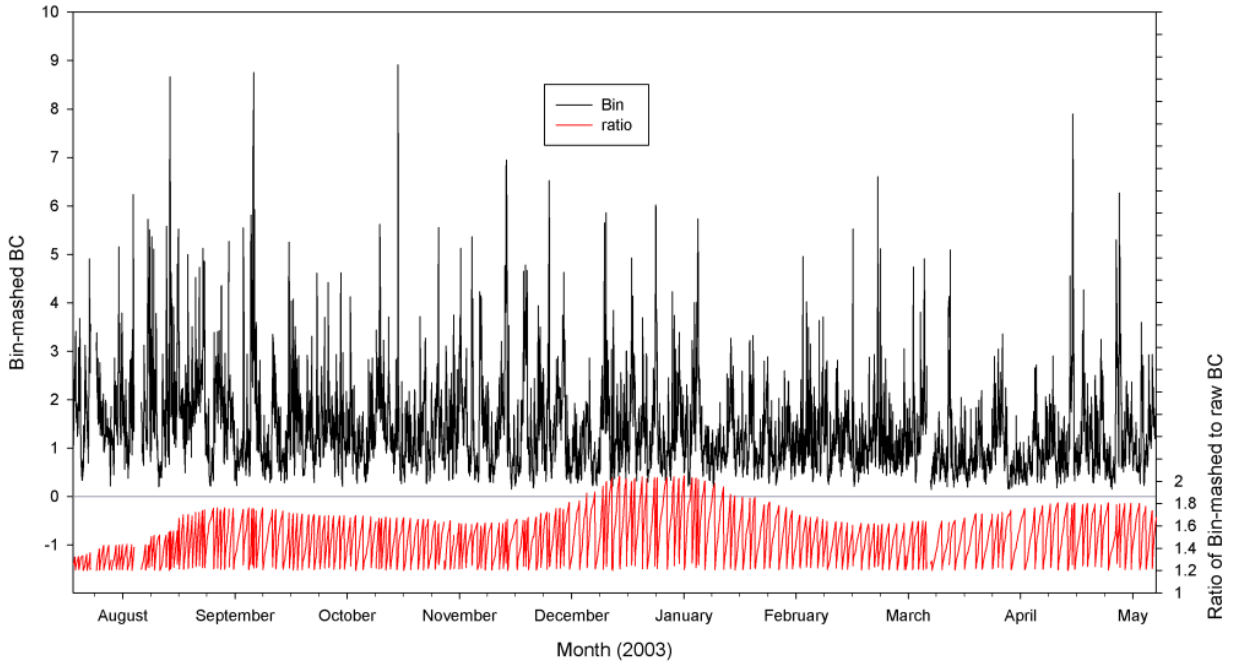

Appendix D: Sonoma Technologies' September 30, 2011 Draft Memo to U.S. Environmental Protection Agency on the Aethalometer Spot Loading Artifact, Including Examples of Difference Between Raw and Bin-corrected BC Data, and Trends Analysis of the HSPH Countway BC Data.

Appendix D.

Sonoma Technology, Inc.
Air Quality Research and Innovative Solutions

DRAFT Technical Memorandum

September 30, 2011 STI-910212-4217

To: Dave Shelow, Neil Frank, EPA OAQPS

From: Steve Brown, Jay Turner (Washington University in St. Louis), George Allen (NESCAUM)

Re: Development and implementation of an updated validation tool for Aethalometer measurements: data acquisition and processing

This draft technical memorandum is part of the deliverable for AIRNow Work Assignment (WA) 2-12, Task 6. It includes key findings on differences between raw and processed (adjusted) Aethalometer data and a summary of the raw data acquired and processed as part of this project. Raw Aethalometer data are biased by optical saturation effects. In an effort to understand these effects and to correct them, the Washington University Air Quality Laboratory (WUAQL) Aethalometer Data Masher was modified as part of this WA and used to process raw data from sites throughout the U.S. Along with the Data Masher software and its user's guide, which provides the technical details of the correction algorithms in the Data Masher, this technical memorandum summarizes the current correction methodology and data changes as a result of this correction.

Key Findings

Key findings from this work include the following:

- There are two major factors that influence the bias caused by the optical saturation (particle loading) effect. First, the effect is influenced by aerosol composition with a highly scattering aerosol reducing the effect. At many locations, the aerosol composition exhibits strong seasonality and in general the adjustments will be higher in locations and during periods with low sulfate, such as the western U.S. and in wintertime.. Second, the bias increases as the particle deposit accumulates on the Aethalometer filter tape. Thus, changes in the maximum attenuation (ATN) setting influence the extent of error. The maximum ATN is a user-controlled parameter; sometimes it is intentionally changed by the user while other times it is unintentionally changed (e.g., following instrument repair when the instrument is returned with default settings, or by turning on or off the ultra-violet (UVC) channel on a 2-channel instrument).
- For default maximum ATN settings, the magnitude of Data Masher adjustments to the Aethalometer black carbon (BC, measured at 880 nm) data are greater for 1-channel instruments (BC only) than for 2-channel instruments (BC and UVC). The majority of data sets collected in this project from state and local air monitoring agencies are for

2-channel instruments. The adjustments to the UVC channel data are larger relative to the BC data.

- The algorithm implemented for this project applies smoothing over several tape advances ("spots"). While most analyses were performed using 30-spot smoothing, larger smoothing ranges may be necessary when the concentration adjustment is small (e.g., low maximum ATN and small optical saturation parameters).
- The algorithm implemented for this project (the "bin" method, described below) typically produces results similar to the legacy "gap" method. However, the bin method has the advantage of providing quantitative metrics of the quality of the adjustments. Also, the time series of adjustments sometimes significantly differs between the two methods when data are very noisy (real noise or instrument noise). In such cases, there is anecdotal evidence that the bin method outperforms the gap method. Data from older Aethalometers (AE16 or AE21) tend to be noisier than the current model (AE22).

Introduction

Filter-based optical methods for estimating ambient particulate matter BC concentrations suffer from a mass loading effect whereby the instrument response decreases with increased BC loading. One such instrument, the Aethalometer, continuously collects particles onto a filter and measures the wavelength-dependent transmission of light through the deposit. The mass loading effect is most commonly observed as a step discontinuity in the reported concentration when advancing the Aethalometer filter tape to deposit aerosol onto a clean filter spot instead of a particle-laden filter spot. **Figure 1** shows an example of this effect using collocated Aethalometers. Initially there is good agreement between the reported BC values, but after the tape advances for the co-sited unit, it reports concentrations that are systemically higher than the primary unit. These higher values after the tape advance are actually closer to the true BC concentration, while the data prior to the tape advance are biased low. Later in the time series, the tape advances for the primary unit and subsequent data again exhibit good agreement. The mass loading effect is not governed solely by deposited absorbing (e.g., soot) aerosol. It is also influenced by the abundance of internally- or externally-mixed scattering aerosol (e.g., sulfate) in the ambient air that co-deposits with the absorbing black carbon particles.

Figure 1. Four-hour time series of 5-minute black carbon concentration data for collocated Aethalometers, East St. Louis. Each instrument exhibited one tape advance during this period. The collocated unit data stream was adjusted for instrument-to-instrument bias.

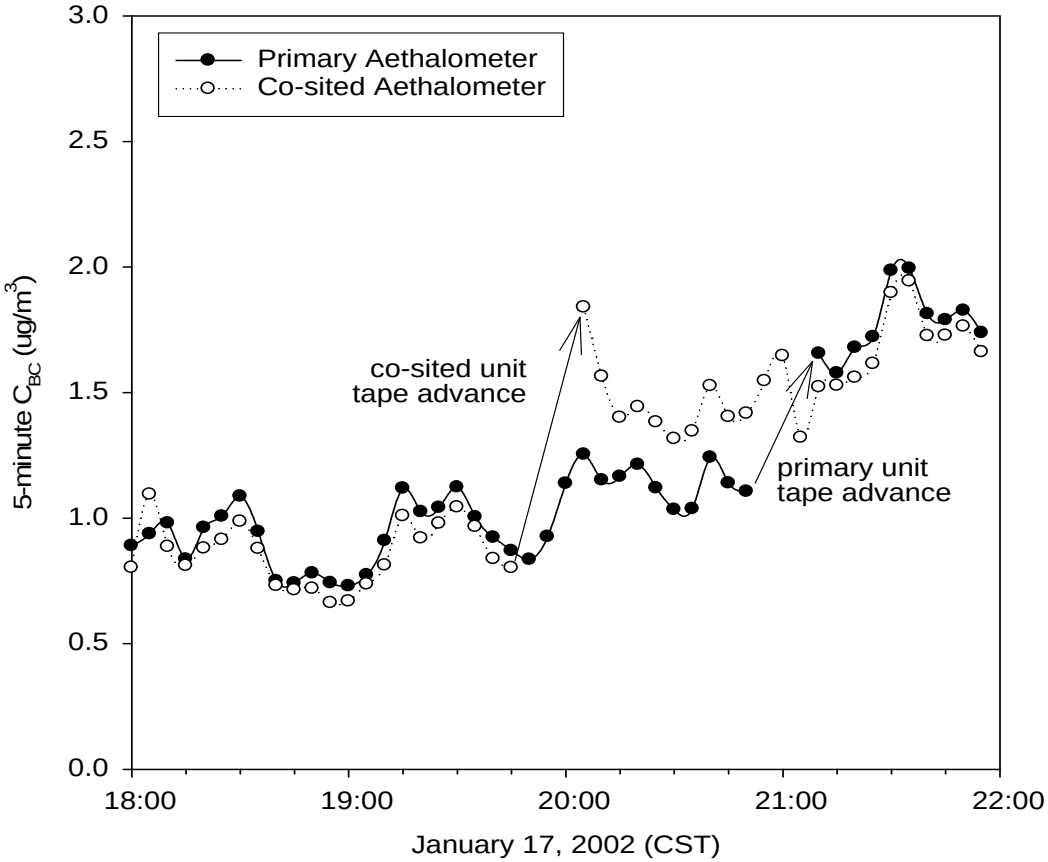

Several approaches have been proposed to adjust the data for these artifacts. For the Aethalometer, one approach uses the difference in reported concentration before and after a filter tape advance to estimate the artifact. Another approach is to perform a regression of the reported concentration on the attenuation using all of the data over a specified time period. Both of these approaches assume the true BC concentration is not changing over the time period of interest (across the tape advance for the first approach, for the entire time period used for the regression in the second approach). Thus, additional temporal aggregation of the data or smoothing of the artifact estimates is needed to dampen the effect of this limiting assumption. As part of this project, the Aethalometer data post-processing program developed at Washington University at St. Louis (the WUAQL Data Masher) that is publicly available to the air quality measurement community has been revised to include an algorithm for adjusting the raw data using both of these approaches. The gap-based algorithm was implemented for prior projects whereas this project focused on implementing a regression-based algorithm that uses all of the data. This latter algorithm has been implemented in the current version of the program and was used throughout this project.

Methods

The loading effect leads to the Aethalometer-reported concentration decreasing with increased ATN (a measure of the light absorption by the deposited aerosol) even when the measured aerosol has a constant BC concentration. The goal of the algorithm is to correct for the ATN effect so that, on average, concentration is independent of ATN. The loading effect is assumed to follow the form:

$$BC_t = BC_r \left(1 + k \cdot ATN\right) \tag{1}$$

where BC_t is the true (adjusted) concentration, BC_r is the Aethalometer-reported concentration, and k is an empirical parameter that, in this algorithm, is obtained from the regression of concentration on ATN. The parameter k is termed the "optical saturation parameter" and is zero for no adjustment to the raw data. For example, at ATN = 50, a k-value of 0.010 would adjust the BC concentration upward by 50%. The remainder of this section summarizes the methodology. More details are provided in the Data Masher User Guide.

Considerable effort was invested to develop a methodology that would stabilize the analysis across a range of data sets. Simply binning the data by ATN was insufficient because some high-concentration extreme values can have considerable influence on the regression. After testing several approaches, the following methodology was adopted. The first step is to bin the raw concentration data (typically collected on a time base of 5 minutes but sometimes 1 minute) by attenuation. The algorithm allows the user to specify either a fixed bin width (e.g., 5 ATN units) or an approximate number of bins to be equally distributed over the attenuation range observed for each channel (Aethalometers can have 1, 2, or 7 channels corresponding to the number of wavelengths for which absorption is measured). The default is a fixed bin width of 5 ATN units. Tape advances are followed by an instrument stabilization period with no data reported. The time duration of all data gaps are identified and the mode gap size (e.g., three consecutive 5-minute missing records) is used to flag the tape advances in the time series. If the second mode gap occurs at a frequency of at least 5% of the mode tape advance gap frequency, the user is given the option to also consider the second mode gap as tape advance events.

Data recorded between each tape advance are stratified into the ATN bins and the mean concentration is calculated for each bin. These concentration values are then normalized to the average concentration over all the bins. These steps ensure that the time series data between each tape advance is given similar weight in the regression. Next, these normalized, binned concentrations are aggregated over a user-specified number of tape advances w (default w = 30) and the median normalized value is calculated for each bin. Bin-specific median values are regressed on ATN to determine the empirical data adjustment parameter, k. **Figure 2** shows an example of the data used for the regression of normalized concentration on ATN (solid circles). Error bars denote the interquartile ranges about the median normalized concentrations. The open circles show the median normalized concentrations estimated from Equation (1) using the fitted k-value. Ideally these values should be tightly clustered around the horizontal line at

normalized concentration of unity (i.e., the ATN dependence of concentration has been removed); in this example they are biased high by less than 2%, which is a minimal bias.

Figure 2. Aethalometer BC concentration for April 2001 through March 2004 at East St. Louis, binned by ATN and normalized within each tape advance. Solid circles are the median normalized concentrations; error bars denote the interquartile ranges. Open circles are the estimated concentration values using Equation (1) and the regression-estimated *k*-value of 0.0025.

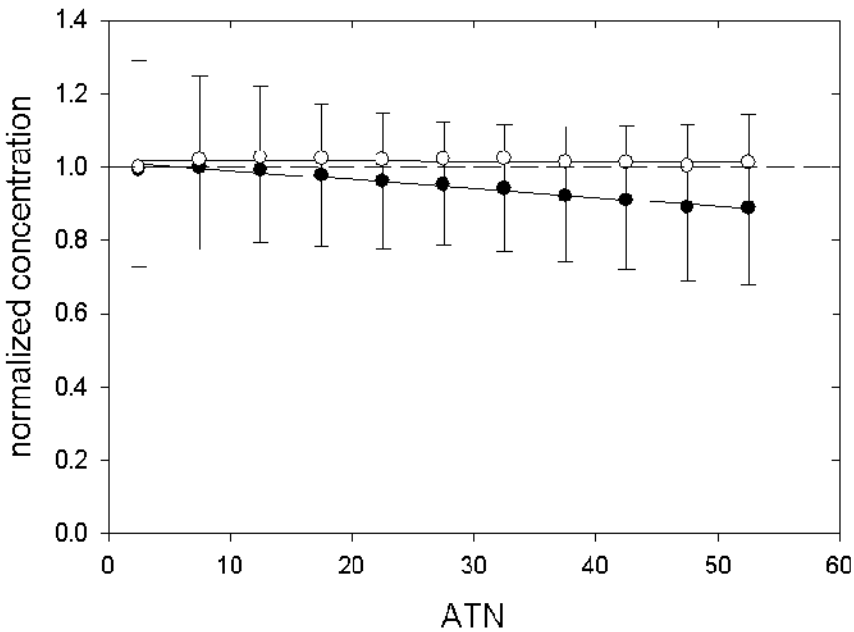

The example shown in Figure 2 is based on all tape advances over the three-year period of April 2001 to March 2004 for BC data collected at East St. Louis with a 2-channel Aethalometer (880 and 370 nm for BC and UVC, respectively). As previously mentioned, the data corrections are not made using a single adjustment for all data but rather the analysis is performed on a user-specified centered moving window of width *w* tape advances. A regression to determine *k* is performed for each tape advance (except the first *w*/2 and last *w*/2 tape advances) using data within the centered window of *w* tape advances. For each regression, the data point with the maximum residual is removed and the regression is repeated. If the leave-one-out regression *k*-value differs from the initial *k*-value by more than 0.001, the data point with maximum residual is deemed to exert too much influence and the leave-one-out slope is used for the *k*-value. **Figure 3** shows the *k*-value time series for the East St. Louis BC data set after smoothing with a centered median smoother of window size *w*=30 tape advances. The *k*-values for the spin-up period (first *w*/2 tape advances) and spin-down period (last *w*/2 tape advances) are imputed using the first- and last-resmoothed *k*-values, respectively.

Figure 3. Aethalometer BC data adjustment parameter time series for April 2001 through March 2004 at East St. Louis. Adjustment parameters from the regressions of median normalized concentration on ATN with a window of 30 tape advances; the time series was smoothed using a centered median smoother with a window of 30 tape advances.

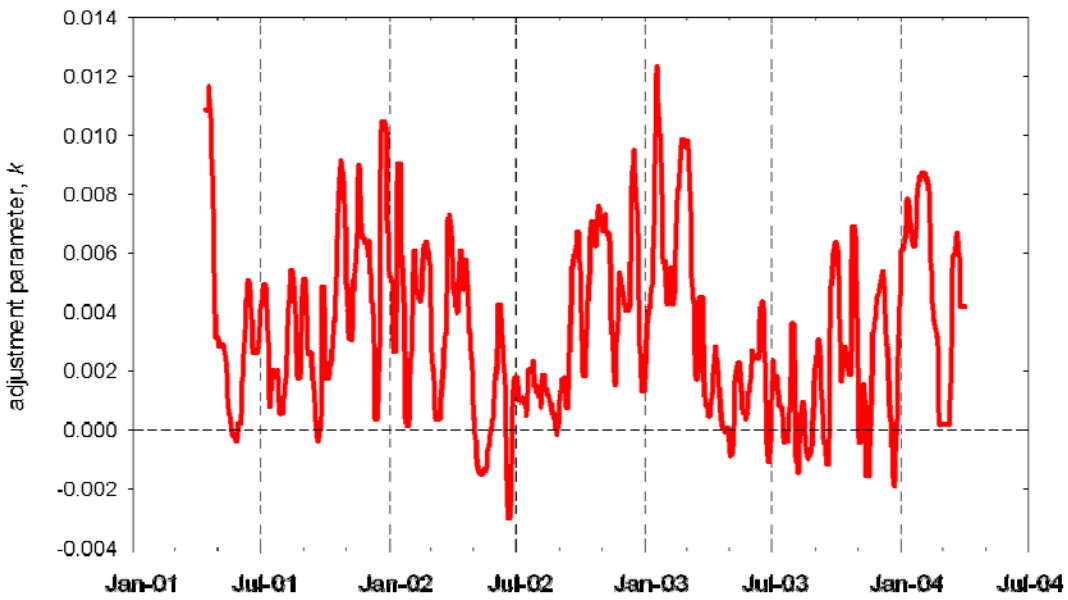

Given the smoothed time series of *k*-values, the raw data are adjusted using Equation (1) with the smoothed *k*-value for tape advance *j* used to adjust all data between tape advances *j* and *j+1*.

The overall process is repeated for each channel of data in addition to the 880 nm BC data (i.e., 370 nm UVC data for a 2-channel Aethalometer or the remaining 6 channels for a 7-channel Aethalometer). Up to three years of data can be processed in a single batch when the raw data is collected with a 5-minute time base.

Aethalometer Black Carbon Data Assembled as Part of this Project

Data were received from local, state, and regional agencies as well as the U.S. Environmental Protection Agency (EPA). Based on available site identifier codes associated with the delivered data, 146 sets of files were received; generally each set is for a single site, but there may be multiple sets of data for a given site if operations or instruments were changed. A summary of data is displayed in **Table 1**. In addition, we paired daily averaged processed data with data reported in the Air Quality System (AQS) provided by EPA. A summary of these data sets is provided in **Table 2**. A comparison of official, AQS data and the processed data for an example site is provided in a later section of this document.

Summary of Aethalometer Data Processing Steps and QC Criteria

The Aethalometer Data Masher program can process data in a single run that spans approximately one year for 1-minute data or three years for 5-minute data. In this work, raw Aethalometer data files were combined from subdirectories into one- or three-year data sets for efficient processing. Multiple subdirectories often contain partial data from the same day and have the same file name. These files were renamed to ensure no data were lost; the Data Masher automatically removes any duplicate data. Each data set was processed using the default Data Masher settings and a site name was added to each file.

The hourly Data Masher output was used for calculation of 24-hr and monthly averages in Microsoft Access. A 75% completeness criterion was required for all averages. 1- and 5-minute Data Masher output was not processed further. Hourly data were used to produce seasonal and diurnal box plots with the requirement that BC-corrected mass concentrations were greater than or equal to -0.5 $\mu g/m^3$. Hourly data were also used to produce monthly box plots with no data screening. These plots are provided electronically with this memo.

Example of Differences between Raw and Processed (Adjusted) Data

As an example, the relationship between raw and adjusted BC concentrations at the Harvard School of Public Health (HSPH) EPA PM-Center Countway site in Boston, Massachusetts, is shown in **Figures 4 and 5** for October 1999 through September 2009. The Aethalometer was a 1-channel unit with a BC maximum ATN setting of 75 used during this period. The average adjusted/raw ratio for this time period is 1.19. In winter the average ratio was 1.30; in summer the average ratio was 1.08. The time series reveals that even within a given season, this ratio can vary. In particular, September time periods show different patterns, likely due to differences in BC sources and/or meteorology.

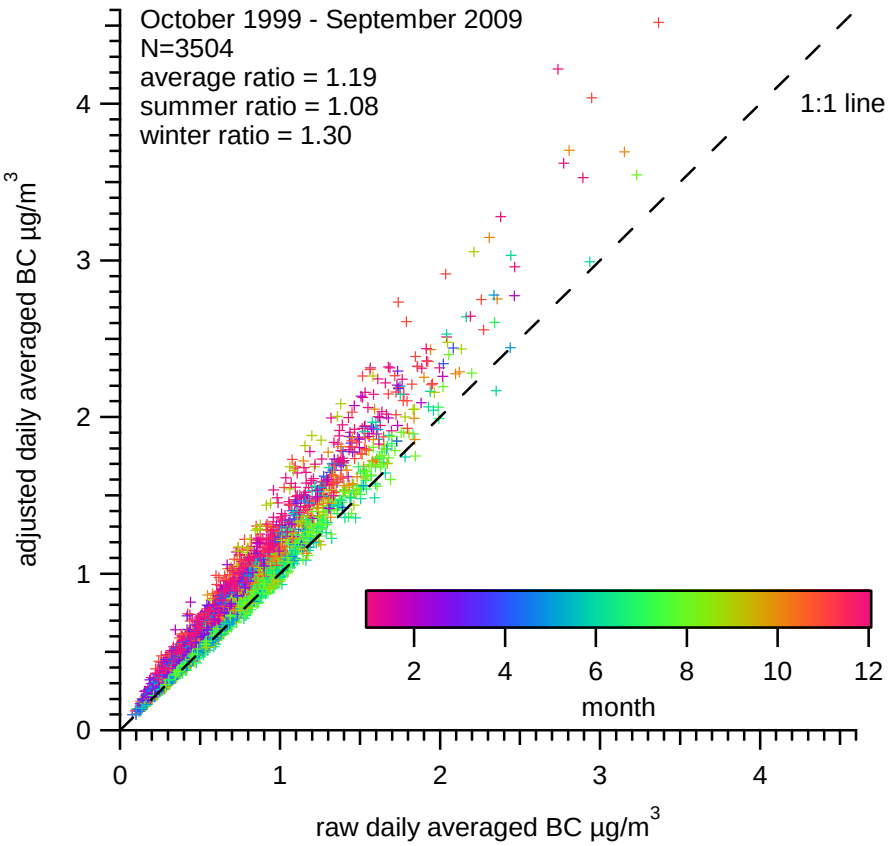

Figure 4. Daily averaged adjusted versus raw BC concentrations (µg/m^3) during October 1999 through September 2009 at the Harvard Boston site, colored by month. Maximum BC ATN = 75.

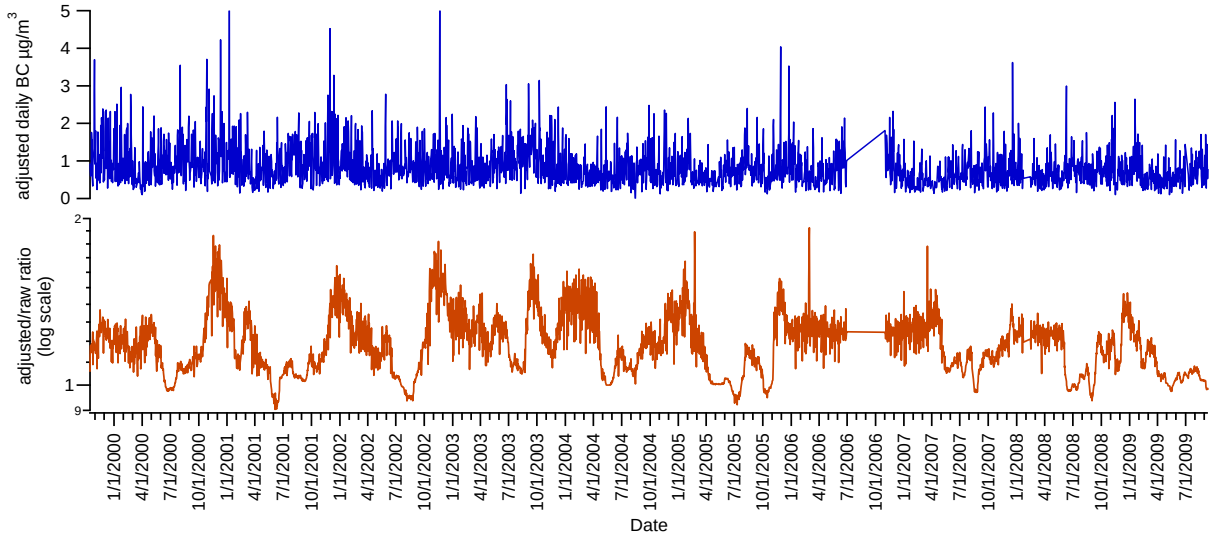

Figure 5. Time series of daily averaged BC concentrations µg/m^3 and daily averaged adjusted/raw ratio at the Harvard Boston site. Maximum BC ATN = 75.

Example of Differences between HSPH Official Data and Processed (Adjusted) Data

As an example, the processed data were compared to the official data as reported in the AQS by HSPH for the Harvard Boston PM-Center site in **Figures 6 through 8**. The HSPH official data set included HSPH validation of the raw data to void certain records but did not include adjustments for the mass loading effect. Raw data, as obtained from the instrument, are used to generate the adjustments; thus, it is necessary to screen the adjusted data to remove all records that were voided in the official data. The average adjusted/official ratio was 1.19 and the average difference between adjusted and official data was 124 ng/m^3. The largest differences between adjusted and official data were seen in wintertime when there is less sulfate to suppress the mass loading effect.

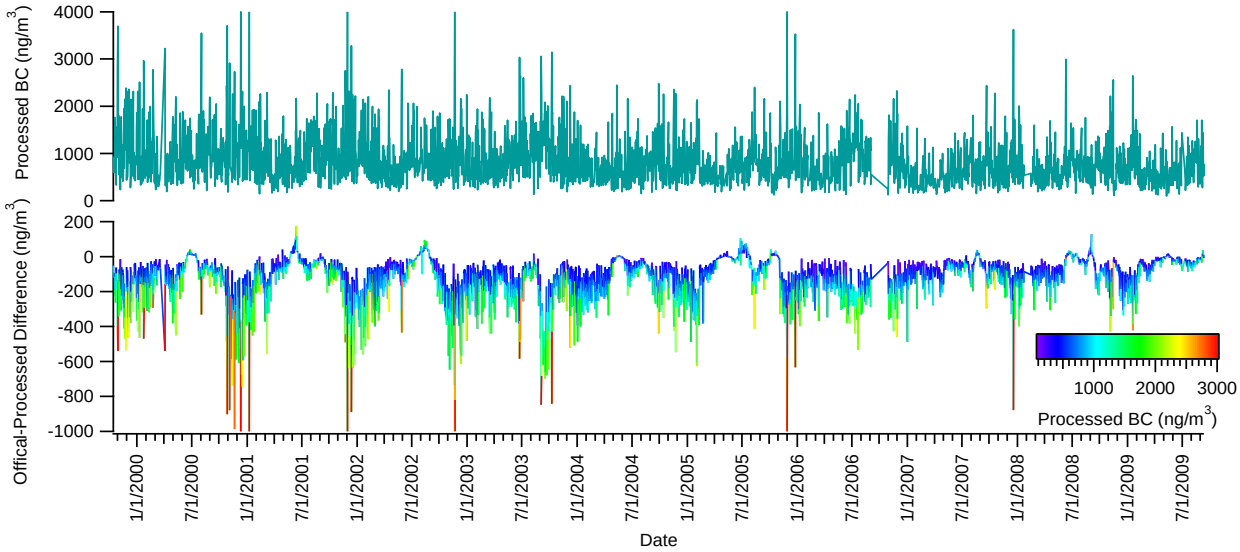

Figure 6. Time series of daily averaged processed (adjusted) BC concentrations and the difference in daily averaged processed BC with HSPH reported BC concentrations (ng/m^3) at the Harvard Boston site in October 1999 through September 2009.

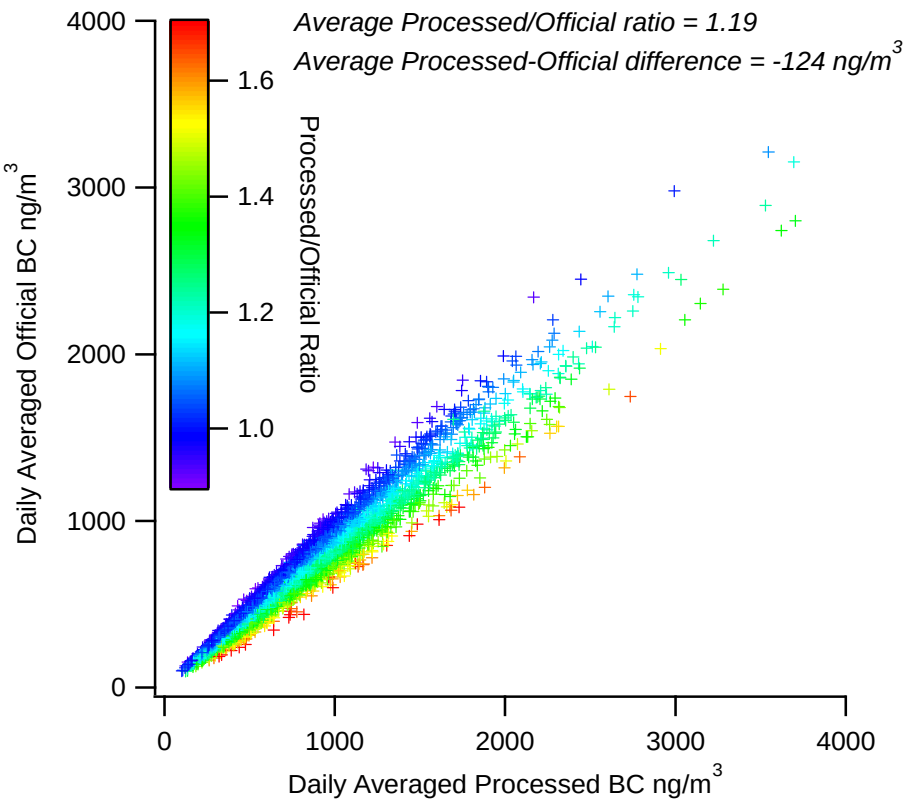

Figure 7. Comparison of daily averaged processed (adjusted) BC concentrations with daily averaged HSPH reported ("official") BC concentrations (ng/m^3) at the Harvard Boston site from October 1999 through September 2009.

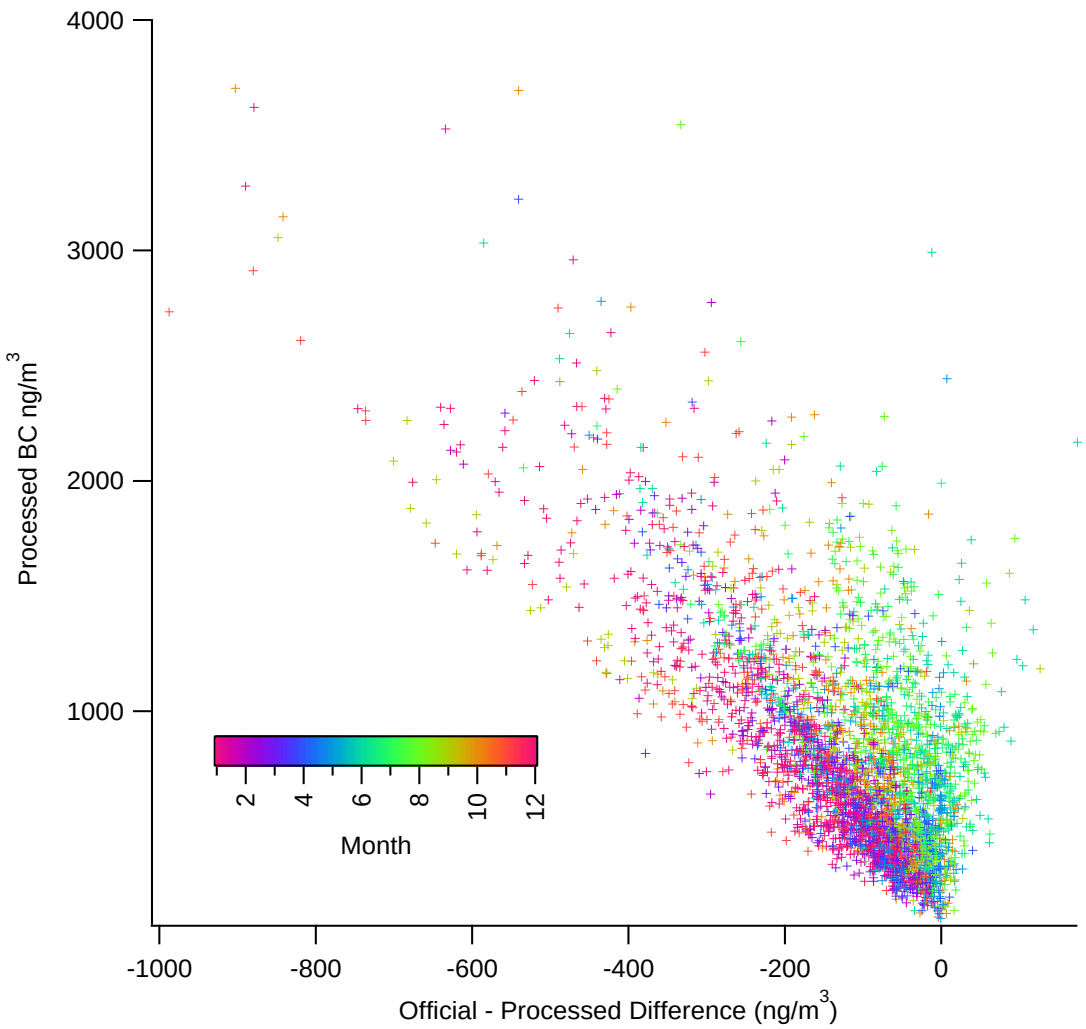

Figure 8. Comparison of daily averaged processed (adjusted) BC concentrations with the difference between daily averaged HSPH reported ("official") BC concentrations and processed BC concentrations (ng/m^3) at the Harvard Boston site from October 1999 through September 2009.

Example of Black Carbon Climatology

Processed (adjusted) data from the HSPH EPA PM-Center Countway site in Boston, Massachusetts, are also used to demonstrate BC climatology. **Figure 9a** shows the day-of-week pattern for daily-average adjusted BC over the entire data set (October 1999 through September 2009). Box plots were constructed for the distributions of daily-average BC divided by the centered seven-day day average BC; this normalization stabilizes the BC concentration with respect to episodic behavior. BC concentrations are consistently high on weekdays, lower on Saturdays, and lowest on Sundays. **Figure 9b** shows the annual distributions of daily-average adjusted BC for 2000-2008. Box plots are omitted for 1999 and 2009 because data for these years were incomplete. While the annual trend is not strictly monotonic, BC concentrations have clearly decreased over the past decade, consistent with

Boston BC measurements made by the Massachusetts Department of Environmental Protection at two sites.

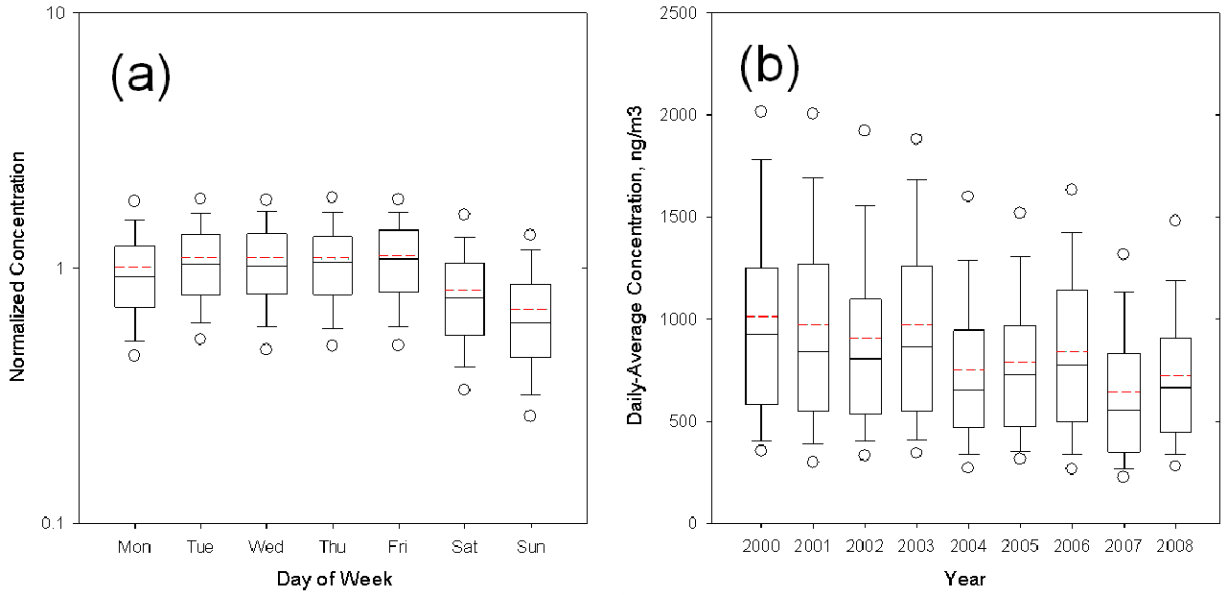

Figure 9. (a) Day-of-week patterns and (b) annual patterns for daily-average processed (adjusted) BC concentrations collected at the Harvard Boston site from October 1999 through September 2009. For (a), normalized concentration was calculated as the daily-average BC divided by the centered seven-day BC. Open circles are 5th and 95th percentiles, whiskers are 10th and 90th percentiles, box boundaries are 25th and 75th percentiles, the interior black line is the median and the interior, and the dashed red line is the arithmetic mean.

Figure 10 shows the long-term trend for seasonal BC concentration distributions. Seasonal median BC concentrations are typically highest in the summer (red boxes) and lowest in the spring (green boxes). Summer season and fall season BC was elevated in 2003 and 2006 compared to the other years. Winter exhibits the largest inter-annual variability with broad distributions during 2000-2002 and narrower distributions and lower median BC in the subsequent years.

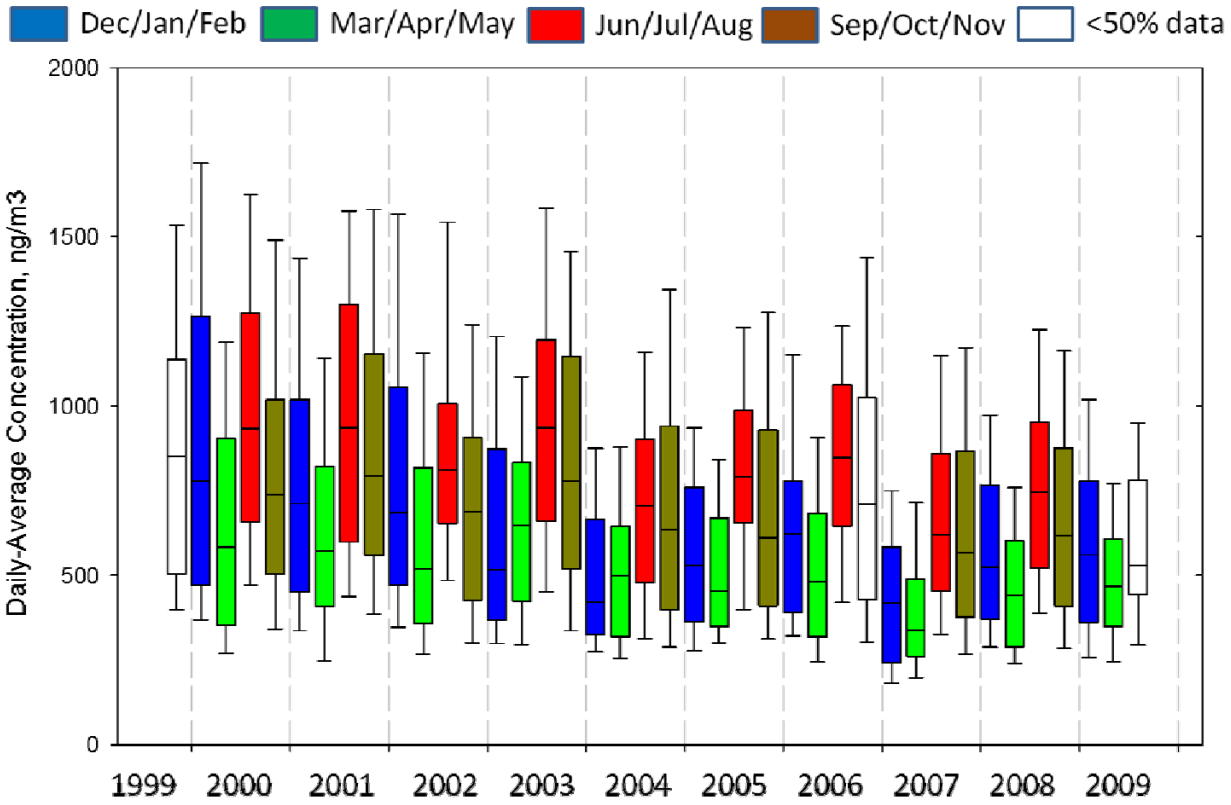

Figure 10. Seasonal distributions of adjusted BC concentration for data collected at the Harvard Boston site from October 1999 through September 2009. Whiskers are 10th and 90th percentiles, box boundaries are 25th and 75th percentiles, and the interior black line is the median.

Appendix E: Reflectance Analysis Method for Estimating BC at the North End Site, February to April 2003.

Appendix E.

Reflectance analysis method for estimating BC at the N.End site for February-April 2003.

The North End site BC measurements started July 1, 2003. For trend purposes, 2003 was an important year. The Harvard School of Public Health (HSPH) has been determining BC from Teflon filters using a EEL Model M43D Smokestain Reflectometer, and analyzed all available Federal Reference Method (FRM) N.End filters for 2003 (there were no FRM filters available before 2003). Figure 1 shows the relationship between reflectance EC reported by HSPH and collocated Aethalometer 24-hour BC for sixteen days between August and November 2003.

Figure 1. Reflectometer EC vs. Aethalometer BC, August-November 2003

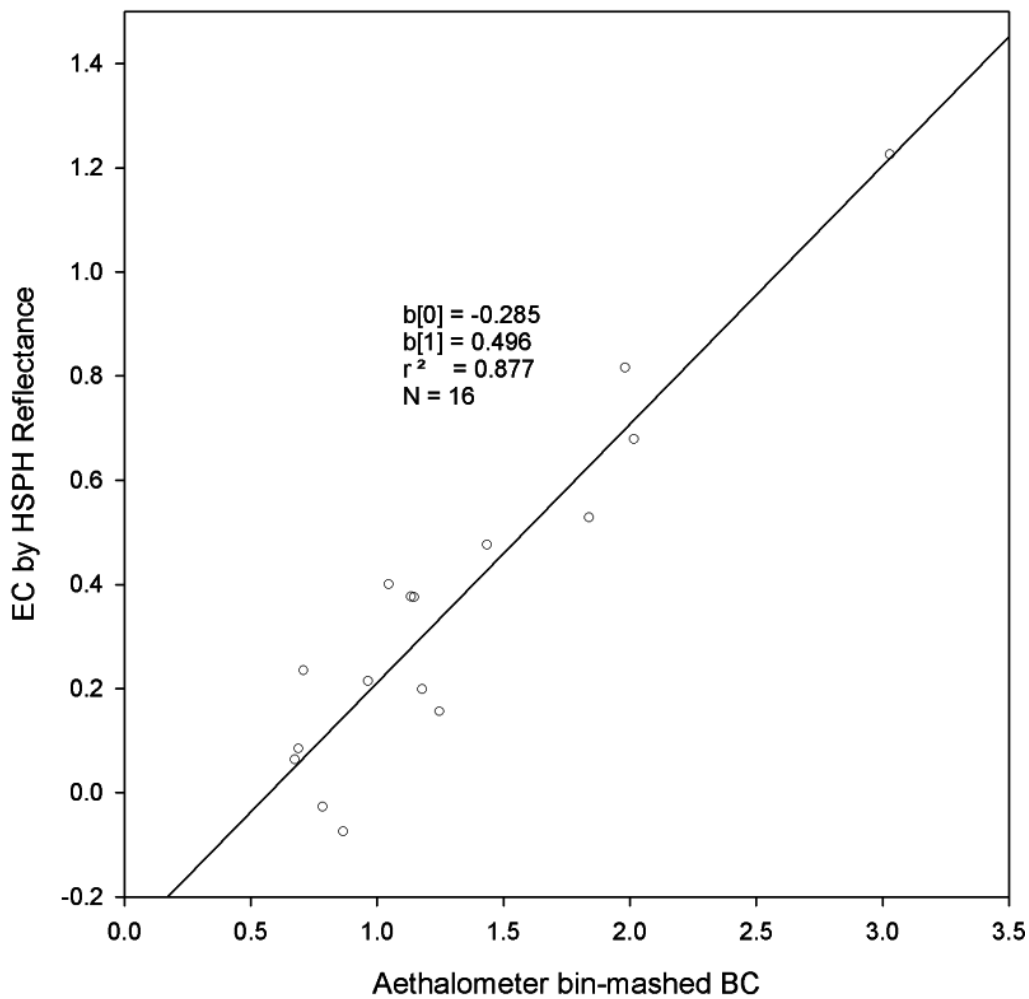

Twenty-one Teflon filters from the every 3rd-day FRM sampler were available for February through April 2003, and analyzed by HSPH. The Reflectometer EC data were converted into equivalent BC data using the regression shown here. The mean estimated BC for these data was 1.35 $\mu g/m^3$, compared to 1.32 $\mu g/m^3$ for the mean Aethalomter BC from July to December 2003.

Appendix F: Turner (2011): Description of the Binned Aethalometer Artifact Correction Method.

Appendix F.

A Refined Methodology to Adjust Aethalometer Black Carbon Data for Measurement Artifacts

Extended Abstract 2011-A-676-AWMA

Jay Turner*
Department of Energy, Environmental & Chemical Engineering; Washington University; Campus Box 1180, One Brookings Drive; St. Louis, MO 63130-4899
George Allen
NESCAUM, 101 Merrimac St., Boston MA 02114
Steven Brown
Sonoma Technology, Inc.; 1455 N. McDowell Blvd., Suite D; Petaluma, CA 94954-6503
Neil Frank
United States Environmental Protection Agency, Office of Air Quality Planning and Standards; 109 T.W. Alexander Drive; Research Triangle Park, NC, 27709

INTRODUCTION

Filter-based optical methods for estimating ambient particulate matter black carbon (BC) concentrations suffer from a mass loading effect whereby the instrument response decreases with increased BC loading. One such instrument, the Aethalometer™, continuously collects particles onto a filter and measures the wavelength-dependent transmission of light through the deposit. The mass loading effect is most-commonly observed as a step discontinuity in the reported concentration upon advancing the Aethalometer filter tape to deposit aerosol onto a clean filter spot instead of a particle-laden filter spot. **Figure 1** shows an example of this effect using collocated Aethalometers. Initially there is good agreement between the reported BC values but after the tape advances for the co-sited unit, it reports concentrations that are systemically higher than the primary unit. These higher values are actually closer to the true BC concentration with the data prior to the tape advance being biased low. Later in the time series the tape advances for the primary unit and subsequent data again exhibit good agreement. The mass loading effect is not governed solely by deposited absorbing (e.g. soot) aerosol. It is also influenced by the abundance of internally- or externally-mixed scattering aerosol (e.g. sulfate) in the ambient air that co-deposits with the absorbing black carbon particles.

* Corresponding author, e-mail: jrturner@wustl.edu

Extended Abstract #2011-A-676-AWMA. "A Refined Methodology to Adjust Aethalometer Black Carbon Data for Measurement Artifacts", Jay Turner, George Allen, Steven Brown, and Neil Frank. Proceedings of the 104th Annual Meeting of the Air & Waste Management Association, Orlando, FL, June 21-24, 2011.

Figure 1. Four hour time series of 5-minute black concentration carbon data for co-sited Aethalometers, East St. Louis. Each instrument exhibited one tape advance during this period. The co-sited unit data stream has been adjusted for instrument-to-instrument bias.

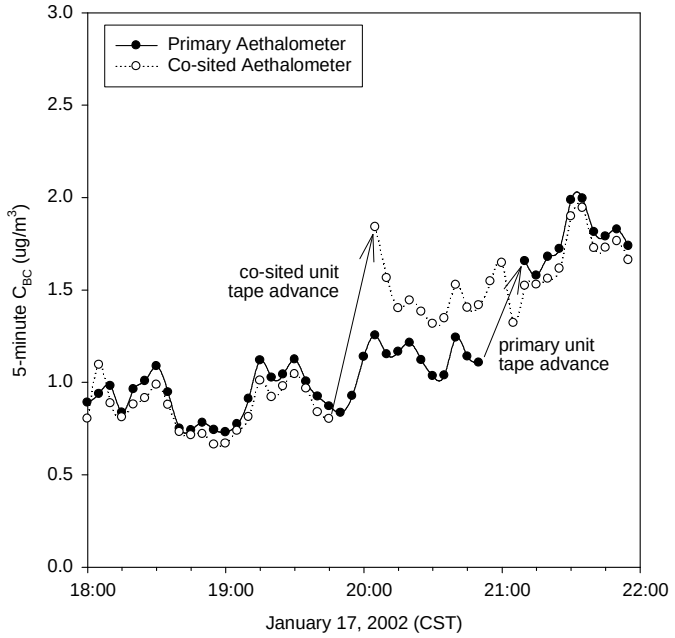

Several approaches have been proposed to adjust the data for these artifacts. For the Aethalometer, one approach uses the difference in reported concentration before and after a filter tape advance to estimate the artifact.[1] Another approach is to perform a regression of the reported concentration on the attenuation using all of the data over a specified time period.[2] Both of these approaches assume the true BC concentration is not changing over the time period of interest (across the tape advance for the first approach, for the entire time period used for the regression in the second approach). Thus, additional temporal aggregation of the data or smoothing of the artifact estimates is needed to damp the effect of this limiting assumption. The Aethalometer data post-processing program developed at Washington University that is publicly available to the air quality measurement community is being revised to include an algorithm for adjusting the raw data using both of these approaches. The gap-based algorithm was implemented for prior projects[3] whereas the current work focuses on implementing a regression-based algorithm that uses all of the data. The latter algorithm is the focus of this extended abstract.

METHODS

The loading effect leads to the Aethalometer-reported concentration decreasing with increased attenuation (ATN, a measure of the light absorption by the deposited aerosol) even when the measured aerosol has a constant BC concentration. The goal of the

algorithm is to regress out this decreasing trend so that, on average, concentration is independent of ATN. The loading effect is assumed to follow the form:[1,2]

$$BC_t = BC_r \left(1 + k \cdot ATN\right) \qquad \text{(eqn 1)}$$

where BC_t is the true concentration, BC_r is the Aethalometer-reported concentration, and k is an empirical parameter that, is this algorithm, is obtained from the regression of concentration on ATN.

The first step is to bin the raw concentration data (typically collected on a time base of 5-minutes but sometimes 1-minute) by attenuation. The algorithm allows the user to specify either a fixed bin width (e.g. 5 ATN units) or an approximate number of bins to be equally distributed over the attenuation range observed for each channel (Aethalometers can have 1-, 2- or 7-channels corresponding to the number of wavelengths for which absorption is measured). The default is a fixed bin width of 5 ATN units. Tape advances are followed by an instrument stabilization period with no data reported. The time duration of all data gaps are identified and the mode gap size (e.g. three consecutive five-minute missing records) is used to flag the tape advances in the time series. Data recorded between each tape advance are stratified into the ATN bins and the mean concentration is calculated for each bin. These concentration values are then normalized to the average concentration over all the bins. This step ensures that the data time series between each tape advance is given similar weight in the regression. Next, these normalized, binned concentrations are aggregated over a user-specified number of tape advances w (default w = 30) and the median value is calculated for each bin. Bin-specific median values are regressed on ATN to determine the empirical data adjustment parameter, k. **Figure 2** shows an example of the data used for the regression of normalized concentration on ATN (solid circles). Error bars denote the interquartile ranges about the median normalized concentrations. The open circles show the median normalized concentrations estimated from equation (1) using the fitted k-value. Ideally these values should be tightly clustered about the horizontal line at normalized concentration of unity (i.e. the ATN dependence of concentration has been removed) and in this example they are biased high by up to 2%.

The example shown in Figure 2 is based on all tape advances over the three year period April 2001 to March 2004 for BC data collected at East St. Louis with a two-channel Aethalometer (880 and 370 nm for BC and UV-C, respectively). As previously mentioned, the analysis is actually performed using a user-specified centered window for the number of data traces between tape advances (w) used to calculate the median normalized concentrations. A regression to determine k is performed for each tape advance except the first w/2 and last w/2 records. These spin-up and spin-down periods are imputed with the first- and last-calculated k-values, respectively. **Figure 3** shows the k-value time series for the East St. Louis BC data set (black line). This time series is further smoothed using a centered median smoother of window size w (red line).

Figure 2. Aethalometer BC concentration for April 2001 – March 2004 at East St. Louis, binned by ATN and normalized within each tape advance. Solid circles are the median normalized concentrations; error bars denote the interquartile ranges. Open circles are the estimated concentration values using equation (1) and the regression-estimated *k*-value of 0.0025.

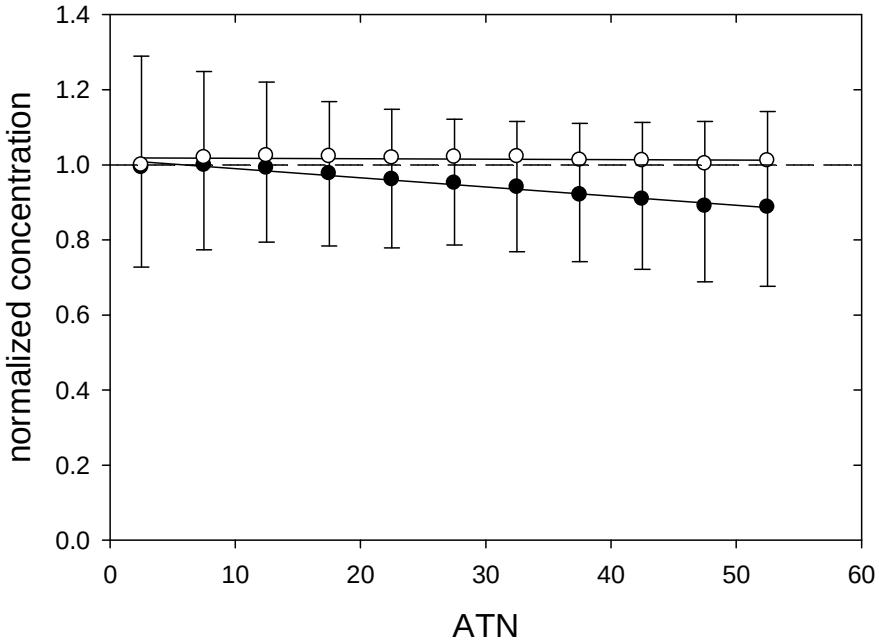

Figure 3. Aethalometer BC data adjustment parameter time series for April 2001 – Mach 2004 at East St. Louis: adjusted parameters from the regressions of median normalized concentration on ATN (black line); and smoothed parameters using a centered median smoother with a window of 30 tape advances (red line).

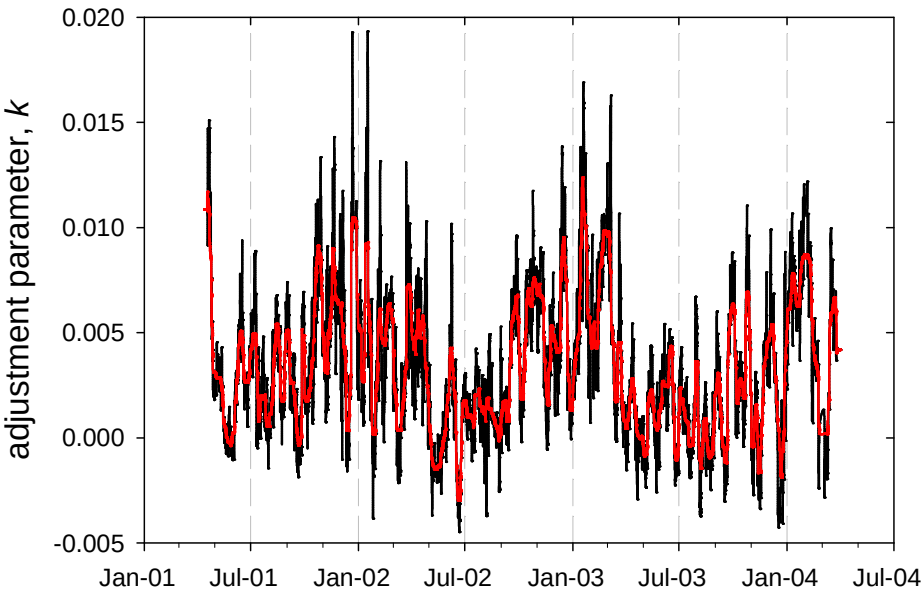

Given the smoothed time series of *k*-values, the raw data are adjusted using equation (1) with the smoothed *k*-value for tape advance *j* used to adjust all data between tape advances *j* and *j+1*.

The overall process is repeated for each channel of data in addition to the 880 nm BC data (i.e. 370 nm UV-C data for a two channel Aethalometer or the remaining six channels for a seven-channel Aethalometer). Up to about three years of data can be processed in a single batch if the raw data were collected at five-minute time base.

RESULTS

The adjustment parameter time series shown in Figure 3 is consistent with the pattern obtained using the tape advance gap method to estimate the parameter.[1] It exhibits a local maximum each winter and local minimum each summer because in St. Louis the concentration of scattering aerosol reaching the Aethalometer filter tape is higher in the summer than the winter and this aerosol partially offsets the BC mass loading effect.[4]

Figure 4 shows scatter plots of the adjusted hourly concentrations on the raw hourly concentrations for black carbon (BC, fig 4a) and UV-absorbing carbon (UV-C, fig 4b) using the April 2001 – March 2004 East St. Louis data set. The mean ratio of the adjusted-to-raw hourly concentrations is 1.09 for BC and 1.28 for UV-C. UV-C is measured at 370 nm and since absorption increases with decreasing wavelength the UV-C channel reaches the user-specified maximum attenuation (which triggers a tape advance) before the BC channel. For the two-channel Aethalometer deployed in East St. Louis the maximum attenuation was set to 125 which is reached for the UV-C channel when the BC channel attenuation is about 50. Thus, the UV-C data have a much larger artifact than BC data as demonstrated by the magnitude of the mean adjustment (9% and 28%, respectively). Note that a one-channel Aethalometer (BC only, 880 nm) with a maximum attenuation set to 125 would exhibit about the same percentage adjustment as the UV-C channel data in this example.

SUMMARY

The Aethalometer data post-processing software developed at Washington University has been revised to include a refined algorithm for adjusting the data for mass loading effects. For well-behaved data such as the example used in this extended abstract, the adjustments are generally consistent with an algorithm that derives adjustment parameters from the concentration change across each tape advance (not shown). The refined algorithm is expected to be superior for noisy data because it uses all the data and thus is more likely to damp the noise. While changes in the mass loading effect can occur on time scales shorter than the time over which this algorithm windows the data and smooths the adjustment parameter time series, the adjustments do capture changes in the mass loading effect that occur on longer times scales (weeks-to-months) and thus it is an improvement over using the raw data. For example, for the East St. Louis deployment there were on average three tape advances per day so the windowing and smoothing with $w = 30$

Figure 4. Raw and adjusted BC (a) and UV-C (b) hourly concentration values for the April 2001 – March 2004 data collected at East St. Louis. The mean ratio of the hourly adjusted-to-raw concentrations includes only those hours with adjusted concentrations greater than 1 μg/m^3.

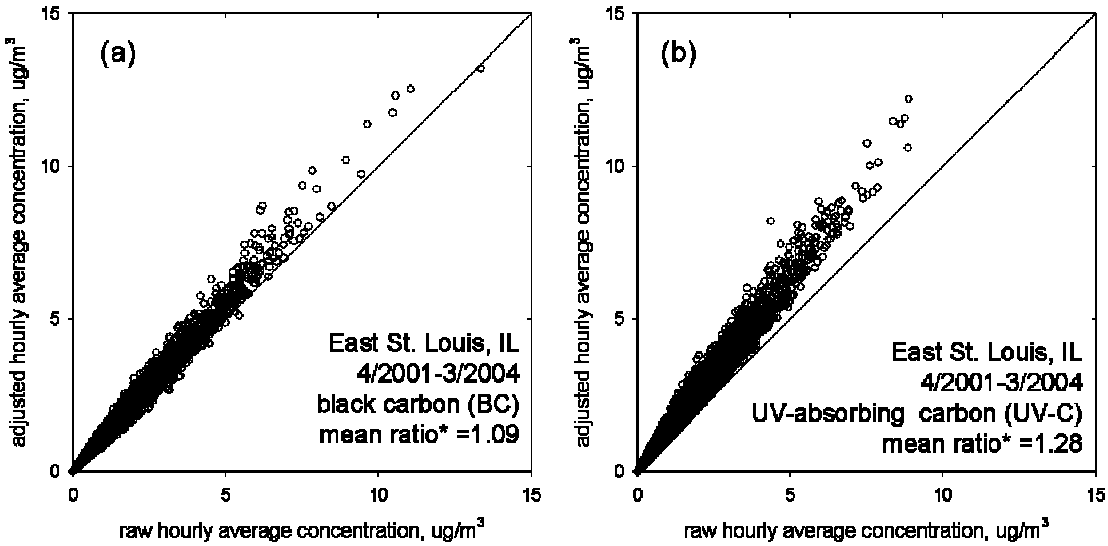

corresponds to about ten days. The software is currently being beta tested and will be publicly available by mid-2011. It is currently being used to reprocess data collected from several sites across the United States towards developing a more robust description of aerosol black carbon climatology.

ACKNOWLEDGEMENTS

The authors gratefully acknowledge David Shelow (USEPA), Natalie LaGuardia (STI) and Theresa O'Brien (STI) for their contributions to this project.

Although the research described in this presentation has been funded wholly or in part by EPA through a contract to the Sonoma Technology, Inc., it has not been subjected to the Agency's required peer and policy review and therefore does not necessarily reflect the views of the Agency, and no official endorsement should be inferred.

REFERENCES

1. Turner, J.R.; Hansen, A.D.A; Allen, G.A.; Methodologies to Compensate for Optical Saturation and Scattering in Aethalometer™ Black Carbon Measurements, Paper #37, Proceedings of the Air & Waste Management Association Symposium on Air Quality Measurement Methods and Technology, San Francisco, CA, April 30 – May 2, 2007.
2. Park, S.S.; Hansen, A.D.A.; Cho, S.Y.; *Atmos. Environ.*, **2010**, *44*, 1449-1455.

3. Turner JR, Allen GA (2008). Temporal Patterns and Source Apportionment of Ambient Fine Particle Aethalometer Black Carbon in Boston, Massachusetts. Transportation Research Board 88th Annual Meeting, Washington, D.C., January 2009.

4. Arnott, W.P.; Hamasha, K; Moosmüller, H.; Sheridan, P.J.; Ogren, J.A.; *Aerosol Sci. Technol.*, **2005**, *39*, 17-29.

KEYWORDS

Aethalometer, black carbon, optical saturation

Appendix G: Turner (2008): Source Apportionment for the North End Site.

Appendix G.

TEMPORAL PATTERNS AND SOURCE APPORTIONMENT OF AMBIENT FINE PARTICLE AETHOLOMETER BLACK CARBON IN BOSTON, MASSACHUSETTS

Jay R. Turner*
Department of Energy, Environmental & Chemical Engineering
Washington University
Campus box 1180; One Brookings Drive
St. Louis, MO 63130 / USA
Telephone 314-935-5480
Facsimile 314-935-7211
Email: JRTURNER@WUSTL.EDU

George A. Allen
Northeast States for Coordinated Air Use Management (NESCAUM)
101 Merrimac Street, 10th Floor
Boston, MA 02114 / USA
Telephone: 617-259-2000
Facsimile 617-742-9162
Email: GALLEN@NESCAUM.ORG

submitted August 1, 2008
for presentation at the *TRB 2009 Annual Meeting*
and publication in the *Transportation Research Record: Journal of the TRB*

word count 7,263 (4,513 words and 11 figures @ 250 words per figure)

* corresponding author

ABSTRACT

Five years of ambient fine particle Aethalometer™ black carbon (BC) data from Boston, Massachusetts, was analyzed for temporal patterns exerted on varying scales. The data were collected by Massachusetts Department of Environmental Protection at the "North End" site which is near the western terminus of the Sumner Tunnel. Diurnal profiles for hourly-average BC on weekdays exhibited a strong mobile source signature with maximum concentration during rush hour. In contrast, on weekends the morning rush hour BC enhancement was quite small and maximum BC was observed in the early evenings. Diurnal profiles stratified by season revealed a local maximum for the winter BC in the evenings for both weekdays and weekends. For nearly three years of data collection at this site, the Aethalometer also collected data for UV-absorbing carbon (UVC). UVC concentrations similar to BC are an indicator for fossil fuel combustion while UVC enhancement above BC is an indicator for biomass combustion. An apportionment of BC to traffic (more generally, fossil fuel) and wood smoke (more generally, biomass combustion) sources yielded 15% contribution from wood smoke on an annual basis; wood smoke was 5% of the summer BC and 28% of the winter BC, and accounted for more than 50% of the BC on weekend nights in the winter. This analysis provides evidence that wintertime biomass combustion, likely including both space heating and recreational fireplace use, is a significant contributor to Aethalometer black carbon concentrations in Boston and it would be erroneous to attribute all of the BC to mobile sources.

INTRODUCTION

This is substantial interest in mobile source contributions to ambient fine particle burdens and their associated adverse health effects. Elemental carbon (EC) has been used in some studies as a surrogate for estimating diesel particulate matter concentrations and exposures, and the potential flaws in this approach have been summarized by Schauer *(1)*. For example, fine particle EC in urban environments can originate from a variety of emission sources including, but not limited to, mobile sources and biomass combustion. EC is conventionally measured by thermal-optical methods with the term EC suggesting carbon that is refractory in nature. Another commonly-measured parameter is black carbon (BC) which is based, as its name suggests, on a measurement of light absorption. While BC and EC are inherently different measurements and both are operationally defined, these parameters are often highly correlated and BC is often used synonymously with EC in an urban air quality and health effects context. One method for measuring BC is the Aethalometer™ (Magee Scientific, Berkeley, CA) which quantifies the absorption of light by aerosol particles continuously deposited onto a quartz fiber filter tape. Certain versions of this instrument measure light absorption at two-or-more wavelengths and it has been shown that the wavelength dependence of absorption is quite different for emissions from fossil fuel combustion and biomass combustion *(2)*. Allen *et al. (3)* and Sandradewi *et al. (4-6)* presented and applied methodologies which use multi-wavelength Aethalometer data and additional fine particle measurements to quantitatively apportion ambient fine particulate matter burdens to wood smoke and traffic emission sources. In this study, we examine a five year time series of ambient fine particle Aethalometer data for evidence of different source types contributing to the BC burden at a site in Boston, Massachusetts.

As previously stated, the Aethalometer measures the absorption of light by aerosol particles continuously deposited onto a quartz fiber filter tape. Wavelength-specific light transmission through the particle-laden filter, *T*, is read at a user defined time interval (typically 5-minutes). The attenuation, ATN, is –

$$ATN = -100 \times \ln(T) = -100 \times \ln\left(\frac{S_B - S_Z}{R_B - R_Z}\right)$$

where S_B and S_Z are the light intensities measured downstream of the particle-laden deposit with the upstream lamp on and off, respectively; and R_B and R_Z are the light intensities measured downstream of the clean section of the filter tape with the upstream lamp on and off, respectively. The effective absorption coefficient, b_{ATN} [L^{-1}], which corresponds to absorption by particles deposited in the quartz fiber filter tape is –

$$b_{ATN} = \frac{A \cdot \Delta ATN}{Q \cdot \Delta t}$$

where A is the particle deposit area [L^2], Q the air sample flow rate [L^3t^{-1}], Δt the time interval between measurements [t], and ΔATN the change in attenuation between measurements. The aerosol absorption coefficient, b_{abs} [L^{-1}] is then given by -

$$b_{abs} = \frac{b_{ATN}}{H(\lambda) \cdot R(\lambda, ATN)}$$

where H(λ) is the absorption enhancement in the massively scattering environment of the quartz fiber filter and R(λ, ATN) accounts for the decrease in the absorption enhancement with particle loading onto the filter. Finally, the ambient concentration of absorbing material, C(λ) [M L^{-3}], is given by –

$$C(\lambda) = \frac{b_{abs}}{E_{abs}} = \frac{b_{ATN}}{E_{ATN}}$$

where E_{abs} [L^2 M^{-1}] is the aerosol mass absorption efficiency and E_{abs} [L^2 M^{-1}] is the effective particle mass absorption efficiency for particles deposited in the quartz fiber filter. Black carbon (BC) is the term used for C(880 nm) while ultraviolet absorbing carbon (UVC or UVPM) is the term used for C(370 nm). The user programs into the Aethalometer for each wavelength an "absorption cross-section", σ(λ) [L^2 M^{-1}], which has been determined from laboratory experiments and corresponds to –

$$\sigma(\lambda) = [E_{abs} H](\lambda) = E_{ATN}(\lambda) \quad \text{with} \quad R = 1$$

The Aethalometer does not account for optical saturation (i.e. R=1 is assumed) and compensation for this phenomenon must be handled by the user during data post-processing. When the light transmission drops below a user-defined threshold (that is, when ATN exceeds a threshold value) the filter tape is advanced and particles are collected on a clean section of the filter tape.

While it has long been known that the absorption per unit mass of deposited absorbing aerosol decreases with increased loading (i.e. R≠1), only recently have there been extensive efforts to compensate the data for such effects. Arnott *et al. (7)* developed a first-principles model for light attenuation in the Aethalometer which showed that the loading-dependent negative bias for the Aethalometer-reported concentration is worst for an aerosol with a low single scattering albedo which is the ratio of the light removed by scattering to the total light extinction. For an aerosol with a high single scattering albedo, the optical saturation phenomenon is further complicated by a matrix effect from co-deposited scattering aerosol which can partially or even wholly offset the optical saturation effect. Turner *et al. (8)* have reviewed various equations proposed to compensate Aethalometer data for these effects, including comparisons to the model of Arnott *et al. (7).* Some equations perform better at low single scattering albedo *(9-11)* with others perform better at high single scattering albedo (*12*). For sites such as Boston with significant seasonal variations in the single scattering albedo, driven to a large extent by seasonal variations in the aerosol sulfate concentration, no single equation is preferred for all conditions and the equation of Virkkula *et al. (11*) has been implemented as described in the Methods section of this paper.

After compensating the data for optical saturation effects, the conditioned data set was mined for insights into the emission sources contributing to BC at the North End site by examining BC diurnal profiles and applying the model of Sandradewi *et al. (4-6)* to apportion BC to traffic and wood smoke sources. This approach assumes that traffic (or more broadly, mobile sources) is the only significant contributor to BC from fossil fuel combustion and wood smoke is the only significant contributor to biomass combustion. No effort is made to determine the total particulate matter burdens from these emission sources since this would require additional air quality parameters that were not measured.

METHODS

An AE-21 Aethalometer (SN #413) has been operated since July 2003 at the Massachusetts Department of Environmental Protection (MADEP) "North End" monitoring site in Boston (174 North Street, AIRS Site ID 25-025-0043), 42.363N, -71.054E. The site is located on the roof of a four-story building with the inlet approximately 20 meters above ground and 25 meters above sea level. The immediate area is a mix of commercial and residential use with substantial traffic activity. The Sumner Tunnel exit (Rt. 1A south) is at the opposite edge of the building from the monitor. The inner harbor of Boston is ~ 500 meters east of the site.

Five years of raw Aethalometer data, from July 2003 through June 2008, were obtained from MADEP for this analysis. While validated hourly-average BC concentration data is uploaded by MADEP to the USEPA Air Quality System (AQS) and is publicly available, this analysis required not only the BC concentration data but also the attenuation data (ATN) to compensate for optical saturation effects; thus, the raw data files were obtained from MADEP and were not subjected to MADEP's validation protocols. Data were collected at five minute time resolution and reported at standard conditions of 1013 mbar and 25°C. A cyclone was placed on the Aethalometer inlet to achieve a particle size cutpoint of 2.5 μm aerodynamic diameter ($PM_{2.5}$). Initially the Aethalometer was programmed to collected data at 880 nm (BC) only; starting in September 2005 the instrument was reprogrammed to also collected data at 370 nm (UVC). The maximum attenuation was initially programmed to 125; thus, tape advances were triggered when the BC channel attenuation exceeded 125. Starting in September 2005 tape advances were triggered when the UVC channel attenuation exceeded 125. The later case typically corresponds to BC attenuation in the range from 30 to 60 (**Figure 1**).

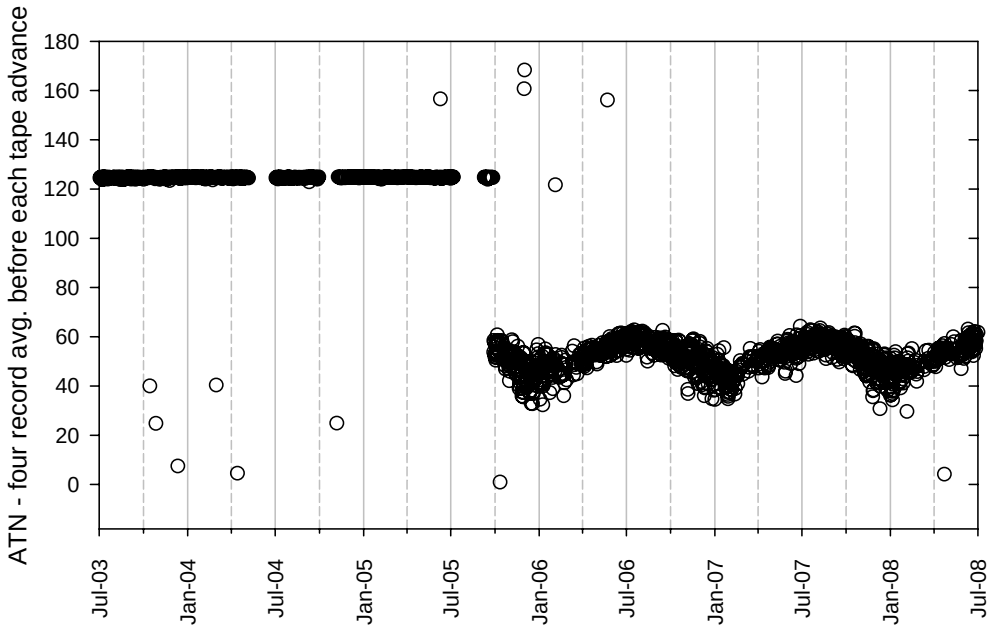

1.

FIGURE 1 Time series for the BC channel (880 nm) attenuation just prior to each tape advance.

The Aethalometer data were compensated for optical saturation using the equation of Virkkula *et al. (11)* as implemented by Turner *et al. (8)*. The governing equation is –

$$R(\lambda) = \left(1 + k(\lambda) \cdot ATN\right)^{-1}$$

or simply -

$$C(\lambda) = C_{AETH}(\lambda) \times \left(1 + k(\lambda) \cdot ATN\right)$$

where $C_{AETH}(\lambda)$ is the concentration reported by the Aethalometer with σ(370 nm) and σ(880 nm) set to 39.5 and 16.6 m^2/g, respectively, and *k* is the compensation parameter. The negative bias from optical saturation causes a step increase in the reported concentration across a tape advance if the aerosol being sampled has a constant composition and concentration. The compensation parameter *k* is calculated for each tape advance assuming the ambient concentration of absorbing material is constant for the 15-minute tape advance-induced instrument stabilization period as well as the averaging times used to estimate the concentrations before and after the tape advance. In reality, the ambient concentration is often changing over this period and thus the individual estimates of *k* are smoothed over numerous tape advances to stabilize the estimates. In this study, a centered rolling median of the tape advance-specific *k* values was used to generate a time series of smoothed *k* which was applied to the raw (C_{AETH}) data.

RESULTS

Aethalometer Data Conditioning

Aethalometer data was compensated for optical saturation effects by smoothing over 20, 40, and 80 tape advances. **Figure 2** shows the smoothed compensation parameter, *k*, for the entire time series. The compensation parameter exhibits a seasonal pattern with maximum values in the winter (relatively large negative bias in the reported concentration values) and minimum values in the summer (relatively small negative bias in the reported concentration values). This pattern is consistent with the role of scattering aerosol on partially offsetting the optical saturation effect. In Boston, ammonium sulfate is the largest contributor to aerosol scattering and exhibits a seasonal pattern with highest concentrations in the summer and lowest concentrations in the winter.

The September 2005 change in the wavelengths measured (from BC only to BC plus UVC) affected the characteristic BC channel attenuation when a tape advanced was triggered (Figure 1). The average time between tape advances was 40- and 20-hours before and after this change, respectively. The tape advance frequency affects the time period corresponding to a given smoothing parameter. Figure 2 shows that smoothing over 80 tape advances yields a similar seasonal pattern for each year of the five year measurement period. It is recognized that this degree of smoothing can only account for seasonal variations in the optical saturation effect and it will not account for changes occurring on finer time scales (e.g. as synoptic weather patterns move through the area on three-to-five day time scales, often altering the aerosol composition). The analyses and interpretation of data presented in this paper are consistent with this limitation. While conditioned data was obtained using a smoothing parameter of 80, the sensitivity of certain results to the smoothing parameter was investigated to ensure the robustness of the results.

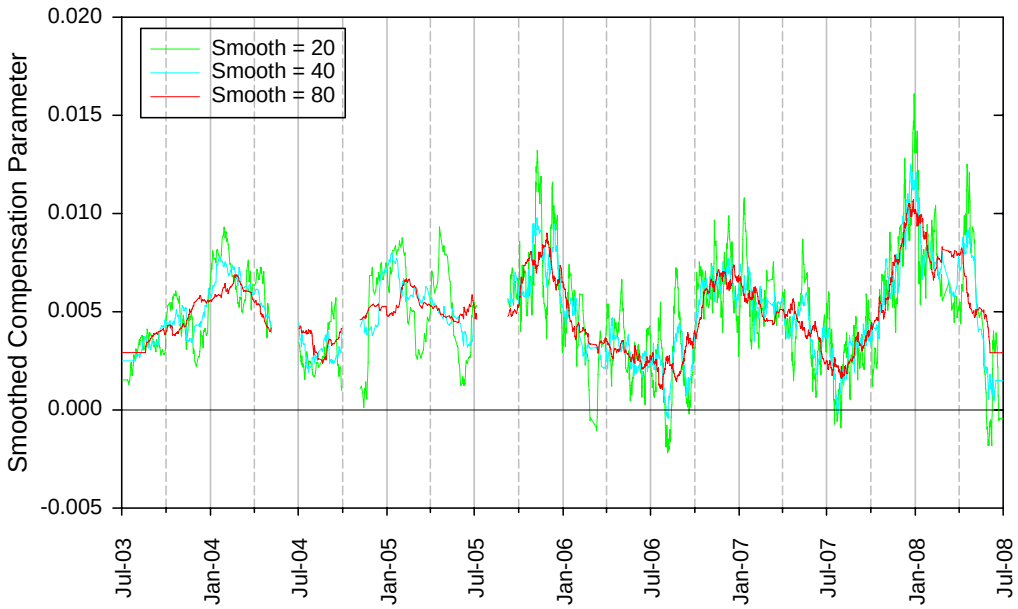

FIGURE 2 Time series for the BC optical saturation compensation parameter, *k*, for various smoothing parameters.

Record-specific adjustments to the data are affected by the compensation parameter and the record-specific attenuation. **Figure 3** shows modeled traces for the Aethalometer-reported concentration as a function of attenuation for a constant 1 μg/m^3 BC aerosol at the 1st and 99th percentiles of the smoothed compensation parameter (k = 0.0015 and 0.010, respectively). Virtually all of the ambient data falls between the two solid curves, corresponding to record-specific concentration adjustments of up to ~50%. Compensated 5-minute data were rolled up to hourly averages. **Figure 4** shows scattergrams for the raw and compensated hourly data for the time periods before and after the change in instrument configuration. The largest adjustments were in the winter prior to the change in the instrument configuration.

Year-to-Year Trends

Figure 5 shows box plots for the hourly BC concentration distributions by year (defined as the period from July through the following June) for the five year data set. The first year (July 2003 through June 2004) exhibits higher concentrations than the subsequent years. This difference is more dramatic for the compensated data compared to the raw data because the higher attenuation values of 125 reached during the first two years corresponds to larger adjustments for optical saturation effects. Compensation is most significant for the winter periods and thus the right-hand plot shows the distributions by year for the period from October through March only. The raw data suggests that the first year was no different from more-recent years and the median concentration was lowest in the second year. In contrast, the compensated data shows the highest median was observed in the first year and the second year no longer exhibits the lowest median. This analysis demonstrates the importance of compensating the data for seasonal trends in the optical saturation artifact, as it leads to different interpretation of year-to-year patterns in

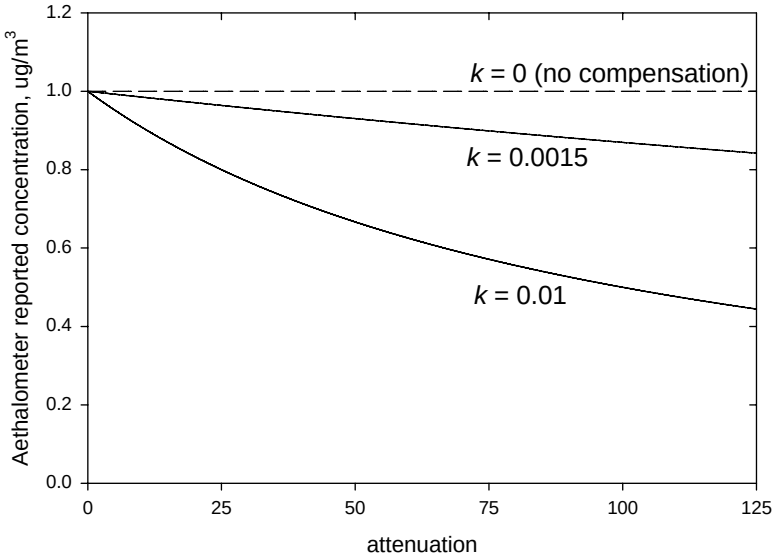

FIGURE 3 Negative bias in the Aethalometer reported concentration as a function of attenuation for the 1st and 99th percentile values of the smoothed BC compensation parameter, *k*.

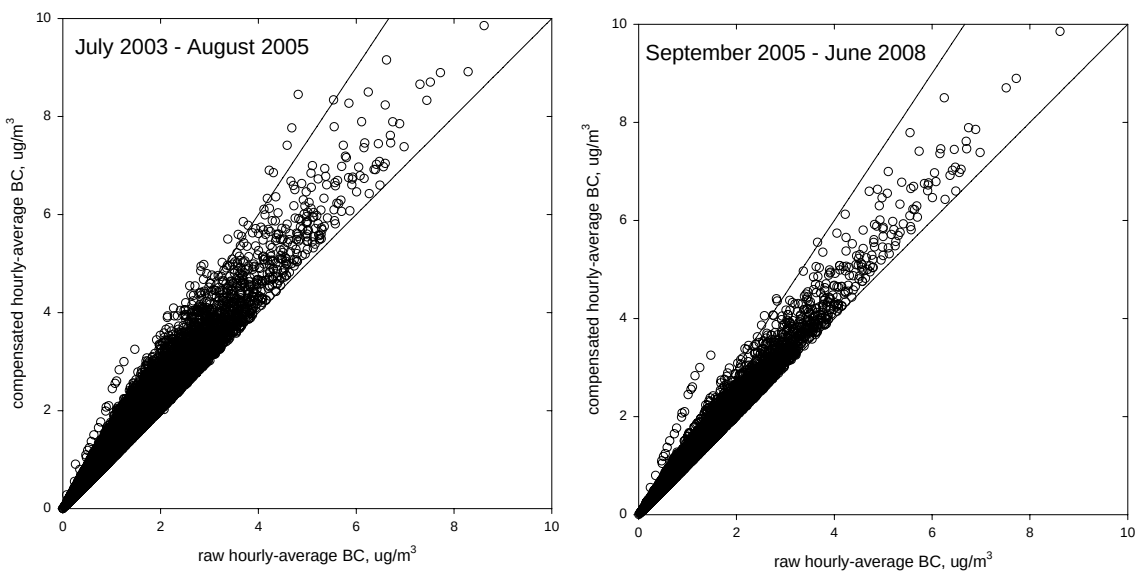

FIGURE 4 Adjustments to the hourly-average BC concentration data for the time periods before (left) and after (right) the change in the instrument configuration from monitoring BC only to monitoring BC and UVC.

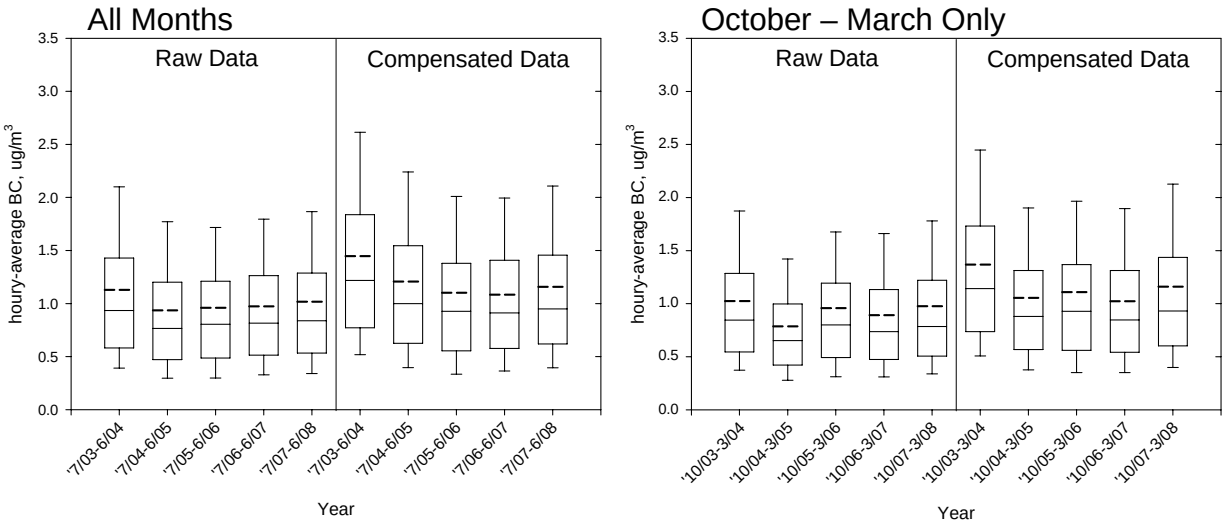

FIGURE 5 Yearly distributions (from July through June) of raw and compensated hourly BC data for all months (left) and from October through March (right). Whiskers are 10th and 90th percentiles.

the BC concentration. The decrease in BC concentrations over the 2003-2004 time period was also observed at two sites in Boston with Aethalometers operating since at least 2000 (G. Allen, unpublished).

Diurnal Trends

Figure 6 shows BC diurnal profiles for the entire five year data set stratified by weekdays and weekends. For weekdays, maximum BC concentrations are observed from 0600 to 0900 EST, consistent with the morning rush hour, followed by a local minimum at midday from 1100 to 1500 EST. A modest secondary maximum occurs from 1600 to 2000 EST, consistent with the evening rush hour. Lowest BC concentrations are observed at night from 2200 to 0400 EST. The midday minimum could arise from reduced emissions during off-peak commute hours coupled with a midday maximum in the mixing layer depth which dilutes the ground-level emissions. The nighttime minimum occurs despite a shallow mixing layer depth which suppresses vertical dilution of any ground-level emissions. The weekend pattern is markedly different with the absence of a BC maximum during morning rush hour and instead a BC maximum in the evening from 1700 to 2100 EST. **Figure 7** shows diurnal profiles for both the summer (June – August) and winter (December – February) periods, again stratified by weekdays and weekends. BC concentrations are higher in the summer compared to the winter, and also exhibit a wider range of concentrations in the summer. Summertime weekdays do not exhibit the evening local maximum in BC concentration that is observed for summer weekends, winter weekdays, and winter weekends. Winter weekends exhibit a modest local maximum in the BC concentration during morning rush hour period that is not observed for summer weekends.

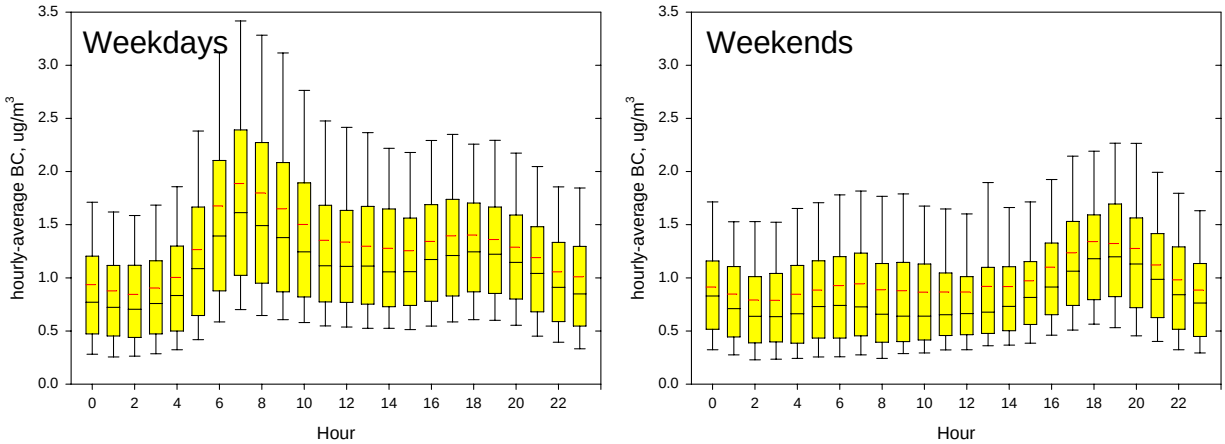

FIGURE 6 Diurnal profiles of hourly-average compensated BC for weekdays (left) and weekends (right). Whiskers are 10th and 90th percentiles. The interior black line is the median and the red line is the arithmetic mean.

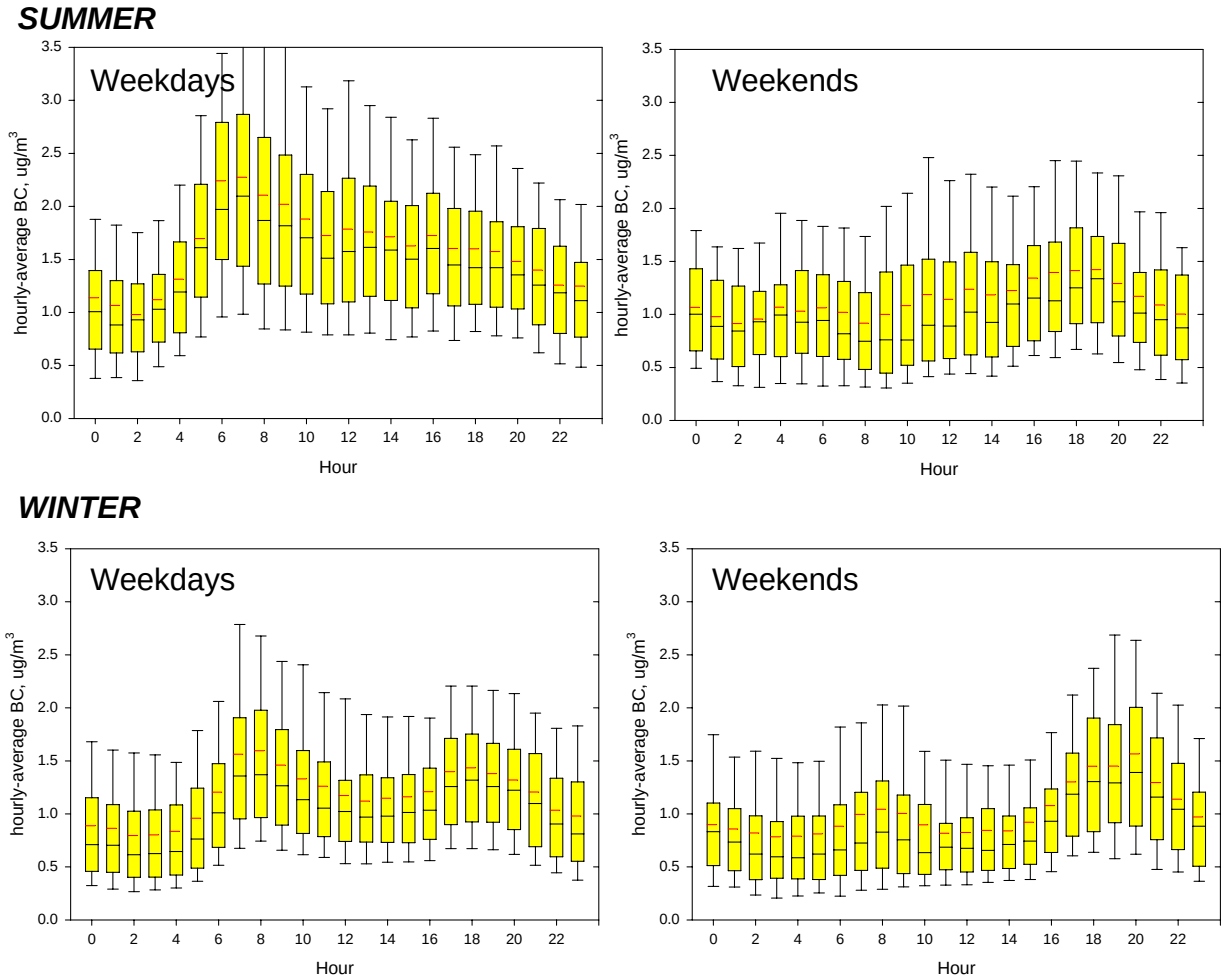

FIGURE 7 Summer (top) and winter (bottom) diurnal profiles of hourly-average compensated BC for weekdays (left) and weekends (right). Whiskers are 10th and 90th percentiles. The interior black line is the median and the red line is the arithmetic mean.

Median diurnal profiles are shown in **Figure 8** for the summer and winter periods stratified by weekdays and weekends, as well the difference between weekday and weekend median diurnal profiles. The enhancement in the weekday BC compared to the weekends exhibits similar diurnal profiles for both seasons with a maximum at 0700-0800 EST followed by a nearly monotonic decrease throughout the day. Within each season, the median nighttime concentrations for weekdays and weekends are nearly identical.

In aggregate, the diurnal profiles of Figures 7 and 8 support mobile sources being the dominant contributor to at least the within-season diurnal variability in the BC concentration. However, this does not mean that mobile sources are the only contributors to BC concentrations. The wavelength dependence of absorption is commonly expressed as a power law relationship –

$$b_{abs}(\lambda) = K\lambda^{-\alpha}$$

where K and α are absorption Angstrom coefficients and α is called the Angstrom exponent. Kirchstetter *et al. (2)* have shown that α ~ 1 for aerosols from fossil fuel combustion and α ~ 2 for aerosols from biomass/biofuel burning and for mineral dust. Given the $PM_{2.5}$ cutpoint will eliminate most of the airborne mineral dust and given the relatively low mass absorption efficiency for mineral dust, high Angstrom exponents in this physical setting are assumed to reflect biomass/biofuel combustion. **Figure 9** shows diurnal profiles for the UVC/BC ratio for the summer and winter periods stratified by weekdays and weekends. This ratio is related to the Angstrom exponent by –

$$\alpha = 1 + 1.15 \times \ln(UVC / BC)$$

for the programmed Aethalometer absorption cross-sections; and UVC/BC and α differ by no more than 5% for UVC/BC ratios between 0.9 and 1.5. Thus, UVC/BC is a reasonable estimate for the Angstrom exponent. Summer UVC/BC ratios are near unity throughout the day with only modest evening enhancements. In contrast, winter UVC/BC ratios exhibit a distinct diurnal profile with a nighttime maximum and midday minimum. Median UVC/BC ratios are slightly

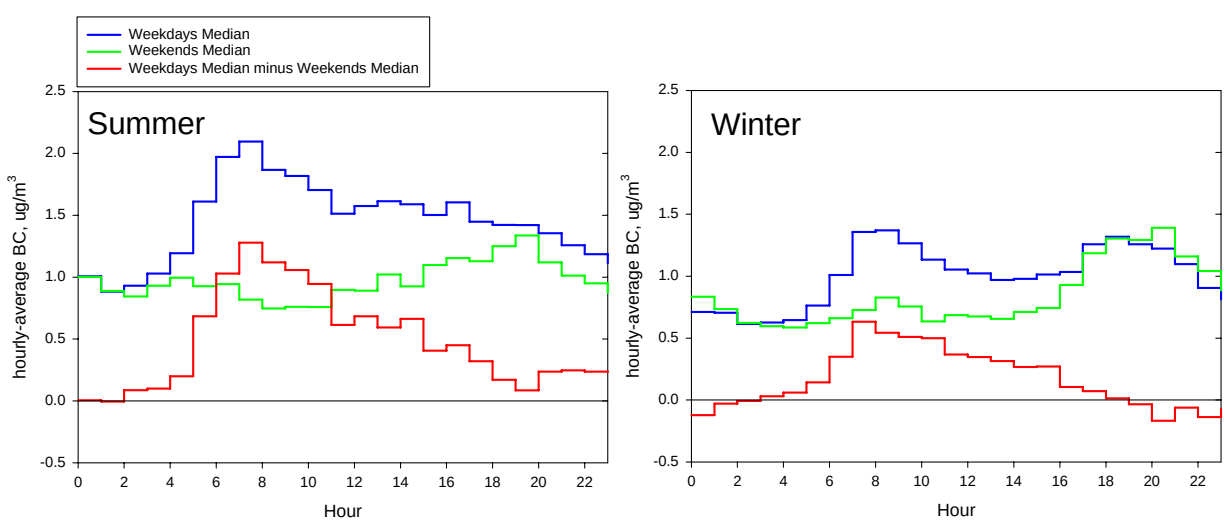

FIGURE 8 Summer (left) and winter (right) diurnal profiles of the median hourly compensated BC for weekdays (blue line), weekends (green line) and the difference between weekday and weekend median values (red line).

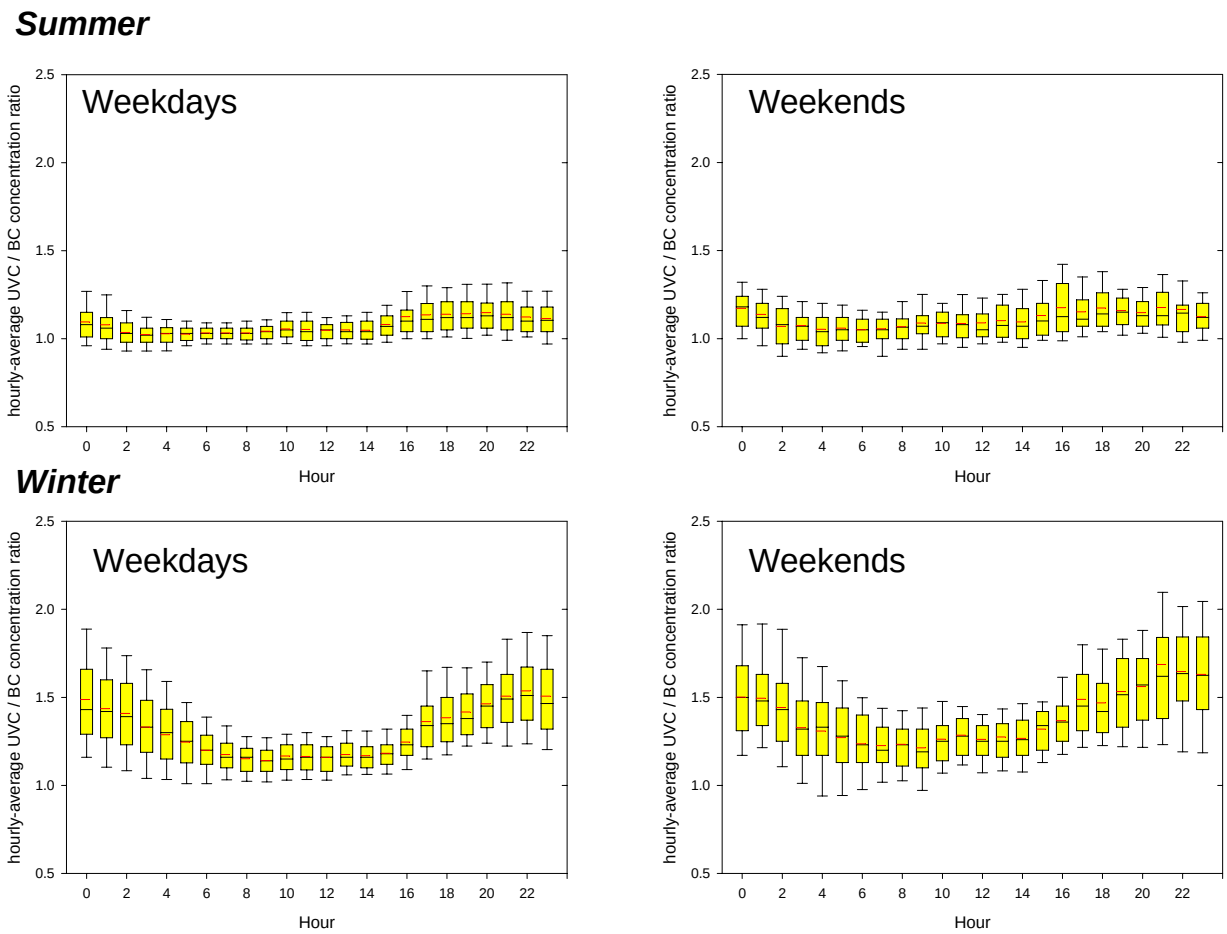

FIGURE 9 Summer (top) and winter (bottom) diurnal profiles of hourly-average UVC/BC ratios for weekdays (left) and weekends (right). Whiskers are 10th and 90th percentiles. The interior black line is the median and the red line is the arithmetic mean. Data from September 2005 through June 2008.

higher on weekends compared to weekdays. This pattern suggests significant biomass combustion contributions during the winter evenings. Sandradewi *et al. (6)* observed similar summer and winter diurnal patterns for the Angstrom exponent of the absorption coefficient measured in an Alpine valley in Switzerland which is known to have both year round traffic influences and wintertime wood smoke influences. Summer median Angstrom exponents were in the range 1.0-1.1 and winter Angstrom exponent diurnal profile exhibited a maximum median value of 1.8 (which corresponds to a UVC/BC ratio of 2.0) at 0000 CET. In this study, we observed summer median UVC/BC ratios of 1.0-1.1 and a maximum in the median winter UVC/BC diurnal profile of 1.5-1.6 at 2200 EST.

Figure 10 shows winter diurnal profiles for ΔC which is defined as UVC minus BC. ΔC increases rather abruptly at 1700 EST with the evening ΔC concentrations higher on weekends compared to weekdays (and modestly higher on Sundays compared to Saturdays). The presence of the evening maximum in ΔC for both weekdays and weekends suggests the use of biomass

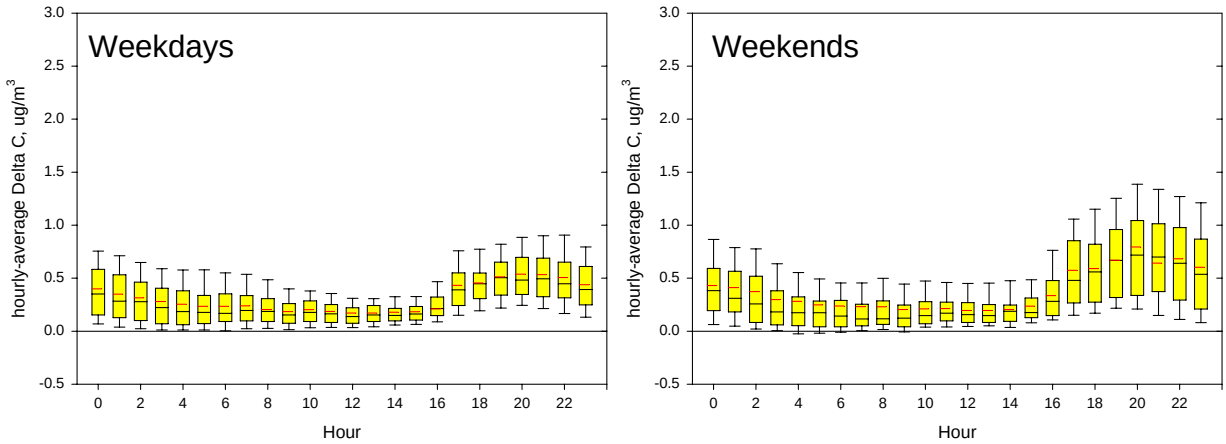

FIGURE 10 Diurnal profiles of hourly-average ΔC (UVC minus BC) for weekdays (left) and weekends (right). Whiskers are 10th and 90th percentiles. The interior black line is the median and the red line is the arithmetic mean. Data from September 2005 through June 2008.

combustion for space heating, and leads to our assignment of this source category as wood smoke. Modestly enhanced evening ΔC concentrations for weekends compared to weekdays suggests contributions from recreational fireplace use, which is also supported by the top 5th percentile of daily-average ΔC including a disproportionately high number of holidays (Thanksgiving weekend, Christmas eve and day, New Year's eve and day).

Sandradewi *et al. (4-6)* presented and applied a two-source model for interpreting multi-wavelength Aethalometer data. Generalizing their derivation to emission sources *A* and *B* with Aethalometer measurements at wavelengths λ_1 and λ_2, using absorption cross-sections which vary inversely with wavelength (as was the case in our study), and assuming the mass absorption efficiencies at a given wavelength are the same for particles from sources *A* and *B*, the concentration $C_i(\lambda)$ apportioned to sources *A* and *B* at λ_2 are –

$$C_B(\lambda_2) = \frac{C(\lambda_1) - [\lambda_2/\lambda_1]^{\alpha_A - 1} C(\lambda_2)}{[\lambda_2/\lambda_1]^{\alpha_B - 1} - [\lambda_2/\lambda_1]^{\alpha_A - 1}}$$

$$C_A(\lambda_2) = C(\lambda_2) - C_B(\lambda_2)$$

where α_i is the Angstrom exponent for source *i*. Sandradewi *et al. (11)* applied the two source model to traffic (source *A*) and wood smoke (source *B*) emissions and assigned Angstrom exponents $\alpha_A = 1.01$ and $\alpha_B = 1.86$ based on literature values and their own estimates. For our measurements at λ_1 =370 nm (UVC) and λ_2 = 880 nm (BC) the BC concentration apportioned to wood smoke (WS) and traffic (T) reduces to –

$$BC_{WS} = 0.91 \times [UVC - 1.01 \times BC]$$

$$BC_T = BC - BC_{WS}$$

Using this approach, wood smoke accounted for 15% of the BC over the entire study period. Wood smoke was 5% of the summer BC and 28% of the winter BC. **Figure 11** shows diurnal profiles for the median BC contribution from wood smoke and traffic (or, more generally, mobile sources). There is very little wood smoke contribution in the summer. In contrast, there are significant wood smoke contributions in the winter with the wood smoke BC on weekday nights approaching 50% of the total BC and the wood smoke BC on weekend nights representing more than 50% of the total BC.

Conclusions

An examination of five years of fine particle Aethalometer black carbon data for the North End site in Boston demonstrates dominant contributions from mobile sources but also significant contributions from biomass combustion, likely wood smoke from space heating and recreational fireplace use, in the winter evenings. While such biomass combustion contributions are generally understood to be important in urban centers in the Pacific Northwest such as Seattle

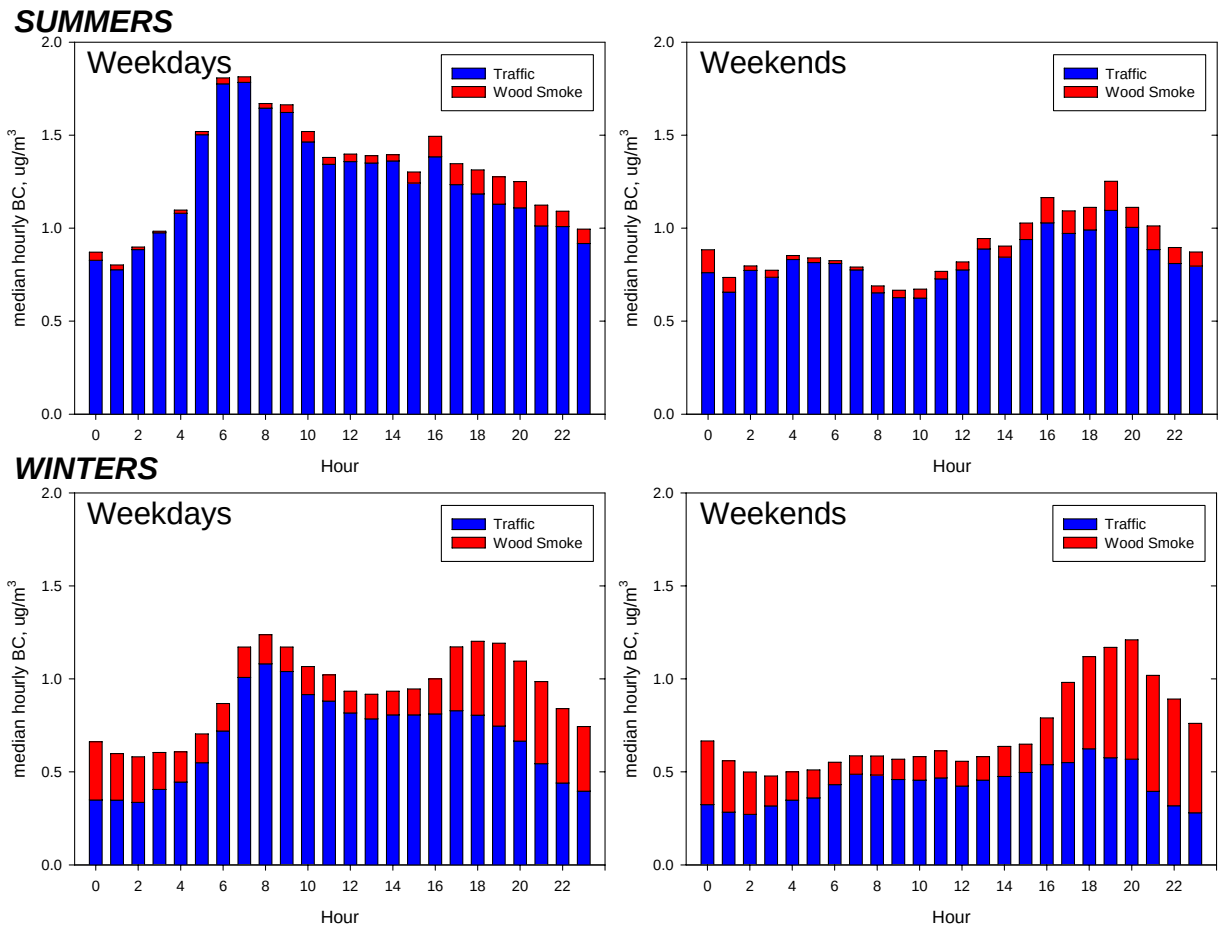

FIGURE 11 Summer (top) and winter (bottom) diurnal profiles of median hourly BC contributions by traffic and wood smoke sources for weekdays (left) and weekends (right). Data from September 2005 through June 2008.

(13), it is now clear that biomass combustion can also be a significant contributor to black carbon in urban centers in the Northeastern U.S. such as Boston. This finding has implications to the interpretation of black carbon as a surrogate for diesel particulate matter in urban centers, and thus to black carbon exposures ascribed to mobiles sources.

ACKNOWLEDGEMENTS

The authors gratefully acknowledge the Massachusetts Department of Environmental Protection, Bureau of Waste Prevention, for providing the raw Aethalometer data.

REFERENCES

1. Schauer, J.J. Evaluation of Elemental Carbon as a Marker for Diesel Particulate Matter. *Journal of Exposure Analysis and Epidemiology*, Vol. 13, 2003, pp. 443-453.
2. Kirchstetter, T., T. Novakov and P.V. Hobbs. Evidence that the spectral Dependence of Light Absorption by Aerosols is Affected by organic Carbon. *Journal of Geophysical Research – Atmospheres*, Vol. 109, 2004, D21208.
3. Allen, G.A., P. Babich, and R.L. Poirot. Evaluation of a New Approach for Real time Assessment of Wood Smoke PM. *Proceedings of the Air & Waste Management Association Visibility Conference in Regional and Global Perspectives on Haze: Causes, Consequences and Controversies*. Paper No. 16. Asheville, NC, October 25-29, 2004.
4. Sandradewi, J., A.S.H. Prevot, S. Szidat, N. Perron, M.R. Alfarra, V.A. Lanz, E. Weingartner, and U. Baltensperger. Using Aerosol Light Absorption Measurements for the Quantitative Determination of Wood Burning and Traffic Emission Contributions to Particulate Matter. *Environmental Science & Technology*, Vol. 42, 2008, pp. 3316-3323.
5. Sandradewi, J., A.S.H. Prevot, M.R. Alfarra, S. Szidat, M.N. Wehrli, M. Ruff, S. Weimer, V.A. Lanz, E. Weingartner, N. Perron, A. Caseiro, A. Kasper-Giebl, H. Puxbaum, L. Wacker, and U. Baltensperger. Comparison of Several Wood Smoke Markers and Source Apportionment Methods for Wood Burning Particulate Mass. *Atmospheric Chemistry and Physics Discussions*, Vol. 8, 2008, pp. 8091-8118.
6. Sandradewi, J., A.S.H. Prevot, E. Weingartner, R. Schmidhauser, M. Gysel, and U. Baltensperger. A Study of Wood Burning and Traffic Aerosols in an Apline Valley using a Multi-wavelength Aethalometer. *Atmospheric Environment*, Vol. 42, 2008, 101-112.
7. Arnott, W.P., K. Hamasha, H. Moosmüller, P.J. Sheridan, and J.A. Ogren. Towards Aerosol Light-Absorption Measurements with a 7-Wavelength Aethalometer: Evaluation with a Photoacoustic Instrument and a 3-Wavelenght Nephelometer. *Aerosol Science and Technology*, Vol. 39, 2005, pp. 17-29.
8. Turner, J.R., A.D. Hansen, and G.A. Allen. Methodologies to Compensate for Optical Saturation and Scattering in Aethalometer™ Black Carbon Measurements. *Proceedings of the Air & Waste Management Association Symposium on Air Quality Measurement Methods and Technology*. Paper No. 37. San Francisco, CA, April 30 – May 2, 2007.
9. Jimenez, J., C. Caliborn, T. Larson, T. Gould, T.W. Kirchstetter, and L. Gundel. Loading Effect Correction for Real-Time Aethalometer Measurements of Fresh Diesel Soot. *Journal of the Air & Waste Management Association*, Vol. 57, 2007, pp. 868-873.

10. Kirchstetter, T.W., and T. Novakov. Controlled Generation of Black Carbon Particles from a Diffusion Flame and Applications in Evaluating Black Carbon Measurement Methods. *Atmospheric Environment*, Vol. 41, 2007, pp. 1874-1888.
11. Virkkula, A., T. Mäkelä, R. Hillamo, T. Yli-Tuomi, A. Hirsikko, K. Hämeri, and I.K. Koponen. A Simple Procedure for Correcting Loading Effects of Aethalometer Data. *Journal of the Air & Waste Management Association*, Vol. 57, 2007, 1214-1222.
12. Weingartner, E., H. Saathoff, M. Schnaiter, N. Streit, B. Bitnar, and U. Baltensperger, U. Absorption of Light by Soot Particles: Determination of the Absorption Coefficient by Means of Aethalometers. *Journal of Aerosol Science*, Vol. 34, 2003, pp. 1445-1463.
13. Gilroy, M., M. Harper, and B. Donaldson. Urban Air Monitoring Strategy – Preliminary Results using Aethalometer™ Carbon Measurements for the Seattle Metropolitan Area. *Proceedings of the Air & Waste Management Association Symposium on Air Quality Measurement Methods and Technology*. San Francisco, CA, April 19-21, 2005.

Appendix H: Annual and Seasonal Boston/Logan Wind Roses, 2000-2012.

Appendix H.

Boston/Logan Wind Roses

Wind speed and direction play a significant role in the seasonal and annual variation of BC. These wind rose plots show the seasonal and year-to-year variation in wind.

Figure 1 shows all wind data for 2000-2012. Figure 2 shows wind for March, and Figure 3 for August for the same time period; these two months are typically the lowest and highest BC months. Figure 4 shows wind for 2009-2012, the duration of the second spatial analysis.

The remaining plots show each year of wind from 2000 to 2012.

Figure 1. 2000-2012

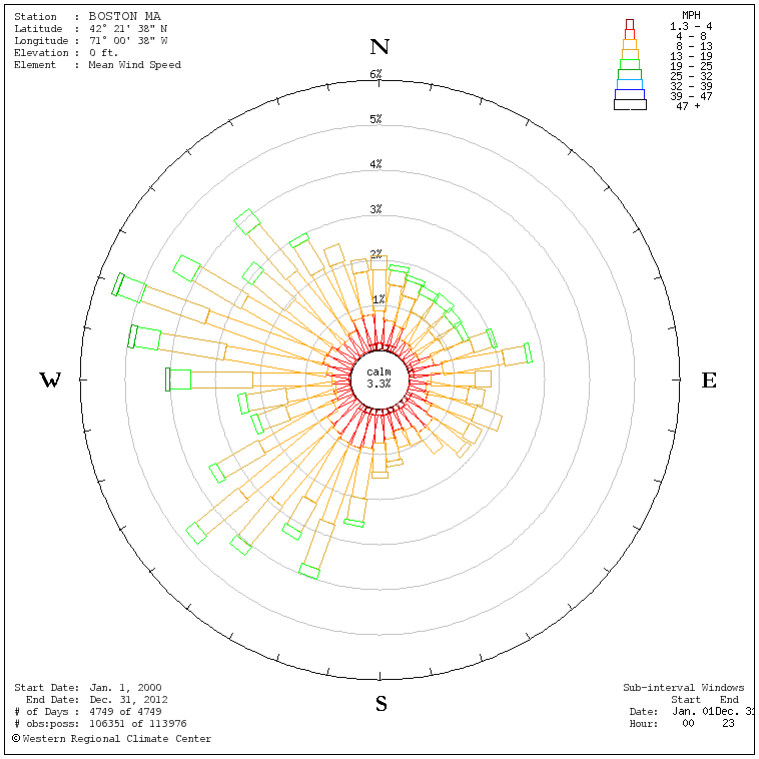

Figure 2. March 2000-2012

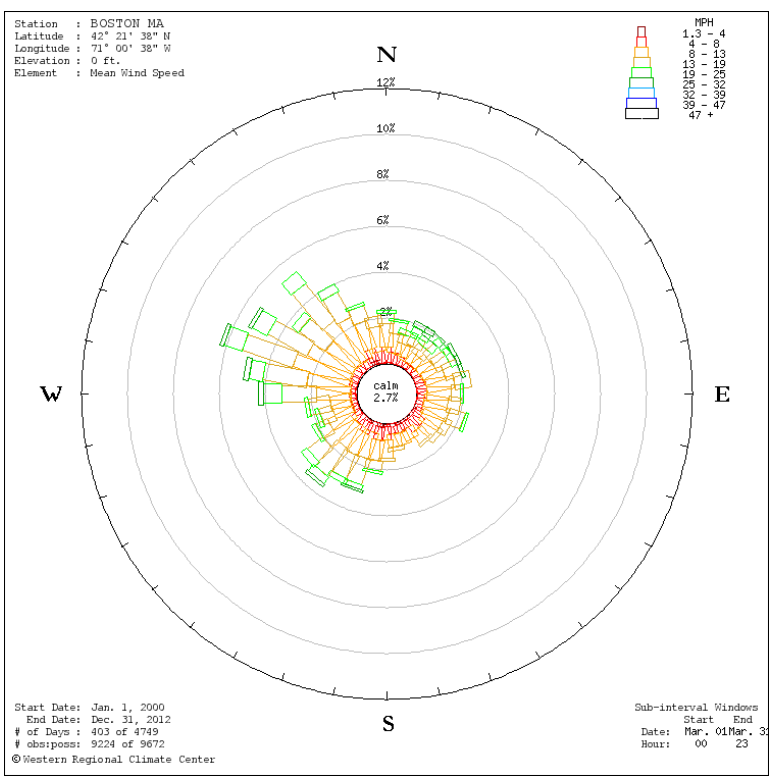

Figure 3. August 2000-2012

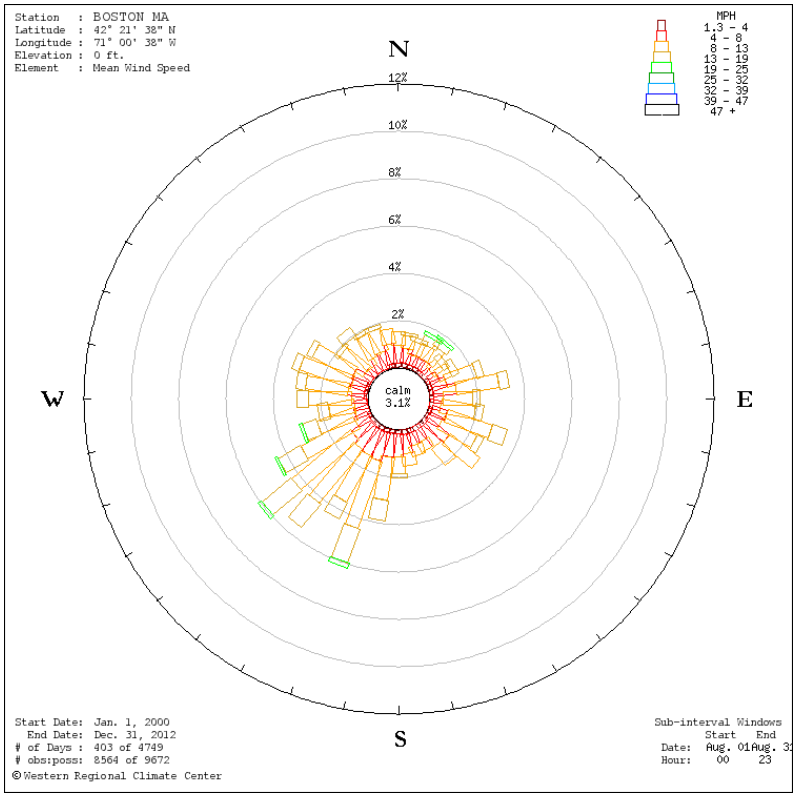

Figure 4. 2009-2012

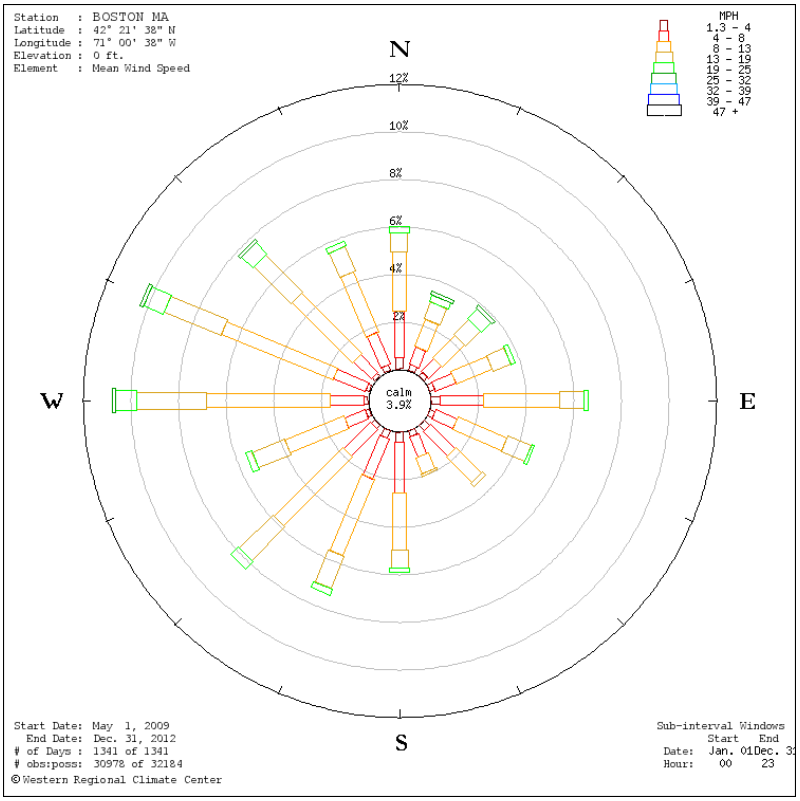

Annual Wind Roses, 2000-2012

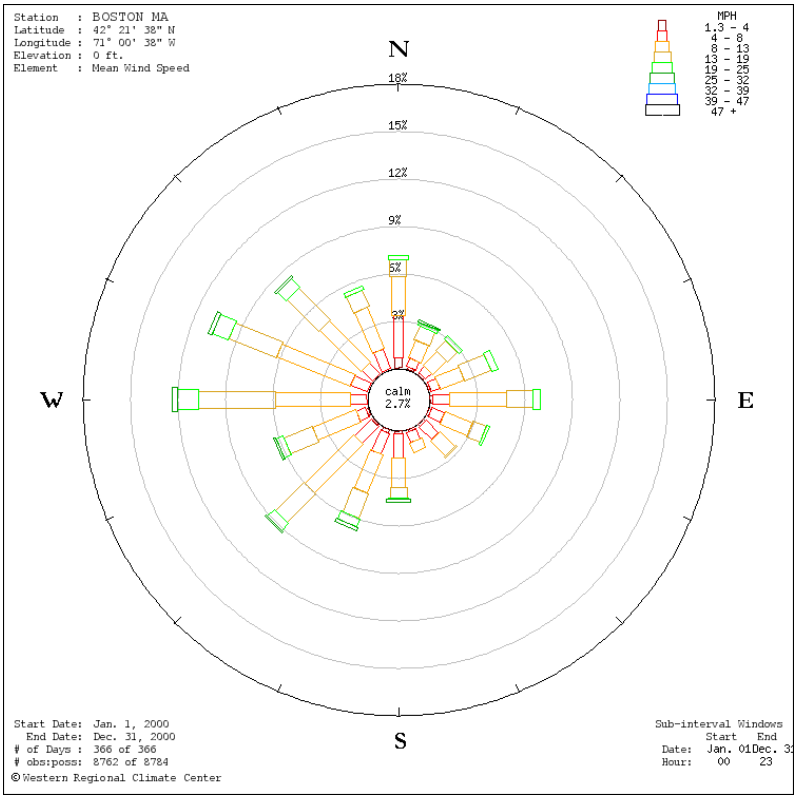

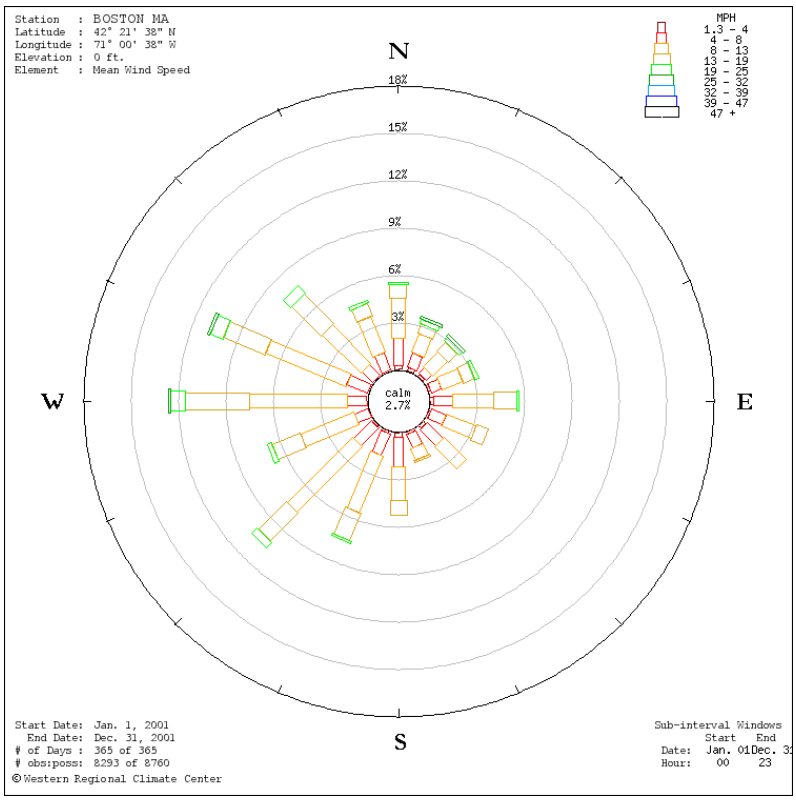

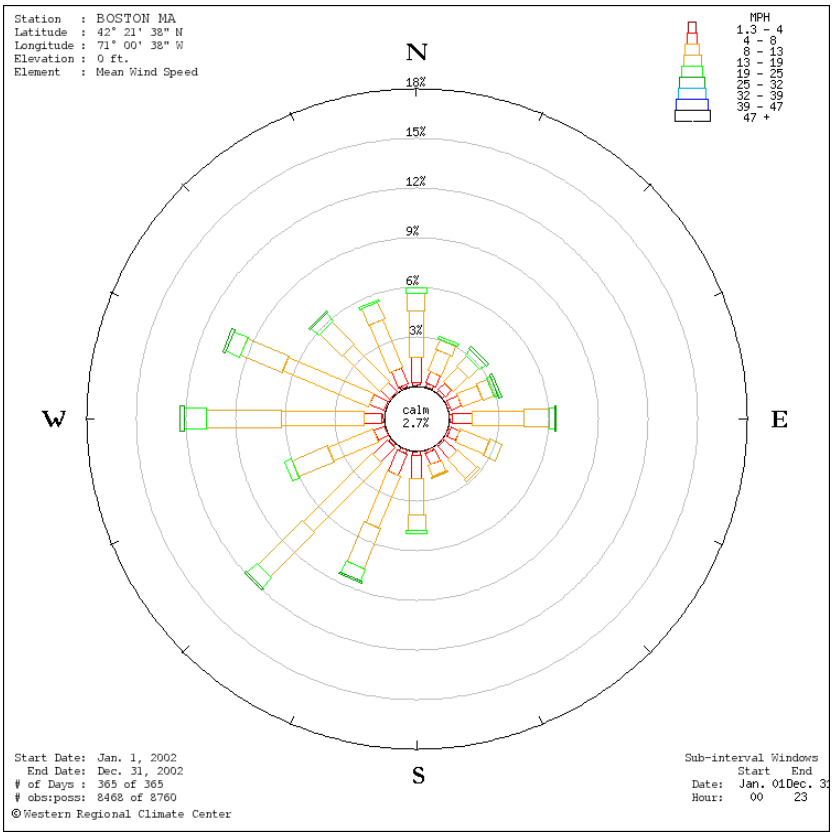
Station : BOSTON MA
Latitude : 42° 21' 38" N
Longitude : 71° 00' 38" W
Elevation : 0 ft.
Element : Mean Wind Speed
MPH
1.3 - 4
4 - 8
8 - 13
13 - 19
19 - 25
25 - 32
32 - 39
39 - 47
47 +
N
W
E
S
18%
15%
12%
9%
6%
3%
calm
2.7%
Start Date: Jan. 1, 2002
End Date: Dec. 31, 2002
# of Days : 365 of 365
obs:poss: 8468 of 8760
©Western Regional Climate Center
Sub-interval Windows
Start End
Date: Jan. 01 Dec. 3
Hour: 00 23

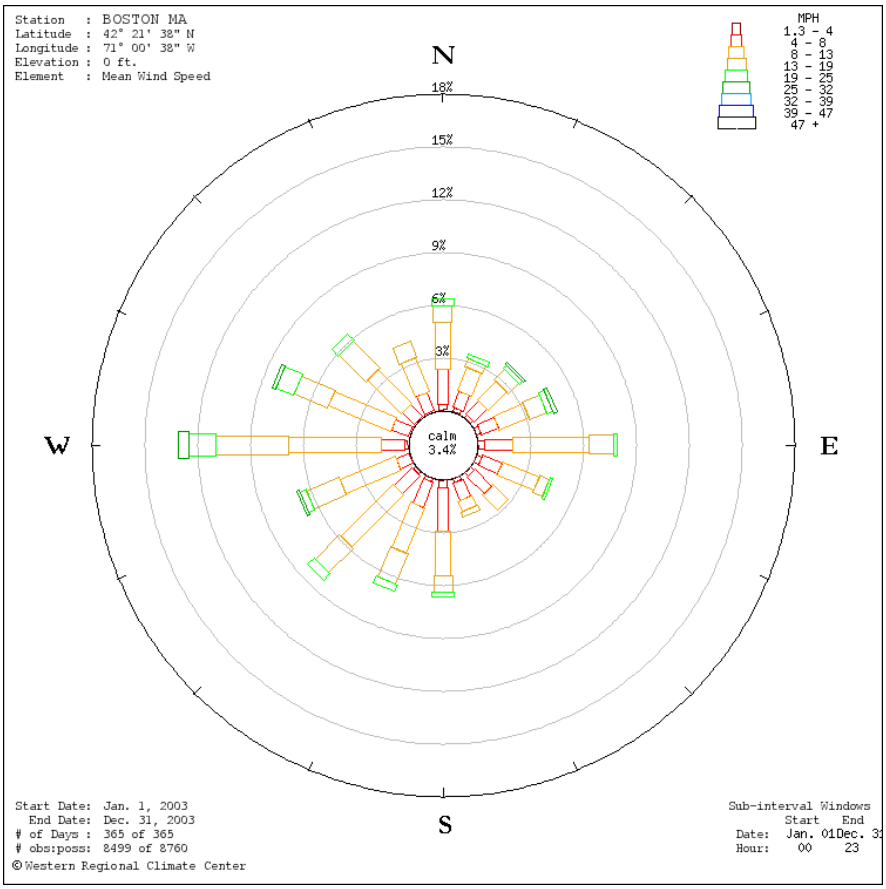
Station : BOSTON MA
Latitude : 42° 21' 38" N
Longitude : 71° 00' 38" W
Elevation : 0 ft.
Element : Mean Wind Speed
MPH
1.3 - 4
4 - 8
8 - 13
13 - 19
19 - 25
25 - 32
32 - 39
39 - 47
47 +
N
W
E
S
18%
15%
12%
9%
6%
3%
calm
3.4%
Start Date: Jan. 1, 2003
End Date: Dec. 31, 2003
# of Days : 365 of 365
obs:poss: 8499 of 8760
©Western Regional Climate Center
Sub-interval Windows
Start End
Date: Jan. 01 Dec. 3
Hour: 00 23

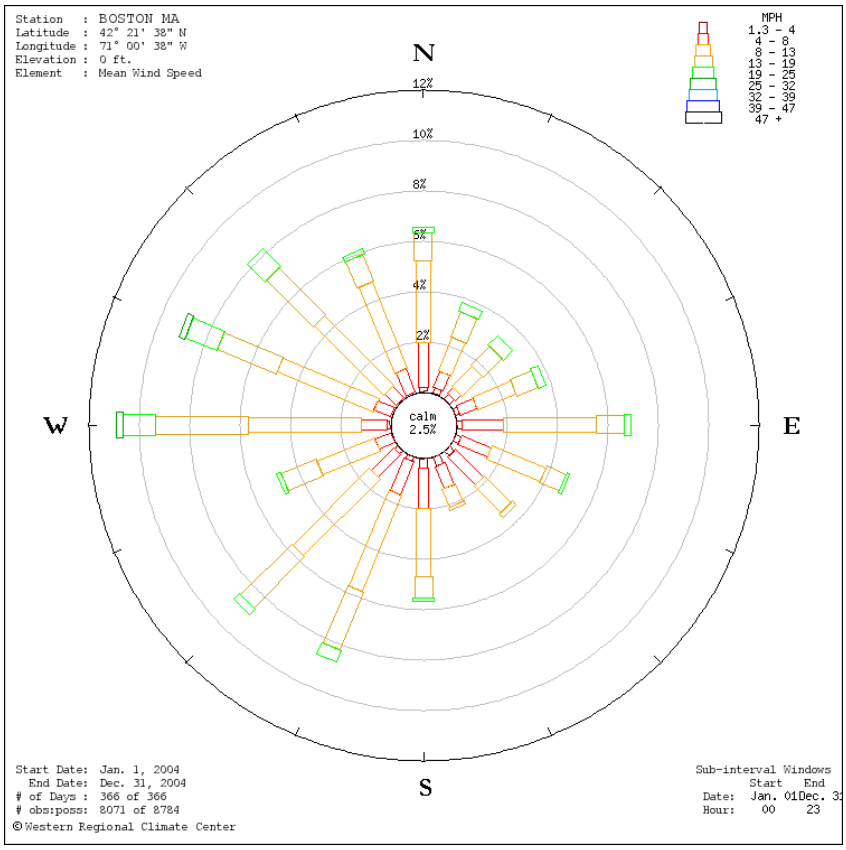
Station : BOSTON MA
Latitude : 42° 21' 38" N
Longitude : 71° 00' 38" W
Elevation : 0 ft.
Element : Mean Wind Speed
MPH
1.3 - 4
4 - 8
8 - 13
13 - 19
19 - 25
25 - 32
32 - 39
39 - 47
47 +
N
W
E
S
12%
10%
8%
6%
4%
2%
calm
2.5%
Start Date: Jan. 1, 2004
End Date: Dec. 31, 2004
# of Days : 366 of 366
obs:poss: 8071 of 8784
©Western Regional Climate Center
Sub-interval Windows
Start End
Date: Jan. 01 Dec. 3
Hour: 00 23

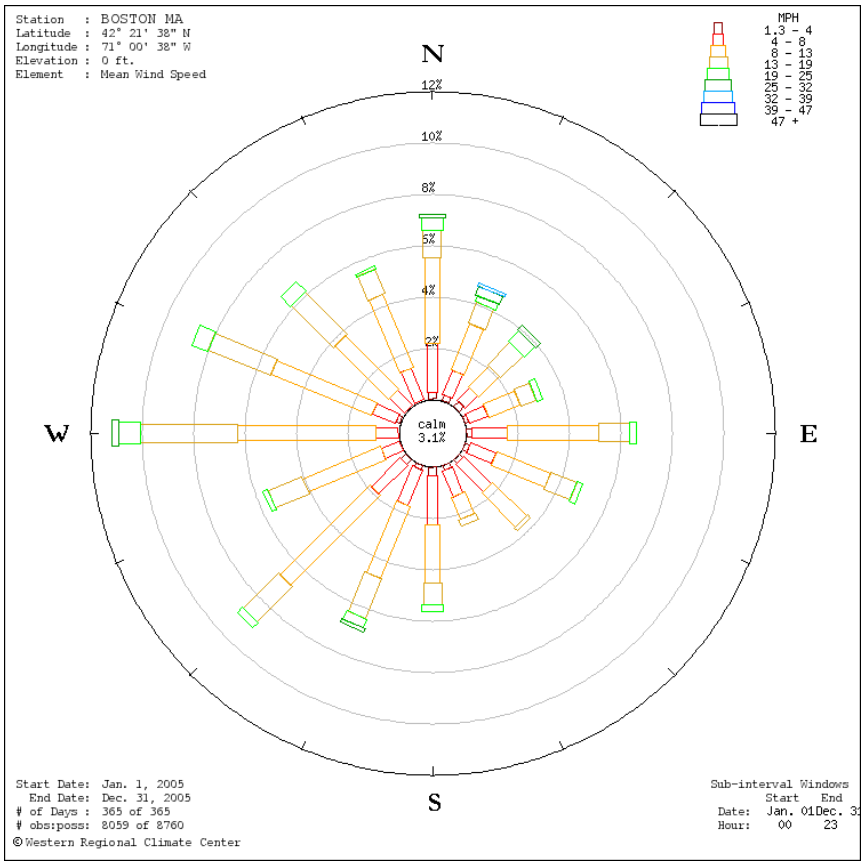
Station : BOSTON MA
Latitude : 42° 21' 38" N
Longitude : 71° 00' 38" W
Elevation : 0 ft.
Element : Mean Wind Speed
MPH
1.3 - 4
4 - 8
8 - 13
13 - 19
19 - 25
25 - 32
32 - 39
39 - 47
47 +
N
W
E
S
12%
10%
8%
6%
4%
2%
calm
3.1%
Start Date: Jan. 1, 2005
End Date: Dec. 31, 2005
# of Days : 365 of 365
obs:poss: 8059 of 8760
©Western Regional Climate Center
Sub-interval Windows
Start End
Date: Jan. 01 Dec. 3
Hour: 00 23

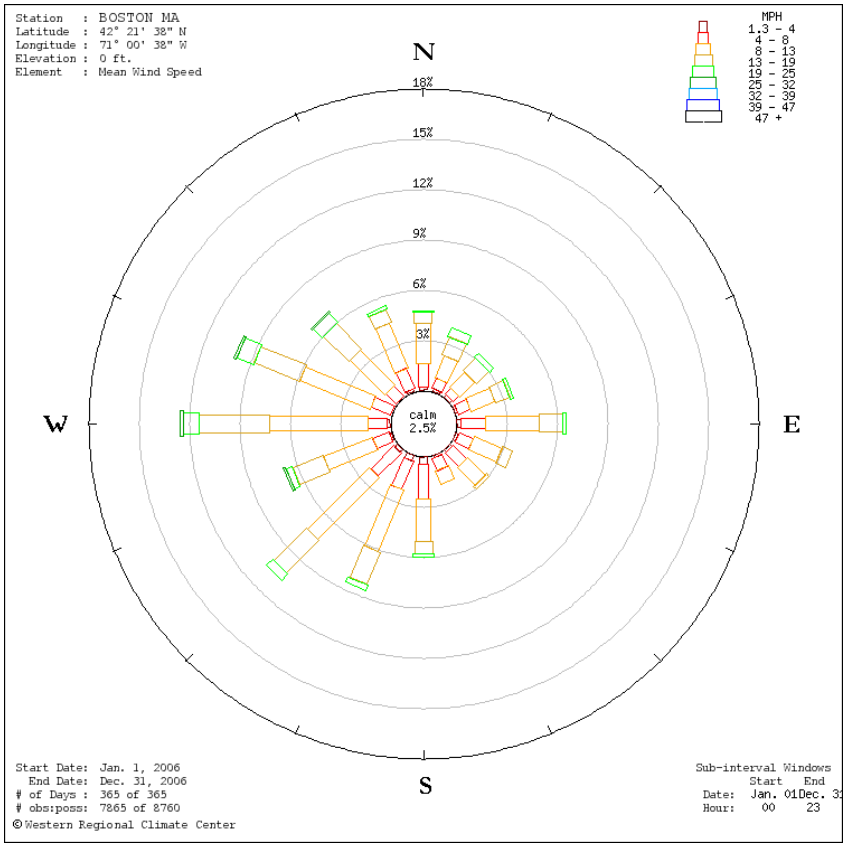
Station : BOSTON MA
Latitude : 42° 21' 38" N
Longitude : 71° 00' 38" W
Elevation : 0 ft.
Element : Mean Wind Speed
MPH
1.3 - 4
4 - 8
8 - 13
13 - 19
19 - 25
25 - 32
32 - 39
39 - 47
47 +
N
E
S
W
18%
15%
12%
9%
6%
3%
calm
2.5%
Start Date: Jan. 1, 2006
End Date: Dec. 31, 2006
# of Days : 365 of 365
obs:poss: 7865 of 8760
© Western Regional Climate Center
Sub-interval Windows
Start End
Date: Jan. 01 Dec. 3
Hour: 00 23

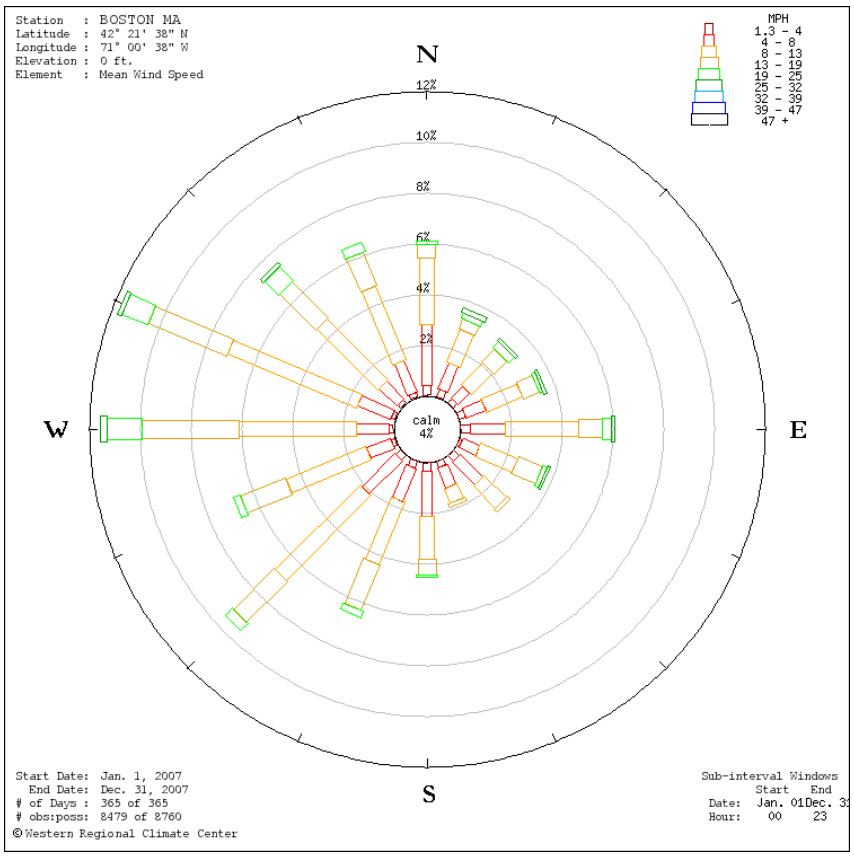
Station : BOSTON MA
Latitude : 42° 21' 38" N
Longitude : 71° 00' 38" W
Elevation : 0 ft.
Element : Mean Wind Speed
MPH
1.3 - 4
4 - 8
8 - 13
13 - 19
19 - 25
25 - 32
32 - 39
39 - 47
47 +
N
E
S
W
12%
10%
8%
6%
4%
2%
calm
4%
Start Date: Jan. 1, 2007
End Date: Dec. 31, 2007
# of Days : 365 of 365
obs:poss: 8479 of 8760
© Western Regional Climate Center
Sub-interval Windows
Start End
Date: Jan. 01 Dec. 3
Hour: 00 23

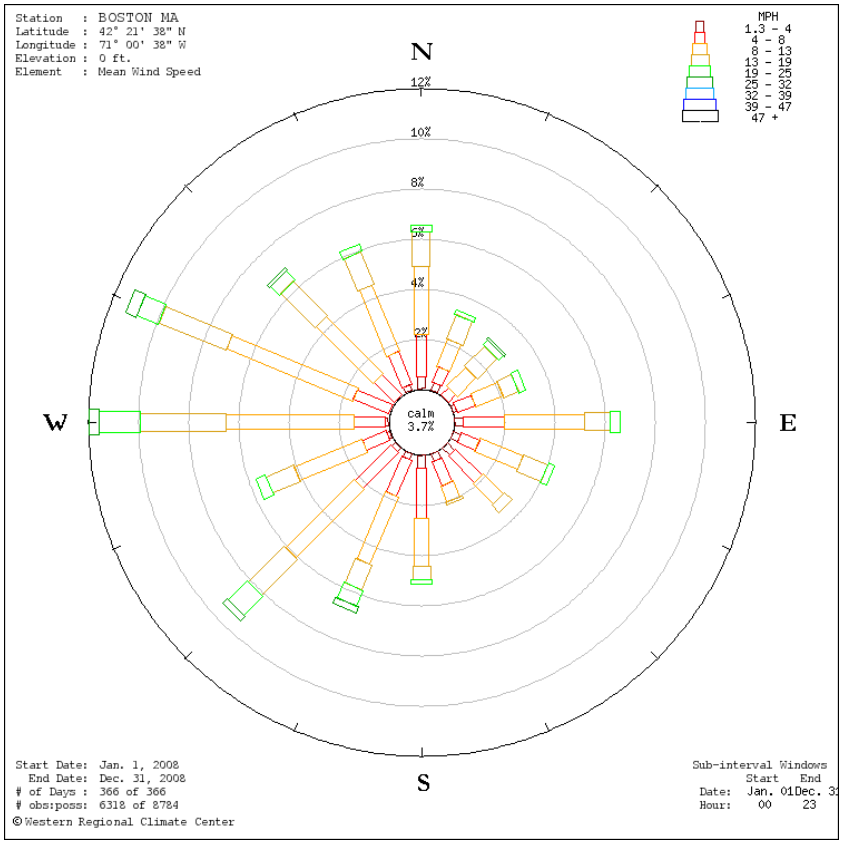
Station : BOSTON MA
Latitude : 42° 21' 38" N
Longitude : 71° 00' 38" W
Elevation : 0 ft.
Element : Mean Wind Speed
MPH
1.3 - 4
4 - 8
8 - 13
13 - 19
19 - 25
25 - 32
32 - 39
39 - 47
47 +
N
E
S
W
12%
10%
8%
6%
4%
2%
calm
3.7%
Start Date: Jan. 1, 2008
End Date: Dec. 31, 2008
# of Days : 366 of 366
obs:poss: 6318 of 8784
© Western Regional Climate Center
Sub-interval Windows
Start End
Date: Jan. 01 Dec. 3
Hour: 00 23

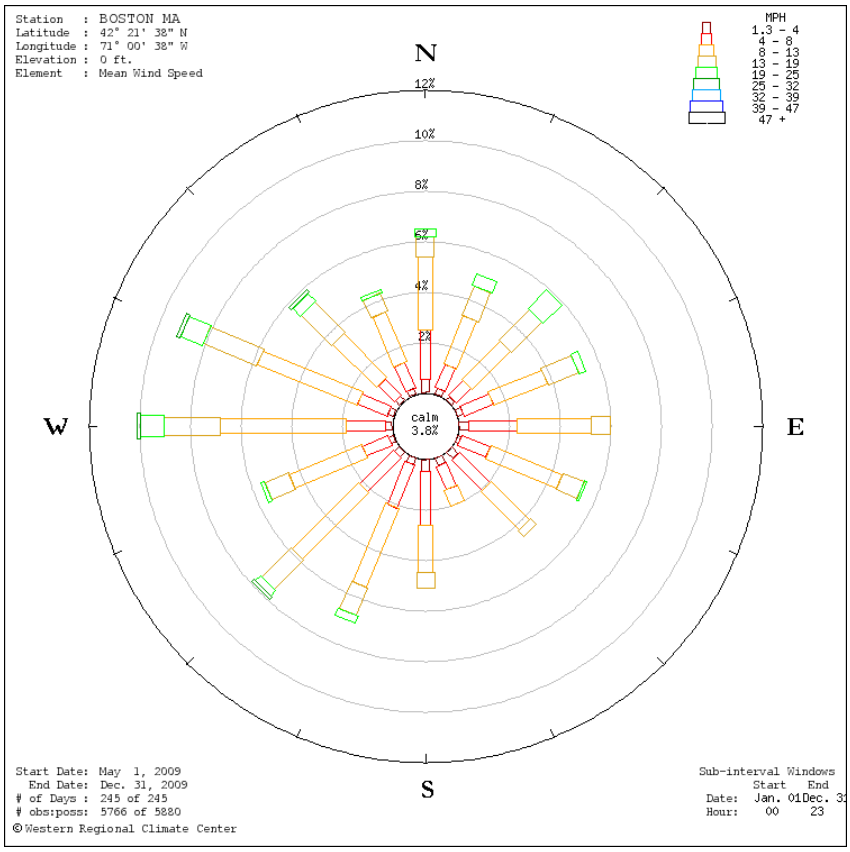
Station : BOSTON MA
Latitude : 42° 21' 38" N
Longitude : 71° 00' 38" W
Elevation : 0 ft.
Element : Mean Wind Speed
MPH
1.3 - 4
4 - 8
8 - 13
13 - 19
19 - 25
25 - 32
32 - 39
39 - 47
47 +
N
E
S
W
12%
10%
8%
6%
4%
2%
calm
3.8%
Start Date: May 1, 2009
End Date: Dec. 31, 2009
# of Days : 245 of 245
obs:poss: 5766 of 5880
© Western Regional Climate Center
Sub-interval Windows
Start End
Date: Jan. 01 Dec. 3
Hour: 00 23

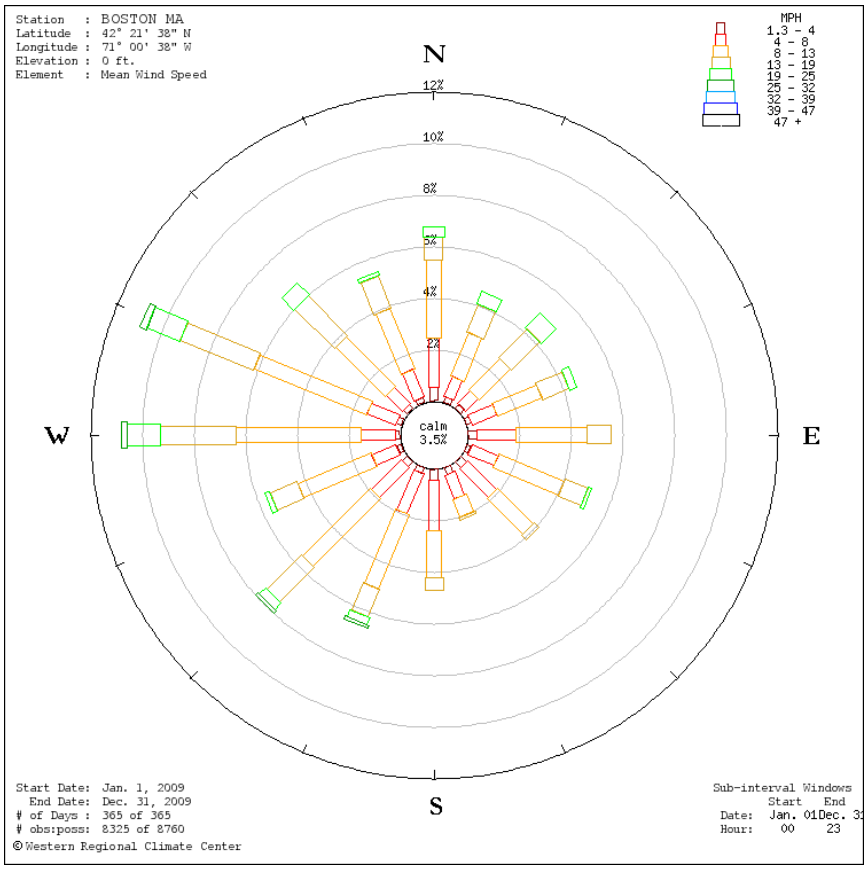
Station : BOSTON MA
Latitude : 42° 21' 38" N
Longitude : 71° 00' 38" W
Elevation : 0 ft.
Element : Mean Wind Speed
MPH
1.3 - 4
4 - 8
8 - 13
13 - 19
19 - 25
25 - 32
32 - 39
39 - 47
47 +
N
W
E
S
12%
10%
8%
6%
4%
2%
calm
3.5%
Start Date: Jan. 1, 2009
End Date: Dec. 31, 2009
# of Days : 365 of 365
obs:poss: 8325 of 8760
©Western Regional Climate Center
Sub-interval Windows
Start End
Date: Jan. 01 Dec. 3
Hour: 00 23

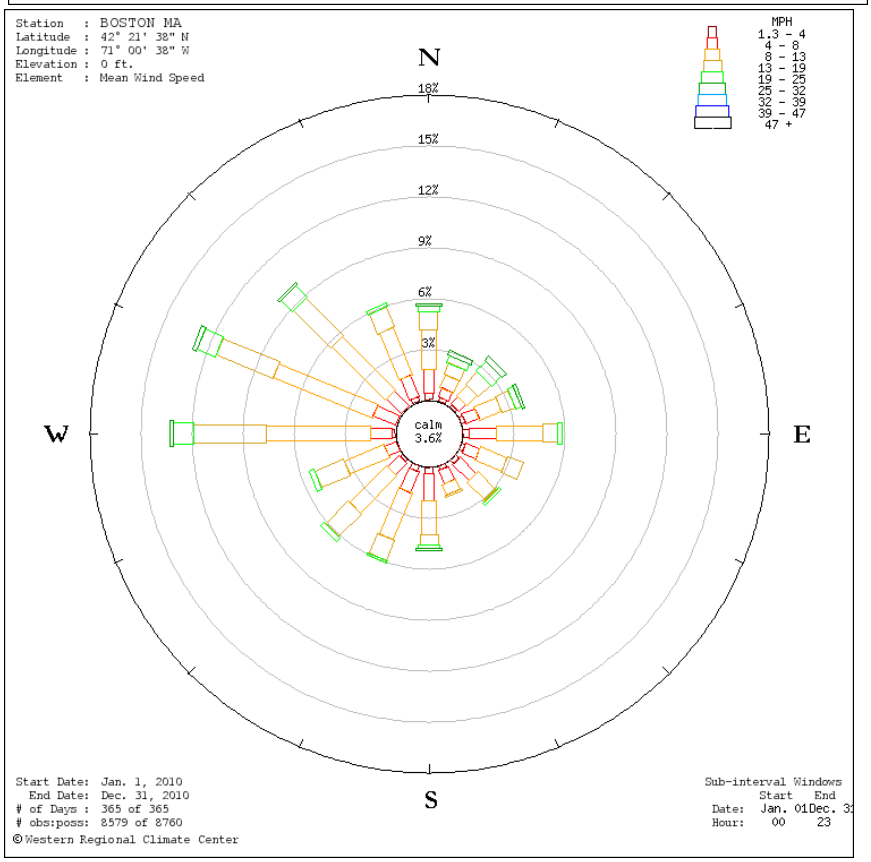
Station : BOSTON MA
Latitude : 42° 21' 38" N
Longitude : 71° 00' 38" W
Elevation : 0 ft.
Element : Mean Wind Speed
MPH
1.3 - 4
4 - 8
8 - 13
13 - 19
19 - 25
25 - 32
32 - 39
39 - 47
47 +
N
W
E
S
18%
15%
12%
9%
6%
3%
calm
3.6%
Start Date: Jan. 1, 2010
End Date: Dec. 31, 2010
# of Days : 365 of 365
obs:poss: 8579 of 8760
©Western Regional Climate Center
Sub-interval Windows
Start End
Date: Jan. 01 Dec. 3
Hour: 00 23

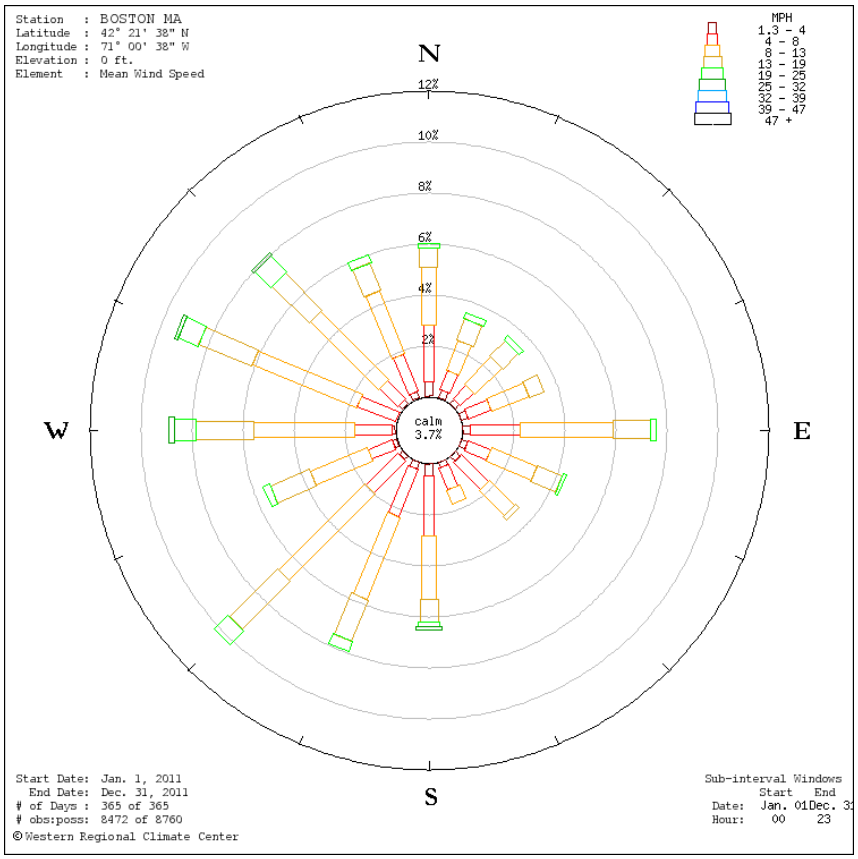
Station : BOSTON MA
Latitude : 42° 21' 38" N
Longitude : 71° 00' 38" W
Elevation : 0 ft.
Element : Mean Wind Speed
MPH
1.3 - 4
4 - 8
8 - 13
13 - 19
19 - 25
25 - 32
32 - 39
39 - 47
47 +
N
E
S
W
12%
10%
8%
6%
4%
2%
calm
3.7%
Start Date: Jan. 1, 2011
End Date: Dec. 31, 2011
# of Days : 365 of 365
obs:poss: 8472 of 8760
©Western Regional Climate Center
Sub-interval Windows
Start End
Date: Jan. 01 Dec. 3
Hour: 00 23

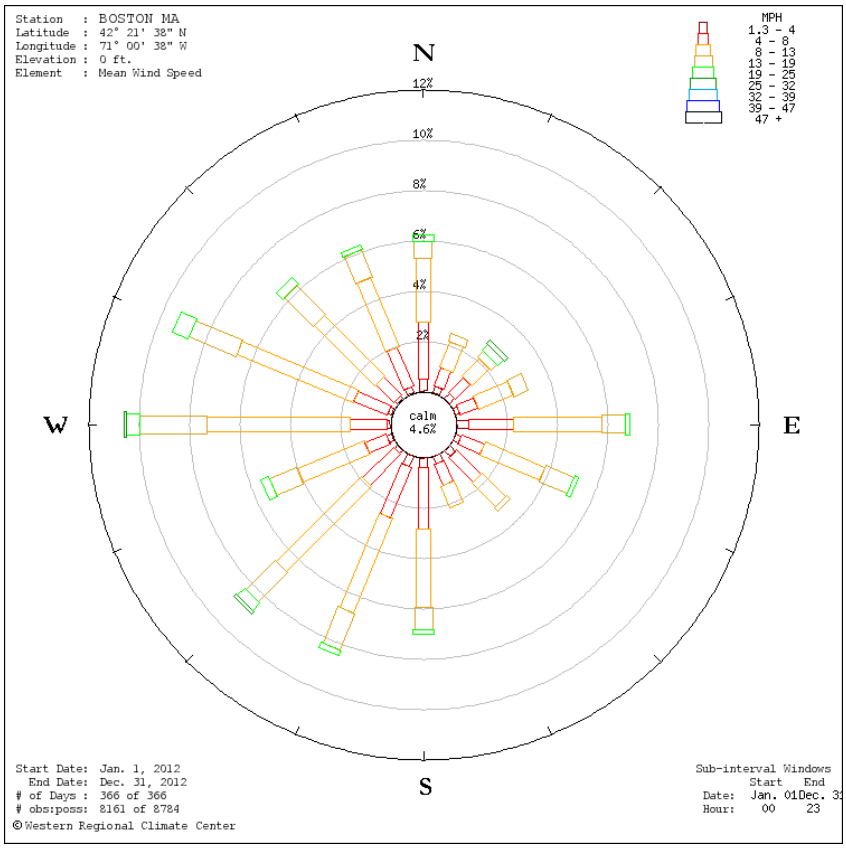
Station : BOSTON MA
Latitude : 42° 21' 38" N
Longitude : 71° 00' 38" W
Elevation : 0 ft.
Element : Mean Wind Speed
MPH
1.3 - 4
4 - 8
8 - 13
13 - 19
19 - 25
25 - 32
32 - 39
39 - 47
47 +
N
E
S
W
12%
10%
8%
6%
4%
2%
calm
4.6%
Start Date: Jan. 1, 2012
End Date: Dec. 31, 2012
# of Days : 366 of 366
obs:poss: 8161 of 8784
©Western Regional Climate Center
Sub-interval Windows
Start End
Date: Jan. 01 Dec. 3
Hour: 00 23